DISSERTATION

submitted to the

Combined Faculties for the Natural Sciences and for Mathematics

of the

Ruperto-Carola University of Heidelberg, Germany

for the degree of

Doctor of Natural Sciences

---

presented by

Diplom Biologe (t.o.) Darius Schwenger

born in Heidelberg

Heidelberg, June 2009

Function of the exocyst complex in the calyx of Held presynaptic nerve terminal

---

Referees: **Prof. Dr. Blanche Schwappach**
Prof. Dr. Thomas Kuner

Acknowledgements

First of all, I would like to thank Prof. Dr. Thomas Kuner for providing the topic and giving me the opportunity to work in his lab. His constant motivation and support gave me the possibility to work independently and to explore a broad spectrum of methods. I also would like to thank Prof. Dr. Blanche Schwappach for scientific advice and quick responses to all my inquiries.

Many thanks to all the people I have been working with and for the priceless atmosphere in the lab! Without you it would have been half of the fun. Thanks to all of you for the time we had and for sharing and contributing to an unforgettable period.

Special thanks to Bob for sharing his deep insights into the calyx prep and his advises in electrophysiology! Thanks to Christoph for keeping track of lunch times and for cookie supply. Big thanks to Claudia, Suse and Michaela for the constant support and for filling the lab with these beautiful spirits, which restock the lab overnight. Thanks to Heinz for unlimited coffee supply and the EM collaboration. Thanks to Nina and Thomas from the Dresbach group for teaching me the hippocampal prep and helping out with reagents.

I would like to express my deepest thanks to my parents for the unquestioned support during my whole life and for opening up all the possibilities I have. Also, I would like to thank my brother for standing by my side and for open ears in any regard.

Last but not least, thank you Marie for being in my life and for sweetening every day.

Table of Contents

1 Introduction

The human brain is a complex organ composed of 100 billion neuronal cells, each of which makes an average of 1000 contacts at specialized sites called synapses. The resulting network, which governs the function of the central nervous system from simple motor tasks to sophisticated emotional and cognitive behaviour, relies on the communication of neurons with each other in a precisely directed and timed manner. This implies that two major aspects have to be fulfilled in order for the central nervous system to function properly: (1) neurons have to connect to a specific neuronal cell and (2) the way in which they receive, generate and transmit action potentials to their connected neuronal cells has to be defined. The first aspect, connectivity, was initially discovered in the early 20th century by Santiago Ramón y Cajal, who performed Golgi stains on brain tissue. He was able to resolve single units, the neurons, which led to the confirmation of the neuron doctrine, the idea that neurons are the basic and functional unit of the nervous system, which was initially introduced by Wilhelm von Waldeyer in 1891. Past research efforts in developmental neurobiology have concentrated on the mechanisms, which direct axons to their particular partner and how the initial contact site, which later would turn into a synapse, is established. Once formed, a synapse is a highly dynamic structure, which can be eliminated or strengthened. This process of synapse elimination or strengthening depends partly on external stimuli and synaptic activity. It represents an essential step in the establishment of an adaptable neuronal network and is thought to underlie learning and memory processes. Recent scientific efforts are aiming to create a connectome, a complete map of neural wiring in the mammalian brain.

Apart from mere connectivity of individual neurons, an individual central nervous system is defined by how synapses transfer and modulate electrical signals. Hodgkin and Huxley (Hodgkin and Huxley, 1952) elucidated the mechanism of action potentials and the elaboration of the quantal theory by Fatt and Katz led to an understanding of transmitter release (Fatt and Katz, 1950; Fatt and Katz, 1951; Fatt and Katz, 1952). Soon thereafter, it was recognized that neurotransmitters, which are released from the presynaptic neuron, have to bind and activate neurotransmitter-gated ion channels on the postsynaptic cell to convey the chemical signal of neurotransmitter release from the presynaptic bouton into an electrical signal caused by an ion flux across the membrane of the postsynaptic cell. This process of chemical synaptic transmission is not constant for every action potential, which arrives at the presynaptic terminal, but is rather dependent on the preceded activity of that synapse. Modulation of synaptic transmission is both pre- and postsynaptic in origin and occurs on different frequency and time scales for an

individual synapse. Together with connectivity, modulation of synaptic transmission is describing brain plasticity and reflects the result of environmental stimuli and experience.

The following subchapters of this introduction will expand on the two mentioned aspects of connectivity and synaptic transmission. The focus will be set on the presynaptic compartment and unresolved questions in these fields, which this thesis addresses by investigating a potential involvement of the exocyst complex in these processes. Thereafter, a summary of the current literature about the exocyst complex will follow to explain the initial interest in this multiprotein complex. Finally, the employed *in vivo* model system will be described before the introduction concludes with the aim of the study.

1.1 Connectivity

The assembly of neural circuits requires the intricate coordination of multiple developmental events. First, cells need to differentiate into a cell type and migrate to a specific location. This is followed by the outgrowth of axons and dendrites, which are guided by various axon guidance cues to the appropriate target field. Once axons reach their target field, they then must identify their appropriate targets and initiate assembly of specialized membrane areas at defined locations to enable information flow between neurons.

1.1.1 Pathfinding and targeting

While traditionally it was believed that only the two involved pre- and postsynaptic neurons communicate to form a specific synaptic contact, there is growing evidence for the existence of so called *guidepost cells*, which are not part of the neuronal circuit itself but assist in axon guidance and synapse assembly (Bentley and Caudy, 1983). Guidepost cells attract axons by secretion of long-range chemoattractants (e.g. netrin, sonic hedgehog), which are sensed via receptors on outgrowing axons (e.g. DCC, BOC) (Charron et al., 2003; Okada et al., 2006; Serafini et al., 1996). Once axons reach their guidepost cell, secretion of repellent factors (e.g. Slit) and binding to axonal receptors (e.g. Robo) has to occur to allow for further outgrowth of axons to the next guidepost cell (Kidd et al., 1999). Since guidepost cells secrete attractive and repellent factors simultaneously, the receptivity of these factors is regulated in a partly interdependent manner. Regulatory proteins (COMM, ROBO3) control surface expression of receptors and repellent and attractive receptors influence each other negatively to silence the contrary response (Stein and Tessier-Lavigne, 2001). Via this regulation axons can reach their target postsynaptic neuron in a *connect-the-dots* like fashion. Apart from secreting

long-range factors guidepost cells also attract or repel outgrowing axons by expression of ligand molecules on their surface (e.g. ephrin-B2, neuregulin-1), which bind to their receptors on axons (e.g. EphB1, ERBB4) and induce the equivalent response (Lopez-Bendito et al., 2006; Williams et al., 2003). In this way guidepost cells can act as a barrier to prevent further axon outgrowth or assist in axon guidance as a scaffold substrate via cell-cell interactions. In some examples guidepost cells serve as synaptic placeholders by defining endpoints for axonal processes before postsynaptic targets are present. After they served as substrate for axon outgrowth they are eliminated by regulated cell death (Del Rio et al., 1997). Apart from directing axons to their respective target field, guidepost cells also provide positional cues for synapse target selection and synaptogenesis. For example glial cells secrete factors, which attract one axon and induce formation of presynaptic specializations in another, and thereby initiate contact between the two neurons in a locally defined area (Colon-Ramos et al., 2007). Interestingly, the same secreted factor induces different responses via the same receptor in these two neurons highlighting the intricate entanglement of cellular cues and responses, which lead to the establishment of axo-dendritic contacts. The discovery of transient cell-cell interactions, which is mediated by cells extrinsic to the final neuronal circuit, offers explanations of how the nervous system is wired in such a delicate and defined way. Nevertheless, the molecular mechanisms that underlie establishment and disassembly of transient circuits are poorly understood. Similarly, the regulation of receptivity of axons during attraction and repulsion to and from guidepost cells offers a model of how axon guidance could occur, but more developmental processes are most likely involved.

Actin dynamics are required for extension of filopodia to the target region. The exocyst complex, a multiprotein complex suggested to act as a tethering factor and the focus of this study, has been associated with cytoskeleton dynamics in this regard. Pommereit and Wouters (2007) proposed, that nerve growth factor (NGF) induced sprouting is locally confined to certain membrane patches by the interaction of Exo70, a subunit of the exocyst complex, and the GTPase TC10. Binding of these two proteins was necessary to induce an activation of the actin nucleation core machinery, the Arp2/3 complex (Pommereit and Wouters, 2007). Thus, the exocyst complex contributes to the events underlying neurite outgrowth by regulating actin dynamics after sensation of neurotrophic factors by the neuron.

1.1.2 Synaptogenesis

Formation of new synapses requires establishment of a pre- and postsynaptic membrane patch (see also above) and targeted delivery of synaptic components along the secretory pathway to the synaptic terminal. Several molecules including synaptic cell

adhesion molecule (SynCAM), cadherins, neural cell adhesion molecule (NCAM), Eph receptor tyrosin kinases and neuroligins and neurexins have been implicated in the early events of synapse formation.

The cadherin protein family has received increasing attention since it clusters at nascent synapses together with synaptic markers and as a cell-adhesion molecule seems well suited to promote adhesion between pre- and postsynaptic elements (Benson and Tanaka, 1998) (Figure 1). Besides cell-adhesion a role in synaptic organization has been suggested for ß-catenin, which binds to N-cadherin and regulates localization of synaptic vesicles through recruitment of PDZ-containing proteins (Bamji et al., 2003). ß-catenin can also mediate interaction between N-cadherin and α-catenin, which in turn is involved in actin dynamics by interaction with several actin-binding proteins that promote or inhibit actin polymerization (Kobielak and Fuchs, 2004).

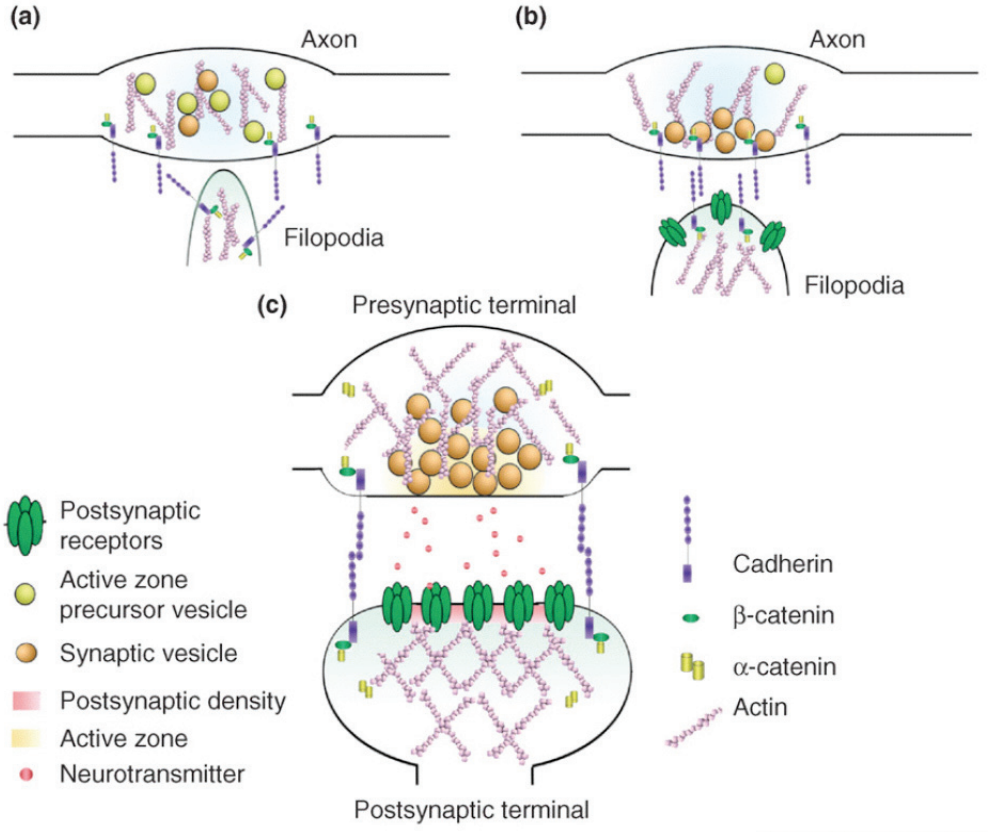

Figure 1. Schematic representation of synapse formation. (a) Synaptogenesis is initiated by cadherins, which are evenly distributed at the dendrite and the axon. **(b)** The axo-dendritic contact is stabilized by cadherin clustering. Active zone precursor vesicles are recruited to the nascent synapse and synaptic vesicles are organized via α- and β-catenin and the actin cytoskeleton. **(c)** A mature synapse is characterized by an aligned pre- and postsynaptic compartment, which is surrounded by cadherin molecules (puncta adherentia). Synaptic vesicles are primed for neurotransmitter release. From (Arikkath and Reichardt, 2008).

The adhesion-molecule protein family of neurexins and neuroligins has also been suggested to act in trans-synaptic signalling (Figure 2). Neurexins are present presynaptically and contain an extracellular domain, a transmembrane region and a cytoplasmatic tail with a PDZ interaction site on the C-terminus (Ushkaryov et al., 1994; Ushkaryov et al., 1992). Neuroligins are postsynaptic proteins, which bind to the extracellular domain of neurexins in a spliceform dependent manner (Ichtchenko et al., 1995). Presentation of oligomerized neuroligins clusters neurexins presynaptically and recruits presynaptic proteins suggesting that binding of those two proteins can induce formation of presynaptic terminals (Dean et al., 2003). The presynaptic signalling events, which are induced by neurexins are currently unknown, but vesicles containing active zone proteins arrive within minutes at nascent synapses (Zhai et al., 2001). The induction of synaptic vesicle recruitment might be dependent on the cytoplasmic tail of ß-neurexin via interaction with Ca^{2+}/calmodulin-dependent serine protein kinase (CASK) and Band4.1 (actin-binding protein) (Biederer and Sudhof, 2001). In addition to CASK, Mint (Munc18-interactin protein) also interacts with the cytoplasmic tail of ß-neurexin and these two proteins bind each other and comprise many PDZ domains and could therefore generate large scaffold with additional ß-neurexin binding sites (Butz et al., 1998). Since neurexins and neuroligin-1 are diffusely distributed in young neurons and become enriched at pre- and postsyanptic terminals upon maturation (Butz et al., 1998; Dresbach et al., 2004; Levinson et al., 2005), it is possible that two protein families are not the sole determinants of the axo-dendritic contact site but are rather recruited by other scaffolding proteins. Either way, binding of neuroligins to neurexins can induce recruitment of presynaptic proteins.

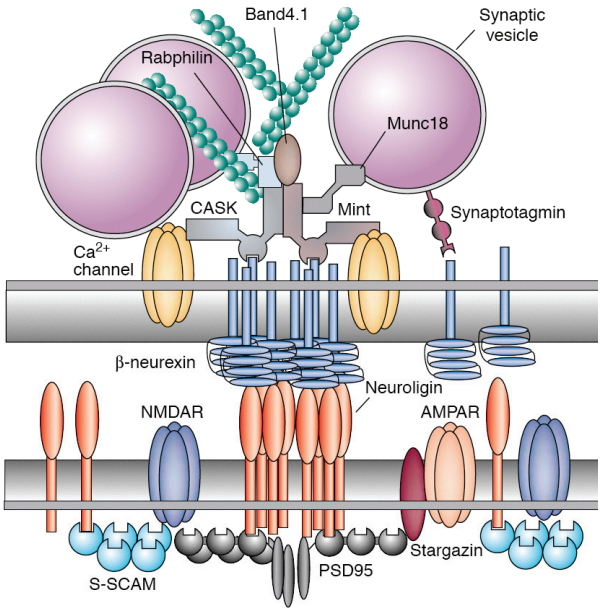

Figure 2. Molecular interactions of postsynaptic neuroligins and presynaptic β-neurexins. Clustered β-neurexin recruits scaffolding proteins via its PDZ binding motif like CASK and Mint. These two proteins bind to each other and could mediate the recruitment of synaptic vesicles through Munc18, the actin binding protein Band4.1 and Rabphilin. CASK also binds to Ca^{2+}-channels and β-neurexin to synaptotagmin. Thus, β-neurexin assembles fundamental components necessary for neurotransmitter release through its PDZ binding motif. From (Dean and Dresbach, 2006).

In summary, it is still not understood how active zone proteins (see also next chapter) are specifically localized to nascent synapses. Secretory vesicles, which contain presynaptic membrane proteins, are synthesized in the soma and are transported along microtubules to the synaptic terminal. These vesicles exhibit differences in size and content. While some vesicles transport synaptic vesicle proteins and calcium channels (Ahmari et al., 2000) other 80 nm large dense-core vesicles contain Piccolo, Bassoon, SNAP-25 and syntaxin (so called PTVs) and are believed to participate in the assembly of active zones as precursor vesicles (Zhai et al., 2001). It has been shown that delivery of Piccolo and Bassoon is dependent on an intact Golgi apparatus, which is consistent with the active zone precursor hypothesis (Dresbach et al., 2006). Similarly, synaptic vesicle proteins are transported in precursor vesicles along microtubules to the nerve terminal. These vesicles are secreted via the constitutive pathway and follow several rounds of exo- and endocytosis during their maturation process to become synaptic vesicles (reviewed in Santos et al., 2009). Taken together, the precise signalling cascades and proteins, which are involved in triggering and targeting the delivery of synaptic vesicle as well as active zone precursor vesicles, is still obscure. An attractive candidate for the delivery of precursor vesicles is the exocyst complex, since it has been associated with site-specific transport of post-Golgi vesicles (see below). Indeed, although the molecular mechanisms were not addressed so far, the exocyst complex has been suggested to mediate the transport of precursor vesicles to nascent synapses. This was inferred from the immunlocalization of exocyst subunits, which preceded the arrival of markers for mature synapses (Hazuka et al., 1999).

1.1.3 Active zone

Fusion of synaptic vesicles is restricted to a specialized area of the presynaptic plasma membrane: the active zone. This area can be recognized in electron micrographs as an electron dense protein network that extents ~50 nm into the cytoplasm and is directly apposed to the postsynaptic density (PSD), where clusters of neurotransmitter receptors, voltage-gated ion channels, scaffold proteins and various second-messenger signaling molecules are concentrated to respond to the release of neurotransmitters which passively diffuse across the synaptic cleft (Figure 3).

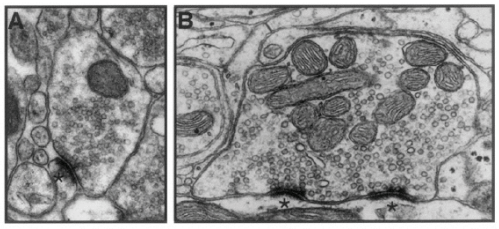

Figure 3. Ultrastructural organization of a presynaptic nerve terminal. (A+B) Two examples of excitatory synapses in vertebrates. The asterisks indicate synapses with electron dense presynaptic active zones opposite to postsynaptic densities. From (Dresbach et al., 2003).

The protein network that constitutes the cytomatrix of the active zone (CAZ) is involved in priming and docking of synaptic vesicles and accounts for use-dependent release of neurotransmitters. While many proteins are present in the active zone, only some protein families are exclusively enriched at the active zone and in contrast to other CAZ proteins are not found in other cell compartments. These families are: Munc13, RIM (Rab3-interacting molecule), ELKS (ERC/CAST) proteins, and Piccolo and Bassoon. Through physical interactions, these proteins form a scaffold at the active zone and play a role in organizing the release and retrieval of synaptic vesicles (Figure 4).

For example, Munc13-1 has been shown to interact via its N-terminal region with RIM1α (Betz et al., 2001) and to be essential for the maturation/priming of synaptic vesicles to acquire a fusion competent state and the generation of the readily releasable pool of synaptic vesicles (Augustin et al., 1999; Varoqueaux et al., 2002). Munc13s are also downstream targets of several signaling cascades and bind directly to diacylglycerol (DAG), β-phorbol esters (β-PE), and calmodulin (Betz et al., 1998; Junge et al., 2004) and therefore seem to be receptors involved in the acute regulation of presynaptic transmitter release.

RIMs form a family of multidomain scaffolding proteins that were initially discovered as putative effectors for the small synaptic-vesicle-binding protein Rab3 (Wang et al., 1997). Binding sites for Rab3 and Munc13 are adjacent but separate, thereby allowing the formation of a tripartite Rab3-RIM-Munc13 complex that would bring synaptic vesicles in close proximity to the priming machinery (Dulubova et al., 2005). RIM1α knockout mice survive to adulthood, and RIM1α-deficient synapses do not exhibit major ultrastructural changes, indicating that RIM1α is not involved in the regulation of synaptic vesicle docking or in the assembly of active zones in mammals (Schoch et al., 2002). In RIM1α-deficient hippocampal CA1 synapses, priming and asynchronous component of release is reduced by 50%, implying that RIM1α functions both during priming and in a post-priming step related to calcium-triggered vesicle fusion (Calakos et al., 2004).

ELKS2 is an insoluble protein that is enriched in the postsynaptic density fraction and is exclusively localized at active zones (Deguchi-Tawarada et al., 2004). In addition to RIM, ELKS bind to Piccolo and Bassoon (Takao-Rikitsu et al., 2004). Expression of ELKS2 deletion mutants in cultured neurons has suggested that ELKS is necessary to localize RIM at the active zone (Ohtsuka et al., 2002). In addition, microinjection of peptides or GST fusion proteins that interfere with ELKS binding to RIM and Bassoon have been shown to diminish synaptic transmission in cultured neurons (Ohtsuka et al., 2002).

Bassoon (tom Dieck et al., 1998) and Piccolo (Cases-Langhoff et al., 1996) are structurally related and are the largest CAZ proteins identified so far (420 and 530 kDa). Both proteins interact with ELKS (Takao-Rikitsu et al., 2004). Expression of a truncated Bassoon protein (180 kDa) in genetically modified mice, which cannot anchor to the CAZ, has been analyzed in various preparations (Altrock et al., 2003; Dick et al., 2003; Dresbach et al., 2003) and suggests that Bassoon is involved in the assembly and functionality of various types of synapses. Several publications about Piccollo have associated this protein with exo- and endocytosis, possibly via an influence on the actin cytoskeleton and interactions with Ca^{2+}-channels (reviewed in Schoch and Gundelfinger, 2006).

Taken together, CAZ proteins are highly enriched at active zones and built a protein scaffold that is important for synaptic vesicle fusion and organization of the active zone. Although the knowledge about interaction sites and regulatory domains of these proteins is constantly growing, a comprehensive overview of how CAZ proteins interact to form the active zone and to organize vesicle traffic and/or fusion is still missing.

1.2 Synaptic transmission

Neurons of the nervous system communicate primarily by releasing neurotransmitters, which bind to adjacent receptors of neighboring cells and cause an ion flux across the plasma membrane thereby passing on information as a change in membrane potential. The following chapter will describe some of the most important proteins, which have been associated with the mechanisms that underlie fusion of synaptic vesicles (SV). Importantly, the release as well as the receptivity of neurotransmitters is not constant for each action potential that arrives at a synapse. Instead, it is dependent on the preceding activity of that synapse, a mechanism, which has been termed synaptic plasticity and is believed to reflect memory and learning processes on a cellular level (Kandel, 2001). The origin of this response behavior is both pre- and postsynaptic in origin and the accounting mechanisms for especially short-term synaptic plasticity will also be described focusing mainly on the presynaptic compartment of glutamatergic synapses.

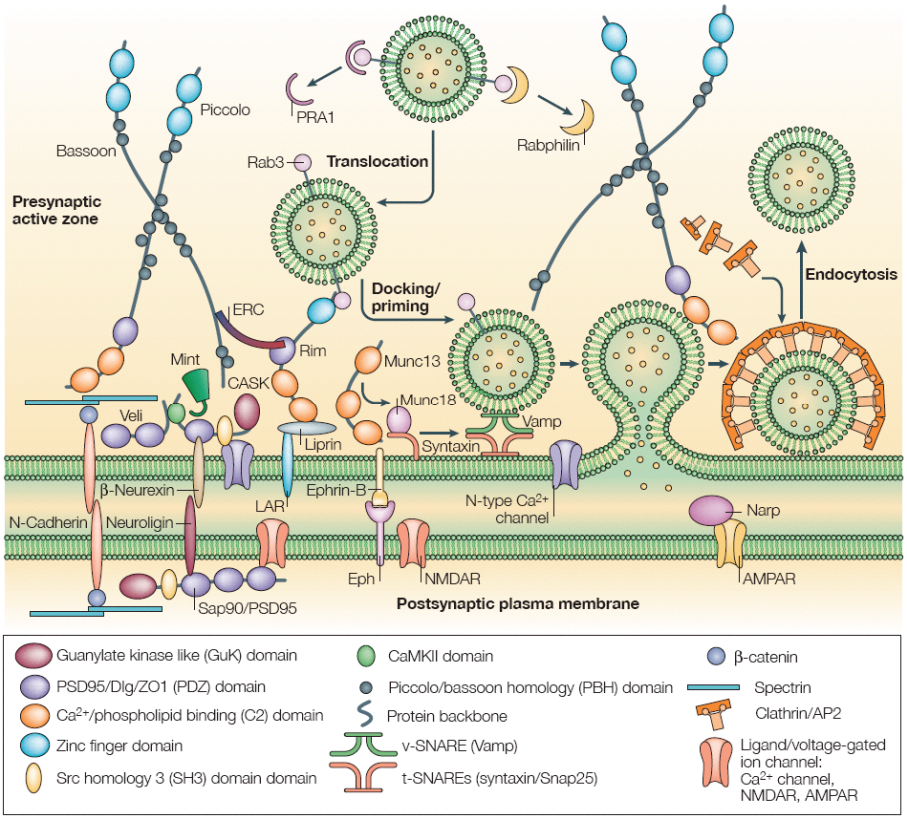

Figure 4. Molecular composition of the active zone. The active zone can roughly be divided into scaffolding molecules and proteins necessary for synaptic vesicle docking and fusion events. Pre- and postsynaptic alignment is ensured by synaptic cell adhesion molecules (CAM) like cadherins, neuroligins and neurexins. Intracellular presynaptic architecture is maintained by scaffolding proteins like bassoon, piccolo, ERC, CASK and Mint. Proteins, which are involved in synaptic vesicles priming and fusion, are RIM, Munc13, Munc18, syntaxin, Vamp, components of the SNARE complex and Ca^{2+}-channels. RIM, Mun13 and Rab3 have been associated with synaptic vesicle docking but no proteins have been identified for translocation of synaptic vesicles to the active zone. From (Ziv and Garner, 2004).

1.2.1 *Evoked release and synaptic vesicle fusion*

Arrival of an action potential at the synaptic terminal is the basic event that triggers evoked release of neurotransmitter (Figure 5). The first step in a chain of events is opening of voltage gated Ca^{2+}-channels due to the membrane depolarization caused by the arrival of an action potential (Llinas et al., 1981). Influx of Ca^{2+}-ions leads to elevated Ca^{2+}-concentrations in microdomains around the Ca^{2+}-channel and to cooperative binding of several Ca^{2+}-ions to its sensor (Schneggenburger and Neher, 2000). Upon elevation of internal Ca^{2+}-concentration synaptic vesicles start to fuse at the active zone in a probabilistic way, which is dependent on the timecourse of internal Ca^{2+}-concentration and the lifetime of the sensor-Ca^{2+} complex, and leads to a jitter in synchronous release that shapes the rising phase of postsynaptic EPSC (Isaacson and Walmsley, 1995). The

most likely calcium sensing protein is synaptotagmin, which enables synchronous release and inhibits Ca^{2+}-independent asynchronous or spontaneous release via different Ca^{2+}-binding domains (Geppert et al., 1994; Nishiki and Augustine, 2004). Synaptotagmin resides in synaptic vesicles and synaptic vesicles reside in a fusion competent state (primed) at the plasma membrane via the SNARE(soluble N-ethylmaleimide-sensitive fusion protein attachment protein receptor)-complex (reviewed in Rizo and Rosenmund, 2008). Upon Ca^{2+}-binding synaptotagmin is supposed to displace complexin from the SNARE-complex, which clamps the fusion machinery to allow for immediate and fast fusion of synaptic vesicles upon Ca^{2+}-entry into the nerve terminal (Tang et al., 2006). Synaptic vesicles can release their content either by full-fusion, i.e. a collapse into the presynaptic membrane, or by a process called kiss-and-run, where opening of a fusion pore is followed by subsequent closure without fusion of membranes (reviewed in Harata et al., 2006). Neurotransmitters released through the fusion pore diffuse passively across the synaptic cleft and are then bound by postsynaptic receptors, which results in ion flux across the membrane and finally transduction of the chemical signal from the presynaptic cell into a membrane polarization of the postsynaptic cell.

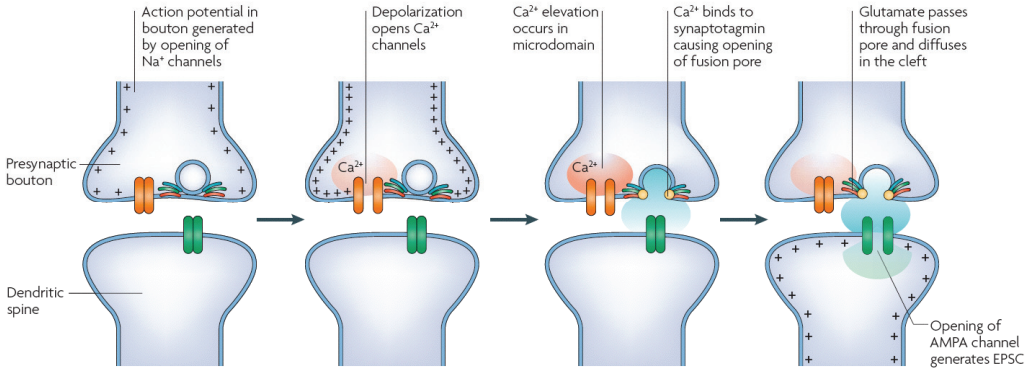

Figure 5. Representation of the sequence of events responsible for chemical synaptic transmission. From (Lisman et al., 2007).

1.2.2 Spontaneous release

Apart form evoked release via arrival of an action potential at the nerve terminal neurotransmitters are also released spontaneously. Despite the frequent usage of these spontaneous events to analyse changes in pre- or postsynaptic parameters the current understanding of the underlying mechanisms is rather limited. From a theoretical point of view it is imaginable that spontaneous events influence synaptic transmission by creating baseline levels of neurotransmitter in the cleft, which will also influence subsequent evoked synaptic transmission and therefore would be a substantial contribution to

information processing. There are also indications that spontaneous events stabilize neuronal circuits and can even lead to postsynaptic action potential firing (Carter and Regehr, 2002; McKinney et al., 1999). It is generally assumed that spontaneous release happens at the active zone, but there are indications for ectopic spontaneous release sites away from the active zone (Colmeus et al., 1982). In addition, the origin of spontaneously released synaptic vesicles is under debate. While Sara and colleagues showed that vesicles from the readily releasable pool (RRP, see also next chapter) have limited crosstalk with spontaneously released SV (Sara et al., 2005) another study claimed that they both originate from the same RRP (Groemer and Klingauf, 2007). In the first case this would imply that a different pool of SV and different molecular machinery mediates spontaneous release whereas in the second case spontaneous fusion would rather be a probabilistic event. Genetic deletions of SNARE proteins show that both evoked and spontaneous release are impaired but to a different extent (reviewed in Wasser and Kavalali, 2009), which could argue for the existence of a different fusion complex in spontaneous release. As mentioned earlier, deletion of synaptotagmin abolishes Ca^{2+}-dependent fusion but augments spontaneous release by an unknown mechanism (Geppert et al., 1994). Similarly, deletion of complexin inhibits Ca^{2+}-dependent fusion but Ca^{2+}-independent fusion persists (Reim et al., 2001). Additionally, deletion of SNARE proteins like VAMP or Munc18 abolishes both forms of synaptic vesicle fusion, which together with the observed synaptotagmin and complexin phenotypes is inconsistent with the idea of one single release machinery for both fusion events (Schoch et al., 2001; Verhage et al., 2000). In summary, further evidence will be necessary to dissect the molecular mechanism, which are shared by the two different fusion events, and to identify whether synaptic vesicles are destined for one or the other fusion or whether SV are able to undergo both pathways.

1.2.3 Synaptic vesicle pools and cycling

The presynaptic terminal is filled with synaptic vesicles of which some are close to the active zone and others reside in the cytoplasm. During synaptic transmission synaptic vesicles fuse with the plasma membrane and are retrieved afterwards via endocytosis. The endocytosed vesicles are refilled with neurotransmitters before they are either transported back to the active zone or are stored in the cytoplasm. Each synaptic vesicle can be assigned to one of three vesicle pools: the readily releasable pool (RRP), the recycling pool and the reserve pool (Rizzoli and Betz, 2005) (Figure 6). The readily releasable pool describes SV, which are located in a fusion competent state (primed) at the active zone. Upon Ca^{2+}-influx these vesicles fuse immediately and release their content into the synaptic cleft. During ongoing physiological synaptic activity the RRP is

depleted and becomes refilled with vesicles from the recycling pool. This is accompanied by a decrease of neurotransmitter release since transport and priming of SV to the active zone now becomes rate limiting for SV fusion. Upon intense stimulation a second decrease in neurotransmitter release occurs, which is attributed to a depletion of the recycling pool and the slow mobilization of SV from the reserve pool. It should be mentioned that this pool might never or rarely be used under physiological stimulus conditions. For example in the calyx of Held high extracellular potassium application is necessary to mobilize vesicles from the reserve pool (de Lange et al., 2003). Those SV that are immobilized in the cytoplasm are believed to be encircled by an actin scaffold (Sankaranarayanan et al., 2003) wherein synapsins are supposed to act as the glue between vesicles (Hilfiker et al., 1999). Until today, it is not understood how vesicles manoeuvre in the presynaptic compartment. Principally, either passive diffusion or active transport could be possible, but no candidate proteins have been elucidated yet. Apart from the unresolved translocation of SV to the active zone, transport of synaptic vesicles to the RRP is classically divided into docking and priming of SV. Several proteins have been identified in these processes of which the most notable ones will be introduced in the following along with the molecular mechanisms that have been elucidated.

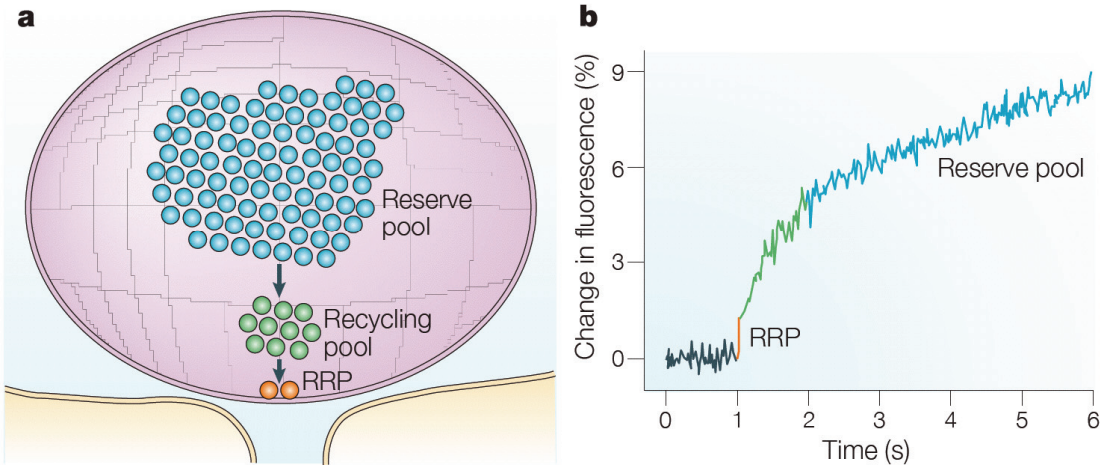

Figure 6. Each synaptic vesicle can be assigned to one out of three vesicle pools. (a) The reserve pool is the largest depot for SV and is employed only after intense stimulation. The recycling pool comprises 10-15% of total SV, whereas only 1% of SV is primed at the active zone and resides in the readily releasable pool (RRP). **(b)** The three pools are differentiated due to their different release kinetics. Note that the spatial orientation of synaptic vesicle pools in real synapses is not as clearly separated. From (Rizzoli and Betz, 2005).

Which proteins are responsible for docking of SV is one of the most unresolved questions in vertebrate synapses. It is tempting to believe that the specificity in SV transport to active zones is directly mediated by active zone resident proteins and thereby

only restricted to this region, although this scenario still leaves the question open of how active zone resident proteins are specifically transported to the active zone in the first place (see above). However, RIM is the only known CAZ protein, which has been identified to interact with a synaptic vesicle associated protein, the GTPase Rab3, and therefore seems a fair candidate to be part in directing SV to the active zone. Indeed, RIM, Rab3 and Munc13 can form a tripartite complex, which was suggested to tether docked vesicles at the active zone to make them available for the priming machinery (Dulubova et al., 2005) (Figure 7). On the other hand neither deletion of Munc13, Rab3 nor RIM abolishes docking of SV in vertebrate synapses as visualized by ultrastructural analysis suggesting that the tripartite complex may rather assist in handing over already docked SV to the priming machinery (Schluter et al., 2004; Schoch et al., 2002; Varoqueaux et al., 2002).

Priming of SV involves the SNARE proteins synaptobrevin (VAMP) on the vesicle side and syntaxin-1 and SNAP-25 on the plasma membrane side (Figure 7). It was shown that Munc18-1 can bind to the closed conformation of syntaxin-1 but this binding hinders SNARE complex assembly, which is contradictory to the total loss of neurotransmitter release seen in Munc18-1 knockout animals (Dulubova et al., 1999; Verhage et al., 2000). On the other side a positive regulatory function for Munc18-1 in SNARE complex assembly has also been suggested since Munc18-1 facilitates complex assembly between synaptobrevin and syntaxin-1-SNAP25 heterodimers (Shen et al., 2007). Thus, Munc18-1 seems to have a negative and a positive influence on SNARE complex assembly. The total loss of synaptic transmission observed in Munc13 knockout mice argues for a crucial contribution of this protein in SV fusion (Varoqueaux et al., 2002). This phenotype can be rescued by either expression of the MUN domain of Munc13 (Basu et al., 2005), which cannot bind to isolated syntaxin-1 but to membrane anchored SNARE complexes (Guan et al., 2008), or by expression of a constitutively open syntaxin-1 mutant (Richmond et al., 2001). Therefore it was suggested that Munc13 promotes SNARE complex assembly by opening syntaxin-1 maybe indirectly in concert with Munc18-1. The finding that expression of the constitutive open form of syntaxin-1 can also rescue the defects observed in RIM deficient animals promoted the hypothesis that RIM acts after vesicle docking via a similar mechanism as Munc13 in priming of synaptic vesicles (Koushika et al., 2001).

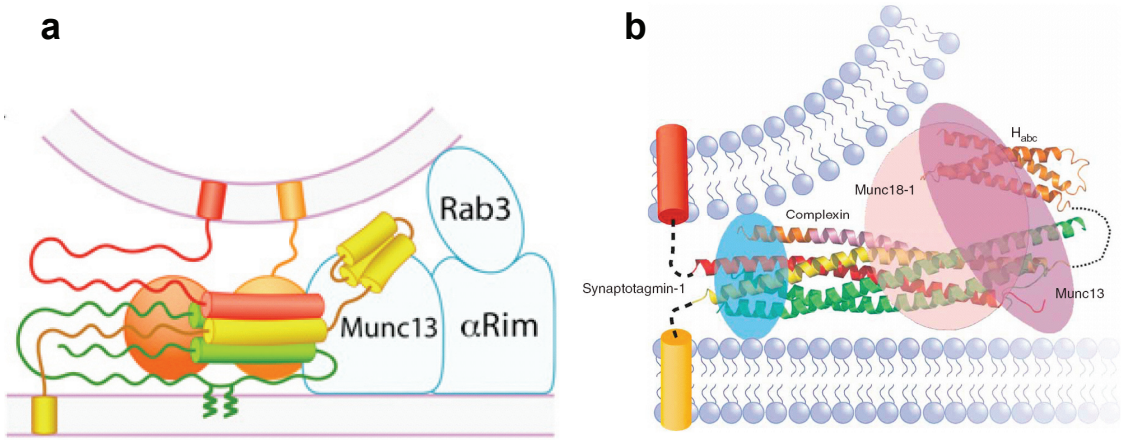

Figure 7. Diagram of the SNARE complex and interacting molecules. (a) Docking of synaptic vesicles might be dependent on the tripartite complex consisting of the synaptic vesicle associated protein Rab3, RIM and Munc13. From (Wojcik and Brose, 2007). **(b)** Munc18-1, Munc13, complexin and synaptotagmin bind to the SNARE complex Only interaction of complexin and the SNARE complex have been resolved at atomic resolution. Where the other illustrated proteins bind is unknown and whether they bind competitively, exclusively or in a compatible way is crucial for understanding molecular mechanisms of synaptic vesicle fusion. From (Rizo and Rosenmund, 2008).

Although the before mentioned studies gave rise to several models of how synaptic vesicles are docked and primed at the active zone these models are likely but undemonstrated and in many cases highly speculative. Ongoing research will be necessary to unify obtained results into a model of neurotransmitter release and to identify potentially remaining players. Especially SV transport and docking mechanisms to the active zone remain unclear. The exocyst, a tethering complex involved in site-specific transport of vesicles, was hypothesized to contribute to translocation events of SVs (Ting et al., 1995). This hypothesis was strengthened by the finding that Sec8, a subunit of the complex, is found on synaptic vesicles and that Sec15, another subunit of the exocyst, binds to the synaptic vesicle resident GTPase Rab3 in drosophila (Wu et al., 2005). However, a direct proof for an involvement of the exocyst complex in mammalian synaptic transmission was never presented. Hence, electrophysiological recordings, which directly address the mechanisms underlying synaptic vesicle fusion, represent a suited approach to reveal the contribution of the exocyst complex to these processes.

1.2.4 Synaptic plasticity

In general, synaptic plasticity comprises any mechanism that is involved in the use-dependent modulation of synaptic transmission. Two forms of synaptic plasticity have been categorized depending on the time scale the modulation lasts: short-term synaptic plasticity describes effects that last for most a few minutes, while long-term synaptic plasticity summarizes mechanisms that tune synaptic responses over longer time periods.

Furthermore, synaptic plasticity can be divided into mechanisms, which decrease synaptic strength, i.e. depression, and those, which increase synaptic transmission, i.e. enhancement. These two forms of synaptic plasticity do not happen exclusively but can contribute to synaptic transmission at the same time and thus the observed signal transduction can exist as a sum of those two modulations. Here, only mechanism of short-term synaptic plasticity will be presented.

Besides the waveform of the arriving action potential, the Ca^{2+}-signal, i.e. intracellular Ca^{2+}-concentration ($[Ca^{2+}]_i$), is the first element that defines synaptic strength. For example if two action potentials arrive at the nerve terminal with a short time delay neurotransmitter release can increase for the second stimulus. The cause for this form of short-term enhancement (STE) called short-term facilitation is believed to be residual calcium from the first action potential that has not been cleared from the nerve terminal (Katz and Miledi, 1968). Per definition facilitation occurs within hundreds of milliseconds, whereas another form of STE, post-tetanic potentiation (PTP), sets in and decays within seconds to minutes. PTP is observed if the number of stimuli in a train is increased and is also dependent on internal Ca^{2+}-concentration, but it seems that the two forms of STE have different Ca^{2+}-receptors which both are different from the SV release machinery. Indeed, PTP seems to multiply the effects of facilitation (Landau et al., 1973; Magleby and Zengel, 1982) and facilitation in turn multiplies with release of neurotransmitter (Bain and Quastel, 1992). The multiple site hypotheses proposes that distinct Ca^{2+}-binding sites reflect the different kinetics observed for the different forms of STE, but no consensus has been reached regarding the properties of these Ca^{2+}-receptors (reviewed in Zucker and Regehr, 2002).

In many synapses the most predominant cause of synaptic short-term depression (STD) upon repetitive stimulation with high (relative to physiological) frequencies is depletion of the readily releasable vesicles. The simplest model emanates from a store S of synaptic vesicles from which a fraction F is released upon action potential arrival. Replenishment of SV to the store during short-term depression is usually assumed to follow a mono exponential function (Betz, 1970). Introducing several SV pools with parameters that describe mobilization of SV inside vesicle pools can further expand this model. Also the fraction F of SV that is released might not be constant but rather be dependent on the individual release sites inside the store S (Murthy et al., 1997). There are also indications that $[Ca^{2+}]_i$ has an accelerating influence on recovery from depression (Sakaba and Neher, 2001) or that increased $[Ca^{2+}]_i$ facilitates the release of reluctantly releasable vesicles thereby making them available during ongoing synaptic activity (Wu and Borst, 1999). Hence, models describing STD due to depletion of RRP vesicles can become quite complex depending on the integrated parameters and are going to be

extended even more with increasing knowledge about the proteins and mechanisms involved.

STD can also originate from desensitization of post-synaptic receptors, which after ligand binding remain in a desensitized conformation that decouples agonist binding from channel opening and thus reduces synaptic efficacy (Armstrong et al., 2006). A third form of STD can arise by feedback activation of presynaptic receptors, which presumably reduce Ca^{2+}-currents and thereby decrease the extent of SV fusion (von Gersdorff et al., 1997).

In summary, although STD has several underlying mechanism replenishment of SV to the AZ is the most predominant cause for this form of information processing. Hence, electrophysiological recordings addressing STD are considered a sensitive approach to identify the mechanisms, which govern transport and docking steps of SV, and to elucidate the functional contribution of the exocyst complex.

1.3 The exocyst complex

1.3.1 Discovery

The transport of vesicles to specific sites of the plasma membrane is essential for membrane growth and polarization of cells. Screening of yeast mutants led to the discovery of genes, whose products are involved in post-translational events of the secretory pathway (Novick et al., 1980). Eight of theses proteins were found to form a multiprotein complex in yeast and mammals, which is referred to as the exocyst and the sec6/8 complex, respectively (Hsu et al., 1996; TerBush et al., 1996; TerBush and Novick, 1995; Ting et al., 1995). The identification of all eight subunits (Sec3, Sec5, Sec6, Sec8, Sec10, Sec15, Exo70, Exo84) and sequence analyses of the underlying genes showed that the sequences from yeast and rat are homologous and that they share 17 – 24 % amino acid sequence identity (Guo et al., 1999a; Kee et al., 1997; Matern et al., 2001). Despite the similarities of the gene sequences the subunits of the exocyst and the sec6/8 complex seem to exhibit slightly different interaction patterns. In yeast, a model for the mechanistic function suggests that the Sec3 subunit serves as a spatial landmark at the plasma membrane for the remaining exocyst subunits (Finger et al., 1998) (Figure 8 and Figure 9 A). Sec15 is an effector for Rab4 in its GTP bound form and binds to Sec10 which then leads to the sequestration of the remaining subunits and to a translocation of the complex to Sec3 on the plasma membrane thereby tethering vesicles to their target membrane (Guo et al., 1999b). By this model exocyst function precedes the assembly of the SNARE-complex and being an effector of Rab GTPases offers a model of how polarized exocytosis is regulated in yeast cells.

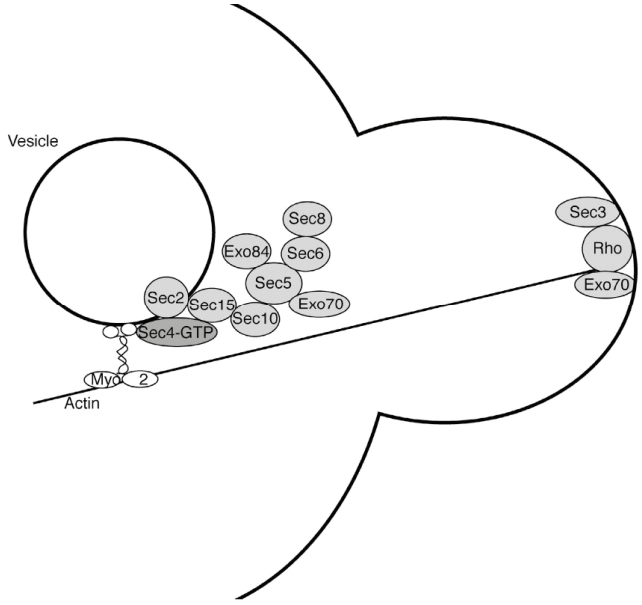

Figure 8. Exocyst mediated vesicle tethering in yeast. Sec3 and Exo70 represent the landmark for the remaining exocyst subunits, which are sequestered after binding of Sec4 to Sec15. Once the vesicle has arrived at the bud tip whole complex formation is completed. From (Boyd et al., 2004).

Homologues of all eight subunits were described in mammalian cells and the whole complex was found to have a combined molecular mass of 734 kDa (Hsu et al., 1996; Kee et al., 1997; Ting et al., 1995). In mammals the exocyst complex, also termed Sec6/Sec8 complex, seems not only to be a tethering factor but appears to be linked to many aspects of the whole secretory pathway and may even be involved in endocytic events. Indeed, its eight subunits, which are not always found together in one complex, make exocyst an attractive candidate for regulating and linking different routes of the cell's membrane trafficking machinery. Because exocyst function has been investigated in many different cell types and organisms, and each study focused only on some of the eight subunits, a diverse picture of what exocyst does and where it is involved developed. Especially the interpretation of localization studies turned out to be restricted due to epitope masking in conjunction with complex assembly and subunit localization. Another characteristic of exocyst research is that publications, which focus "only" on up to four subunits, cannot offer a mechanistic model of how exocyst subunits and its binding partners interact, but are rather bound to assumptions regarding the action of the remaining subunits. Thus, a patchwork of findings emerged, which until now did not lead to a clear understanding of exocyst function in mammals.

The following literature summary will concentrate on work done in the mammalian system, i.e. permanent cell culture, primary cultures and tissue. No *in vivo* study has ever been performed for exocyst in mammals as null mutations display deadly phenotypes already during gastrulation (Friedrich et al., 1997). The involvement of exocyst will be discussed starting from the beginning of the secretory pathway, the endoplasmatic

reticulum (ER), and proceed towards Golgi and post-Golgi trafficking. Finally, the state of the art of exocyst function in neuronal systems will be presented.

1.3.2 Endoplasmatic reticulum

The first subunit of the exocyst complex, which is found along the secretory pathway, is Sec10 in the endoplasmatic reticulum (ER). Sec10 coimmunoprecipitates with Sec61β, a subunit of the heterotrimer Sec61, that forms the main subunit of the endoplasmic reticulum translocon. A very small portion (~4%) of Sec6 and Sec8 also coimmunoprecipitate with Sec61β and overexpression of Sec10 increases this association indicating complex formation. In addition, overexpression of Sec10 results in increased protein synthesis of basolateral proteins on a post-transcriptional level but does not increase synthesis or delivery of an apical protein in MDCK cells (Lipschutz et al., 2003). Thus, the interaction between Sec10 and Sec61β illustrates a link between cellular membrane traffic and protein synthesis machinery. Immunoprecipitation and localization studies could show, that Sec8 coimmunoprecipitates the ER resident 1,4,5-trisphosphate receptors (IP_3R1) from brain microsomal extracts (Shin et al., 2000) and that Sec8 colocalizes with the NR2B subunit of the NMDAR receptor in the ER. The interaction of Sec8 and NR2B is mediated by SAP102 (synapse-associated protein) and this interaction is dependent on the C-terminal PDZ-binding motif of both Sec8 and NR2B (Sans et al., 2003).

1.3.3 Golgi apparatus

So far no interaction of an exocyst subunit with a Golgi-resident protein was published. Localization studies could show that Sec8 is partially overlapping with Golgi markers but disruption of the Golgi network with brefeldinA treatment does not disrupt Sec8 localization. In addition, immunoprecipitation of Sec8 does not coimmunoprecipitate Golgi-resident proteins like βCOP, Golgi 58K protein or mannosidase II from pancreatic acinar cells (Shin et al., 2000). Similarly, localization studies with Golgi markers like GM130 could show a partial overlap with Exo70 but brefeldinA does not alter the staining pattern of the exocyst subunit in PC12 cells. In contrast, the microtubule destabilizing drug nocodazole disrupts the vesicular structures, which is indicative that the subunit positive structures are associated with microtubules and reside near or at the MTOC (microtubule organizing centre) (Vega and Hsu, 2001). Cell fractionation shows that Sec6, Sec8 and Exo70 are associated with a subcompartment of the TGN (trans Golgi network) that is accessible to exocytic cargo (tsVSVG) but distinct from regions containing TGN proteins (VAMP4, furin) in normal rat kidney (NRK) cells (Yeaman et al., 2001). In agreement to the before mentioned findings, Sec10 shows a partial overlap with GM130 and immuno EM (electron

microscopy) studies localize Sec10 to tubulo-vesicular structures close to Golgi cisternae (Prigent et al., 2003). Sec15 and Exo84 are also found in a perinuclear compartment in PC12 cells and are relocated to the growth cone upon differentiation with NGF (Wang and Hsu, 2003). Overexpression of GFP-Sec15 shows a perinuclear distribution pattern, which is disrupted upon nocodazole treatment of COS-7 cells. The dot-like structures remain upon nocodazole treatment which indicates a non-direct interaction of GFP-Sec15 with microtubules (Zhang et al., 2004). Taken together, exocyst subunits Sec6, Sec8, Sec10, Sec15, Exo70 and Exo84 seem to reside in a late TGN compartment and are directly or indirectly associated with microtubules.

1.3.4 Cytoskeleton

1.3.4.1 Septins

Immunoprecipitation of Sec8 pulls down four members of septins indicating an interaction with these filaments (Hsu et al., 1998). This finding was further confirmed by colocalization and coimmunoprecipitation studies between Exo70 and Nedd5 (septin) at a perinuclear compartment in undifferentiated PC12 cells (Vega and Hsu, 2003).

1.3.4.2 Actin

Actin filaments mediate the interaction between Sec8 and Ca^{2+} signalling complexes and latrunculin B treatment redistributes a fraction of Sec6 and Sec8 from the plasma membrane to the cytoplasm (Shin et al., 2000). In contrast, the perinuclear enrichment of Exo70 is not altered if cells are treated with actin destabilizing drugs but membrane pools of exocyst subunits were not monitored in this study (Vega and Hsu, 2001). These findings suggest that the interplay between actin and exocyst does not take place at a perinuclear compartment but rather near or at the plasma membrane. A report from Sugihara et al. showed that the N-terminal region of RalA, a GTPase involved in cell growth, differentiation, organization of the actin cytoskeletal and membrane trafficking, binds to the N-terminal fragment of Sec5. Induction of filopodia formation by the inflammatory cytokine interleukin-1 but not TNFα was blocked if the association of RalA and Sec5 was impaired or antibodies against Sec5 were introduced into Swiss 3T3 cells. The authors proposed a signalling pathway where cytokines activate Cdc42, which in turn activates RalA and that binding of RalA·GTP to Sec5 is necessary for filopodia formation (Sugihara et al., 2002). In a similar study Zuo et al. found that Exo70 (aa 404-653) binds to Arpc1A and to its isoform Arpc1B, which are subunits of the Arp2/3 complex, and this binding sequesters Sec8. The Arp2/3 complex is the core machinery that nucleates actin for the generation of the filamentous actin network. SiRNA against Exo70 inhibits cell migration, disturbs directed movement, impairs filopodia formation

and alters Arp2 distribution. In agreement with previous findings they placed Exo70 downstream of Cdc42 and Rac1 (Zuo et al., 2006). Thus, subunits of the exocyst are part of the signalling cascade for actin cytoskeleton remodelling.

1.3.4.3 Microtubules

It was discussed earlier, that exocyst subunits reside in structures, which are directly or indirectly coupled to microtubules. Colocalization studies could confirm these findings and also revealed that exocyst subunits seem to play a role in microtubule dynamics. Sec8, Exo70 and Exo84 colocalize with microtubules, but only Exo70 is able to inhibit tubulin polymerisation by 80% *in vitro*. Overexpression of GFP-Exo70 but not GFP-Exo84 induces membrane protrusion, which can be compensated for with taxol, a microtubule stabilizing drug (Wang et al., 2004b). Coimmunoprecipitation, fractionation, colocalization and downregulation studies suggested that centriolin, a protein present at the midbody ring and required for abscission, interacts with Sec3, Sec5, Sec8, Sec15, Exo70 and Exo84 in HeLa cells and enables exocyst subunits to be present at the midbody ring. Cytokinesis is delayed and abscission impaired if cells are treated with siRNA against Sec5, Sec8 or Sec15 and secretory vesicles are accumulated around the midbody ring in cells treated with siRNA against Sec5 (Gromley et al., 2005). Apart from its action at the midbody, exocyst is also present at the centrosome, where it colocalizes with pericentrin. During mitosis Sec8, Exo70 and Sec5 are present at the mitotic apparatus and overexpressed Sec5 and Sec8 are present at the abscission site. Sec8 and Exo70 are found in midbody preparations but Sec10 is not. Sec8 or RalA knockdown by siRNA leads to bi-nucleated cells and to the formation of syncytia by intracellular bridges indicating failures in cytokinesis (Chen et al., 2006). Again, how exocyst interacts with these microtubular structures is unknown and whether there is a direct or indirect interaction is still not clear. The tubulin destabilizing effect of Exo70 argues for a direct interaction with microtubules, whereas on the other hand centriolin is necessary for exocyst binding to the midbody ring. The accumulation of vesicles at the midbody ring suggests defects in membrane fusion, maybe due to exocyst proposed function as a tethering complex.

1.3.5 Polarized secretion and complex assembly

There are several publications which argue that exocyst is recruited from the cytosol to cell-cell contact sites upon initiation of calcium-dependent cell-cell adhesion in MDCK cells (Figure 9 B). In polarized MDCK cells the distribution of the complex is restricted to the apical-junctional complex on the lateral membrane domain and Sec8 is associated with a large, cadherin-containing protein complex (Grindstaff et al., 1998; Yeaman et al., 2004). Antibodies against Sec8 specifically inhibit the transport of

proteins to the basolateral membrane but not to the apical membrane (Grindstaff et al., 1998). Similarly, overexpression of Sec10 results in increased protein synthesis of basolateral proteins on a post-transcriptional level but does not increase synthesis or delivery of apical proteins (Lipschutz et al., 2003). The transport of basolateral proteins to their destination via exocyst seems to be regulated by RalA, because overexpression of the Ral-binding-domain of Sec5 leads to mislocalization of basolateral proteins to also the apical membrane. Downregulation of RalA by siRNA decreases the assembly or stability of Sec6 to Sec10 indicating that RalA facilitates the assembly of exocyst subunits (Moskalenko et al., 2002). Thus in MDCK cells the exocyst seems to be necessary for trafficking basolateral membrane proteins to the apical junction and this process is regulated by RalA. Protein synthesis of apical and basolateral secretory proteins might also be regulated by the exocyst complex.

A series of studies have connected the insulin signalling pathway to the exocyst complex. Exo70 binds to the G-protein TC10 and activation of TC10 via insulin stimulation translocates Exo70 to the plasma membrane in 3T3-L1 adipocytes. Sec6, Sec8 appear to exist in a preformed complex with Exo70 and overexpression of an N-terminal fragment of Exo70 (aa 1-384) inhibits glucose uptake but transport of the glucose transporter Glut4 to the plasma membrane persists indicating a defect in plasma membrane fusion events (Inoue et al., 2003). The same authors could show in a consecutive study, that Glut4, Sec8 and Exo70 are competitively displaced from lipid rafts upon overexpression of the N-terminal fragment of Exo70. In addition, knockdown of Sec6, Sec8 or Exo70 with siRNA reduces glucose uptake upon insulin stimulation in 3T3-L1 adipocytes without effecting proliferation, cell shape or protein expression. Exo70 and Sec8 translocate to lipid rafts upon activation of TC10 via insulin stimulation, whereas RNAi against Exo70 decreases protein levels of Glut4 and Sec8 in lipid rafts. SAP97 (synapse-associated-protein) binds to the PDZ-binding motif of Sec8 and knockdown of this protein prevents Sec8, Exo70 and Glut4 from being present in lipid rafts upon insulin stimulation, but no general secretion defects were observed (Inoue et al., 2006). Thus, TC10 and SAP97 regulate the trafficking of exocyst and its designated cargo Glut4 to lipid rafts through Exo70 and Sec8, respectively. A specific involvement of the exocyst in insulin stimulated glucose transport was found by overexpression of Sec6 or Sec8 in 3T3-L1 adipocytes, which upon insulin stimulation leads to relocation of these subunits to the plasma membrane and to an elevation of glucose transport but not to an increase in general secretion (Ewart et al., 2005). Similarly, overexpression of deletion constructs of Sec8 (Δ1-339aa) or Sec10 (Δ536-709aa) diminishes the number of docked insulin vesicles at the plasma membrane without reducing the overall insulin vesicle content in pancreatic β cells suggesting that exocyst subunits are responsible for the

supply of vesicles from a reserve to a readily releasable pool (Tsuboi et al., 2005). Initiation of Glut4 trafficking is supposed to be mediated by RalA, which is activated after insulin stimulation and initiates transport of Glut4 containing vesicles via interaction with Sec5 and the molecular motor protein Myo1c (Chen et al., 2007). Another study showed that insulin also stimulates phosphorylation of Sec8 in 3T3-L1 adipocytes but this process was not found to be sufficient for surface expression of Glut4 (Lyons et al., 2008). However, overexpression of the N-terminal fragment of Exo70 (aa 1-384) in adult primary adipocytes does not ablate Glut4 insertion to the membrane, but instead induces tethering of Glut4 containing vesicles (Lizunov et al., 2009). The contradictory results obtained in these studies were explained by the unique architecture of adult adipocytes highlighting potential differences in exocyst function between closely related cell systems and pointing out that we are just beginning to understand the molecular mechanisms which govern exocyst mediated exocytosis.

Apart from Sec5 also Exo84 binds to RalA·GTP through a predicted PH domain (aa 122-333) and this PH domain also binds to phospholipids with a preference for phosphatidylinositol 3,4,5-trisphosphate ($PI(3,4,5)P_3$) suggesting a regulatory mechanism of protein/lipid interaction via a GTPase. Sec5 and Exo84 also bind to each other and this interaction seems to regulate complex assembly. Distinct distribution of Exo84, Sec10 and Sec5, Sec6 to cytosol and plasma membrane, respectively, argues for the existence of subcomplexes in the cell. Consistent with this idea siRNA against Exo84 decreases the complex formation between Sec6 and Sec10 (Moskalenko et al., 2003). RalB but not RalA is required for cell migration in NRK cells. In a scratch assay siRNA against RalB, Sec5, Sec8 or Sec10 but not against RLIP76/RalBP1 (a Rac/CDC42 Gap and effector of RalA) slows migration of cells and wounding of the cell layer activates RalB and RalB·Sec5 complex formation. Levels of Sec5/Sec8 complex stay the same but Sec8/Sec10 complex forms after wounding indicating complex assembly. Sec6, Sec10 and Exo70 are found on the cell-cell contact free forefront of cells and this localization is inhibited by depletion of RalB or Sec5 (Rosse et al., 2006). Taken together, the exocyst is an effector for RalA and RalB and binding of Sec5 or Exo84 to the activated form of these GTPases induces complex assembly.

In yeast, Sec3 resides at the plasma membrane and is thought to represent a landmark for the remaining exocyst subunits thereby directing the exocyst at sites of vesicle fusion. Recruitment of Sec3 to the plasma membrane in turn is dependent on the Rho1 GTPase (Finger et al., 1998; Guo et al., 2001). In mammals however, Sec3 lacks the Rho1 binding site reported in yeast and its GFP-fusion protein is cytosolic. Indeed all N- and C-terminal fusion proteins of Sec3, -5, -8 and -10 as well as a C-terminal Sec15-GFP fusion protein show a cytosolic distribution in MDCK cells. The only exocyst subunit, which

localizes to the plasma membrane, is GFP-Exo70 and demonstrates a function in establishing and maintaining cell-cell contacts. (Matern et al., 2001). Plasma membrane localization of Exo70 is mediated by C-terminal amino acids K632 and K635, which bind to phosphatidylinositol 4,5-bisphosphate ($PI(4,5)P_2$). Upon mutation of these amino acids Exo70 does not localize to the plasma membrane and recruitment of other exocyst subunits is also impeded. Additionally, these amino acids are crucial for docking and fusion of post-Golgi secretory vesicles, but not for their transport to the plasma membrane. These results suggest that Exo70 serves as a landmark for the remaining exocyst subunits by interaction with $PI(4,5)P_2$ and that this interaction is crucial for exocyst mediated secretion of proteins (Liu et al., 2007). Exo70 interacts via an N-terminal coil-coil domain (aa 1-99) with Snapin, which was originally identified as a SNAP-25 interacting protein, and competes with SNAP-23 for Snapin binding. This interaction was suggested to mediate crosstalk between the exocyst and the SNARE complex (Bao et al., 2008).

In summary, the exocyst is an effector of GTPases and activation of their signalling cascades triggers assembly of subunits and leads to transport of cargo to specific areas of the plasma membrane. There are indications for subcomplexes in the cell but a complete scheme of how all the subunits are assembled has not been established yet. Actually it is not clear whether certain subcomplexes may exert a function on their own without the need for entire complex assembly. Based on the present studies Exo70 is the most likely candidate to serve as a spatial landmark for the remaining exocyst subunits at the plasma membrane and localization of Exo70 to the plasma membrane is necessary to recruit other exocyst subunits.

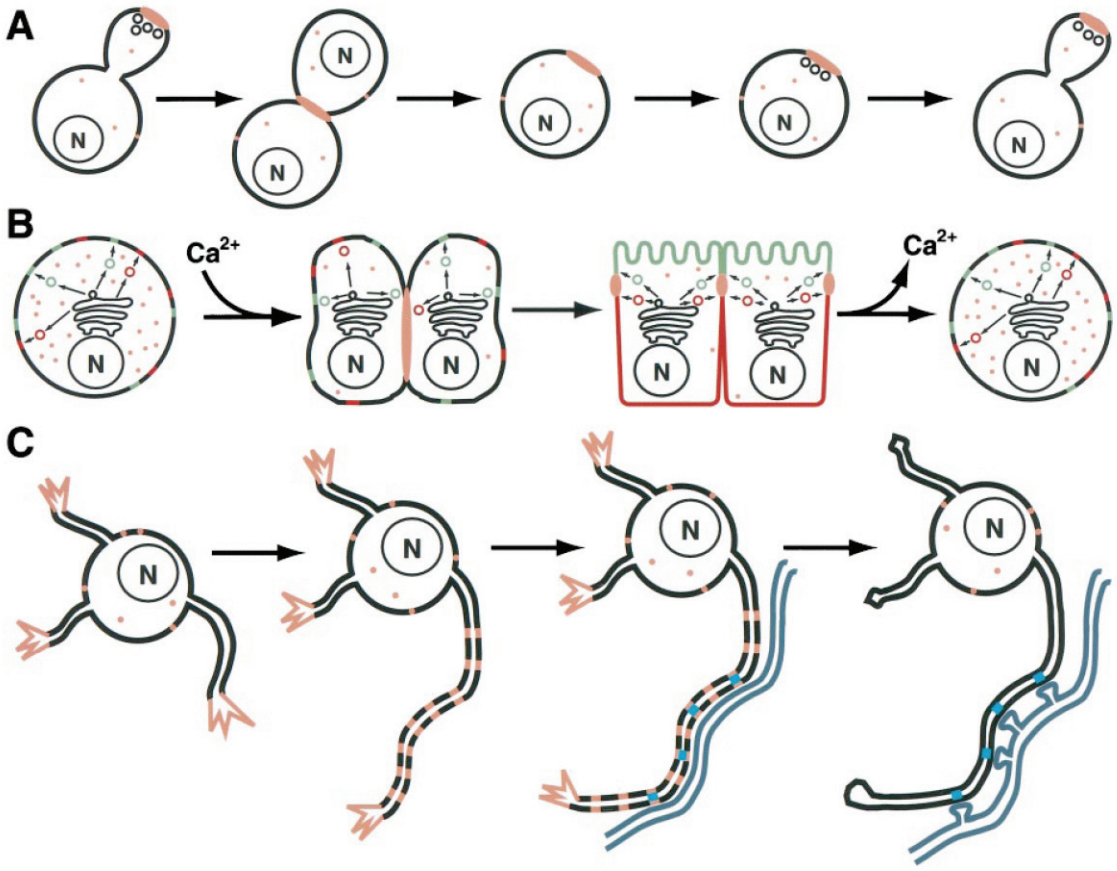

Figure 9. Polarized vesicle trafficking by the exocyst complex (peach). (A) In yeast, the exocyst is present at sites of membrane addition like the bud tip, sites of cytokinesis in dividing cells and remains at the bud scar, which designates future exocytosis sites for bud formation. Note the presence of also a cytosolic pool. **(B)** In MCDK cells, vesicles (red and green) are targeted randomly and the exocyst is randomly distributed in the cytosol. After contact initiation through addition of Ca^{2+} the exocyst concentrates at the junction and organizes apical and basolateral membrane traffic. Ca^{2+}-depletion unpolarizes the cell and the complex is dispersed. **(C)** In young neurons, the exocyst is present at growth cones of neurites. As the neuron matures the complex is found in periodic domains along the axon, which specify nascent synapses. After the synapse has formed between axon and dendrite (gray), the exocyst is downregulated. From (Hazuka et al., 1999).

1.3.6 Involvement in neuronal processes

1.3.6.1 Neurite outgrowth, targeting and synapse formation

Already in initial exocyst studies the complex was associated with membrane addition during neurite outgrowth since immunostaining of Sec6 and Sec8 shows presence of these subunits at the tip of neurites, filopodia and growth cones in hippocampal cultures. Thereby Sec6 staining precedes synaptotagmin and synapsin-1 staining along axons indicating that exocyst specifies sites during synaptogenesis (Hazuka et al., 1999) (Figure 9 C). In brain tissue Sec6 is mostly found colocalized with

segretograninII (SgII) containing vesicles and shows lesser overlap with synaptophysin. On an ultrastructural level Sec6 is found at the inside of the boutonal membrane but nearly absent at the active zone. These findings suggest that exocyst is rather involved in transport of dense core vesicles maybe to build and/or maintain synaptic structures than in contributing to synaptic vesicles exocytosis (Vik-Mo et al., 2003). The subcellular localization of Sec15, Sec6, Exo84 and Exo70 in PC12 cells is shifted upon differentiation with NGF from a perinuclear region to growth cones (Vega and Hsu, 2001; Wang and Hsu, 2003). Overexpression of a Sec10 deletion construct in PC12 cells represses NGF induced outgrowth of neurites indicating an involvement of the exocyst during differentiation (Vega and Hsu, 2001). A molecular basis for actin polymerisation dependent neurite outgrowth was suggested by the interaction of Exo70 with TC10, which antagonizes nWASP (neural Wiskott-Aldrich syndrome protein, an actin nucleation promoting factor) activation through Cdc42 and subsequent activation of the Arp2/3 complex thereby establishing a Cdc42 independent mechanism of NGF induced neurite outgrowth via the TC10-Exo70 interaction (Pommereit and Wouters, 2007). Regulation of neurite branching through Ral GTPases is also in part dependent on its ability to interact with exocyst. While RalA seems to induce neurite branching through the exocyst, RalB acts through phospholipase D (Lalli and Hall, 2005). RalA is also involved in neuronal polarization, since depletion or constitutive activation of this protein decreases the number of polarized cortical neurons in culture. Depletion of exocyst subunits Sec6, Sec8 and Exo84 leads to a similar phenotype, but neurons do polarize if a RalA mutant is overexpressed, which cannot interact with the exocyst subunit Sec5. Additionally, exocyst subunits coimmunoprecipitate with Par3 and atypical protein kinase C (aPKC), proteins of the partitioning defect complex involved in actin nucleation, and translocation of this polarization factor to neurite tips is dependent on the presence of exocyst subunits and RalA (Lalli, 2009). In summary, the exocyst has been associated with synaptogenesis, polarization and branching of mammalian neurons by delivering vesicles to the growth cones. The exact molecular mechanisms of subunit assembly and hierarchy are far from being understood, but Ral GTPases have been associated to trigger exocyst function in membrane addition. Several lines of evidence have pointed out a crosstalk between the exocyst and actin polymerisation factors, thereby establishing a tempting link in neurite outgrowth between vesicle traffic and actin dynamics that is regulated by central signalling cascades.

Several studies in drosophila have also pointed out an involvement of the exocyst in the establishment of the nervous system. Flies depleted of Sec5 die as growth arrested larvae with growth defects in the neuromuscular junction. Retrieved neuronal cultures also show defects in neurite outgrowth and membrane trafficking (Murthy et al., 2003).

Mutant animals for Sec6 fail to grow as larvae and die 72 hours after egg laying. Partial rescue of Sec6 revealed that it is necessary to target specific proteins to the rhabdomere in differentiating photoreceptor cells (Beronja et al., 2005). Mutations in Sec15 do not allow fly development to proceed beyond the second instar larvae stage. While Sec15 does not decrease neurite extension it leads to the formation of synapses between inappropriate partner neurons. This loss of synaptic specificity is attributed to the incorrect delivery of cell adhesion and cell signalling molecules after growth cones have reached their targets. The authors also proposed a model in which exocyst subcomplexes act independently (Mehta et al., 2005), whereas another group argued that at least Sec5, Sec6 and Sec8 act as a complex and are dependent on each other for proper localization and function (Murthy et al., 2005). Depletion of Sec10 results in postembryonic lethality but tissue specific depletion does not influence morphogenesis of the neuromuscular junction (Andrews et al., 2002). Taken together, findings in drosophila support a function of the exocyst complex in neurite outgrowth and targeting but they also highlight individual phenotypes for different mutated exocyst subunits reflecting the unexplored interplay between subunits and also the poorly characterized existence of subcomplexes acting on their own.

1.3.6.2 Synaptic vesicle cycle

The presence of exocyst subunits in the presynaptic compartment was shown by colocalization studies. Sec8 localizes to nerve terminals in the absence and presence of synaptotagmin, but does not show perfect colocalization with the SV marker. Instead it is found more towards the plasma membrane and in a cloud around SV. Sec8 also coimmunoprecipitates with a very small fraction of syntaxin indicating that it is only bound to a restricted pool of this protein. Since it does also not coimmunoprecipitate Munc18, Rab3A and NSF (N-ethylmaleimide-sensitive factor) it was hypothesized that the exocyst transports SV to the SNARE complex, but is not associated with vesicle fusion (Hsu et al., 1996). Sec6 localizes similarly as Sec8 to sites of exocytosis in nerve growth factor differentiated PC12 cells. It resides juxtaposed to DβH, an antigen contained in the lumen of synaptic vesicles, but is not perfectly colocalized with synaptic vesicles (synaptotagmin) (Kee et al., 1997). In functional synapses Sec6 is absent from active release sites undergoing endocytosis, which are marked by FM1-43 uptake, indicating that the sec6/8 complex does not contribute to synaptic vesicle cycling (Hazuka et al., 1999). However, the before mentioned conclusions were deduced from the immunoreactivity of antibodies against Sec6, which were later shown to label only a subpopulation of this subunit (Yeaman et al., 2001). In addition the presence of one (incompletely detected) subunit was supposed to reflect the presence and function of the

entire complex, which might not necessarily be true since subcomplexes might function without the need for entire complex assembly (see above). Wang et al. showed that inhibition of Sec5-RalA interaction abolishes GTP-dependent exocytosis in PC12 cells, but Ca^{2+}-dependent exocytosis remained normal under these conditions (Wang et al., 2004a). These findings clearly show that RalA-Sec5 interaction is not necessary for Ca^{2+}-dependent fusion, which anyway is not expected since RalA signalling was not associated with synaptic transmission so far. Therefore, the obtained findings about exocyst function in synaptic transmission are in need for further confirmation. Interestingly, not a single functional study about exocyst function in neurosecretion was performed since then in mammals. One of the major missing links between exocyst and neurotransmitter release was established when it was shown that Sec15 binds to Rab3, a synaptic vesicle associated GTPase involved in synaptic transmission (Wu et al., 2005). However, this interaction was found in drosophila and remains to be shown in mammals. Similarly, the findings that depletion or mutation of Sec5, Sec10 or Sec15 in drosophila do not influence neurotransmission await equivalent studies in higher organisms (Andrews et al., 2002; Mehta et al., 2005; Murthy et al., 2003). In addition, the potential existence of subcomplexes could obscure an involvement of exocyst function in neurosecretion in experiments based on single subunit depletion. A recent proteomic analysis of synaptic vesicles found Sec8 to be part of this trafficking organelle raising the question of its functional presence (Takamori et al., 2006).

In this regard, authors of a review about the involvement of exocyst in synaptic transmission stated correctly: “However, its (exocysts) involvement in the docking of synaptic vesicles at the active zone … remains to be demonstrated” (Becherer and Rettig, 2006).

1.3.6.3 Postsynapse

Most of the interactions between exocyst and the postsynaptic compartment concentrate on the C-terminal PDZ motif of Sec8 (-TTV). SAP102 (synapse-associated protein) interacts with this PDZ-binding domain of Sec8 and removal of the PDZ-binding domain of Sec8 decreases the surface expression of NMDARs (N-methyl D-aspartate receptor) at the postsynapse. The deletion of the PDZ motif does not interfere with exocyst complex formation, because $Sec8^{\Delta 4}$ is still able to interact with Sec6 and Sec10. As mentioned earlier Sec8, NR2B and SAP102 already form a complex in the ER and this interaction is also dependent on the PDZ-motif (Sans et al., 2003). Another MAGUK (membrane-associated guanylate kinases), which interacts with the PDZ-motif of Sec8, is PSD95 (postsynaptic density protein-95) and this interaction is regulated by cypin, a cytosolic PSD-95 interactor, which shows competitive binding with Sec8 to PSD-95

(Riefler et al., 2003). A recent study from Gerges et al. could decipher the different roles of Sec8 and Exo70 at the postsynaptic compartment. By expression of dominant-negative constructs of Sec8 ($Sec8^{\Delta C16}$) and Exo70 (aa 1-384), which are both able to interact with endogenous exocyst subunits, they found decreased levels of Sec8, AMPARs (α-amino-3-hydroxy-5-methyl-4-isoxazolepropionic acid receptor), NMDARs and PSD95 and an accumulation of Sec8, Rab8 and AMPARs at the postsynaptic density, respectively. Through transport and surface labelling assays they suggested that Sec8 is responsible for transporting AMPARs along the dendritic shaft, whereas Exo70 is needed to insert the receptor into the postsynaptic membrane (Gerges et al., 2006). The C-terminus of GLYT1 (glycine transporter 1) (last 11 aa) binds to Sec3 and overexpression of GLYT1 translocates Sec3-GFP to the plasma membrane in MDCK cells. GLYT1 also coimmunoprecipitates Sec6 and Sec8 from rat brain lysates. The transporter activity of GLYT1 is increased if GLYT1 and Sec3-GFP are overexpressed in COS cells (Cubelos et al., 2005).

In summary, exocyst subunits are involved in the transport and incorporation of postsynaptic receptors to the postsynaptic density. These processes seem to be mediated by different subunits along the secretory pathway and postsynaptic density proteins interact with exocyst subunits along this trafficking route.

A reoccurring scheme though is, that Exo70 represents the final step in vesicle cargo incorporation into the plasma membrane. In adipocytes as well as in the postsynaptic compartment of neurons overexpression of the N-terminal fragment of Exo70 leads to the accumulation of transport vesicles at the plasma membrane, but impedes their surface expression. A second characteristic of this dominant-negative truncation construct is its inability to interact with the Arp2/3 complex, which prevents the formation of actin based membrane protrusions and thus impedes cell migration. Hence, two proposed functions of the exocyst complex are impeded by overexpression of the N-terminal fragment of Exo70 making subunit Exo70 an attractive target to perturb exocyst function in the cell (Figure 10).

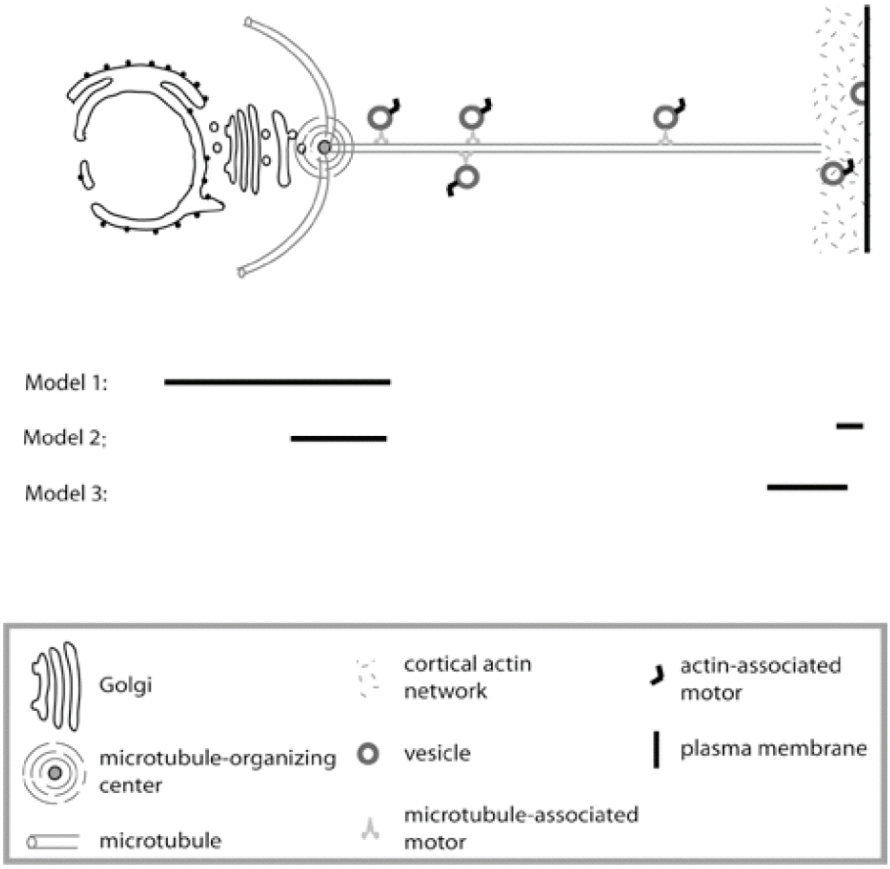

Figure 10. Different models on exocyst function. The first model describes exocysts influence on protein synthesis and sorting. Perturbation of exocyst function would be expected to change the protein composition of various plasma membrane domains. The second model is based on exocysts involvement in post-Golgi trafficking of cargo vesicles and in subsequent docking and fusion events at the plasma membrane. Perturbation of exocyst function would result in accumulation of secretory vesicles at the Golgi or near the plasma membrane. The third model reflects exocysts influence on cytoskeletal elements and its potential involvement in mediating transfer of vesicles from microtubules to the actin scaffold at the plasma membrane. Perturbation of exocyst function would stall vesicles near the plasma membrane and would influence morphological aspects governed by the cytoskeleton. From (Wang and Hsu, 2006).

1.4 The calyx of Held: a model system for excitatory synaptic transmission in the CNS

The calyx of Held was named after its discoverer Hans Held in 1893 (Hans Held 1893). It is the tertiary synapse of the auditory pathway and involved in sound-source localization. The nerve terminal projects from globular bushy cells, which reside in the ventral cochlear nucleus (VCN), towards the contralateral side of the brainstem into the medial nucleus of the trapezoid body (MNTB) where it releases glutamate onto principal cells in a one-to-one synaptic relationship. The calyx of Held has emerged as a model

system to elucidate presynaptic mechanisms of synaptic transmission during the last 15 years, because it is one of the few synapses in vertebrate central nervous system, which are large enough to enable accessibility of the presynaptic compartment with glass electrodes. Therefore, many parameters like vesicle pool sizes, short-term depression, release probability, quantal size and content, number of release sites, Ca^{2+}-microdomains and endocytic events have been described in great detail for several different developmental stages (reviewed in Schneggenburger and Forsythe, 2006). The morphology of individual maturational stages has also been described (Kandler and Friauf, 1993): at P3 the calyx contacts postsynaptic cells as a flat growth cone with many collaterals extending from it. At P14 no collaterals can be detected any more and the structure of the nerve terminal has started to fenestrate, which results in a meshwork of lobes that are connected by thinned membrane patches. Finally at P21 the calyx has arrived at its mature state, which resembles a floral calyx and is characterized by a palm at the axon entry side and emanating finger like stalks with multiple swellings that contact the principal cell from all sides.

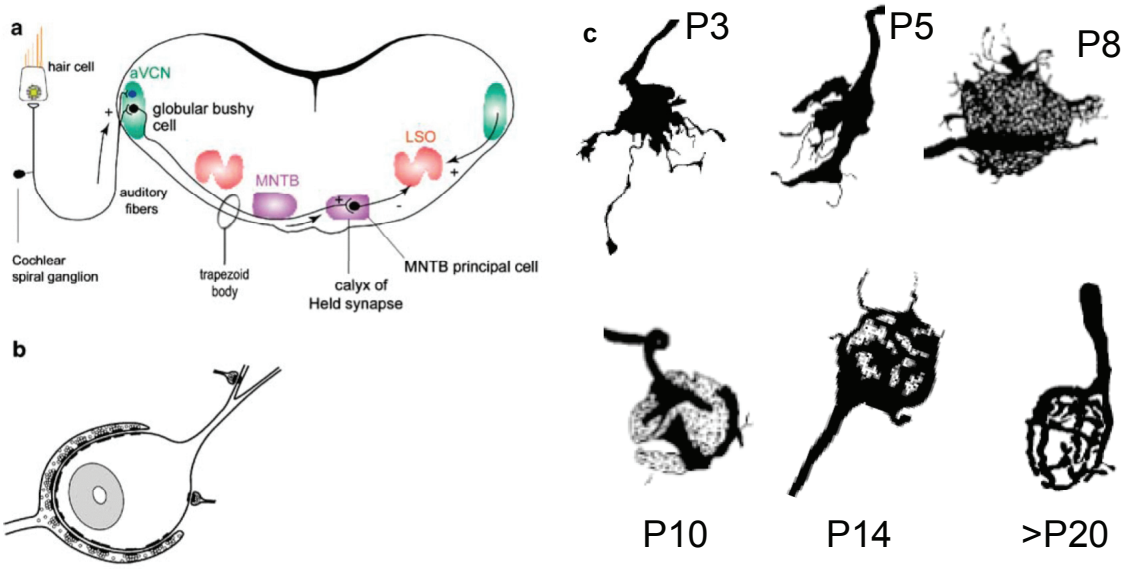

Figure 11. Model system calyx of Held. (a) The calyx of Held is the tertiary synapse in the auditory pathway. It projects from globular busy cells residing in the ventral cochlear nucleus (VCN) towards the contralateral side into the medial nucleus of the trapezoid body (MNTB). **(b)** The giant nerve terminal engulfs postsynaptic principal cells and releases glutamate to evoke excitatory responses. From (Schneggenburger and Forsythe, 2006). **(c)** Maturation of the calyx is accompanied by pronounced morphological changes. At P3 the nerve terminal is already established and shows many collaterals. At P5 the calyx adopts a spoon like shape and collaterals are still present. From P8 to P14 the nerve terminal develops lobes, which surround the principal cell and are connected by a plasma membrane meshwork. At P21 the calyx has reached its mature developmental stage, which is characterized by finger like stalks and resembles a floral calyx. From (Kandler and Friauf, 1993).

The development of viral vectors has opened up the possibility to introduce nucleic acids into globular bushy cells via stereotaxic injections and to analyse synaptic transmission under acute genetically modified conditions (Wimmer et al., 2004). This experimental paradigm allows for investigation of a protein of interest without the need for lengthy creation of knockout animals. In addition, genes, whose elimination causes lethal phenotype in knockout animals, can also be investigated by protein depletion methods, e.g. RNAi, or overexpression of dominant-negative constructs. Importantly, the separation of the pre- and postsynaptic compartment remains intact since viruses transduce only a limited number of cells due to the locally controlled application by stereotaxic injections. This feature separates the pre- from the postsynaptic functions of a protein, which is not maintained in an ubiquitous knockout of a gene in genetically altered animals or in some transiently transfected/transduced permanent cell culture systems.

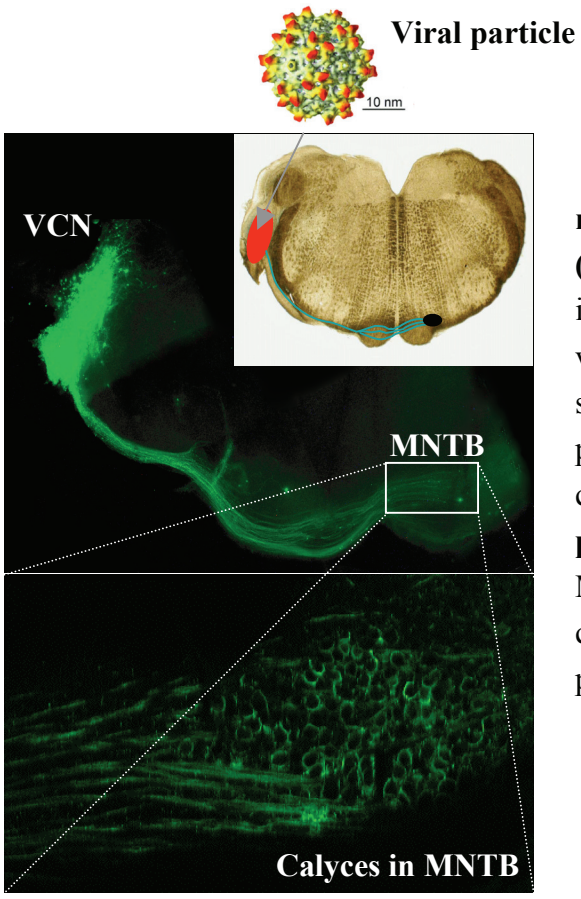

Figure 12. **Acute targeted genetic modification of the calyx of Held. (upper panel)** Brainstem slices are shown into which viral vectors are injected to the ventral cochlear nucleus (VCN) by stereotaxic injections. The fluorescent projections of transduced globular bushy cells can readily be identified. **(lower panel)** shows a magnification of the MNTB region. Calyces are recognized as circular identities, which surround the postsynaptic principle cells.

2 Aim of study

The aim of this study was to address exocyst function in the calyx of Held *in vivo*. The main focus rested on the unresolved question whether the exocyst complex is involved in synaptic vesicle cycling by transport and/or tethering of synaptic vesicles to the active zone. Another goal was to investigate the proposed involvement of the exocyst complex in neuronal outgrowth and in delivery of active zone proteins *in vivo*. It was also of interest where in the presynaptic compartment exocyst subunits reside and whether they are preferentially found as separate single subunits or whether they form complexes with other protein members of the complex.

The localization of the exocyst complex and its involvement in constitutive and regulated secretion was supposed to be addressed *in vivo* by the following experimental paradigm. Globular bushy cells should be transduced by viral vectors, which were delivered into the ventral cochlear nucleus by stereotaxic injection. Since developmental events were to be observed and expression of transgenes occurs with a delay after neuron transduction, a surgery procedure and stereotaxic coordinates for the injection of viral particles into the ventral cochlear nucleus of 2-day-old rats had to be developed first to allow for experimental investigations before the adult stage at P21.

The giant size of the calyx of Held comprises advantages for localization studies in the presynaptic compartment. Therefore, immunohistochemistry against exocyst subunits in combination with overexpression of GFP-fusion proteins of exocyst subunits *in vivo* should reveal the location and the potential existence of subcomplexes inside the presynaptic compartment.

To address exocysts involvement in cellular transport its function was to be perturbed by two independent approaches. The first approach aimed to decrease the protein levels of one or more exocyst subunits by virus mediated transduction of RNAi into globular bushy cells. The successful downregulation was to be shown on the protein level by immunohistochemistry of fixed brainstem slices against the exocyst subunit, which was targeted by the introduced RNAi. The second approach made use of an already characterized dominant-negative truncation construct of Exo70 (Exo70Nter, aa 1-384), which should be overexpressed by virus mediated transduction of globular bushy cells. Subsequent electrophysiological analysis should reveal, whether changes in presynaptic parameters are evident upon perturbation of exocyst function. Similarly, confocal imaging of calyx morphology and immunlocalization of presynaptic marker proteins was meant to disclose the role of the exocyst in neuronal outgrowth and in the transport of CAZ proteins *in vivo*.

3 Materials and Methods

3.1 Transcardial perfusion and fixation procedure

Sprague Dawley rats were perfused as indicated in the results chapter either 13±1 days after birth or at postnatal day 21. Rats were injected with 2.5-5 µl/g bodyweight pentobarbital (Merial, Narcorene) intra peritoneal and observed until no eyelid or toe reflexes could be evoked by touching the eyelid with a cotton stick or by pinching the toes with fingernails or a forceps. When animals were deeply anesthetized, the skin was removed around the area of the apex and the abdominal wall was opened. The skin opening was enlarged and the pleura diaphragm opened to reveal the heart completely. The left ventricle was first slit slightly by using a fine scissor and breached afterwards completely with a blunt steel needle (Becton, Dickinson, REF 301900). The needle was inserted into the aorta and fastened with a bulldog clamp (Fine Science Tools, No. 18050-35). The right atrium was cut widely to open blood circulation and pressure was applied immediately by opening the vent of the PBS (Gibco, 14200) container. Approximately 20 ml of room temperature PBS were flushed through the needle before the animal was perfused with 50 ml freshly thawed, room temperature PBS containing 4% paraformaldehyde (Aldrich, 16005). Thereafter, animals were detached from the perfusion apparatus and left approximately 10 min at room temperature, but covered with wet paper towels to prevent drying. Animals were decapitated and the skullcap opened by entering through the medulla and making tiny cuts close to the skullcap towards the rostrum. The skullcap was removed and a coronal cut approximately 2 mm rostral to lambda was performed. The brain was dissected by cutting all attached nerves and dropped into 10 ml 4% paraformaldehyde PBS and postfixed for another 2 hours at 4 °C. Brains were either immediately sliced or stored in 0.02% sodium azide in PBS after postfixation.

3.2 Slicing of fixed brain tissue

Fixed rat brains were freed from excess liquid and the dura removed with forceps. The brain was glued onto the tissue holder with instant glue (World Precision Instruments, 7341). Vibratome sections of 50-100 µm thickness were prepared with razerblades (American Safety Razor Company, Personna) and collected in PBS for short-term (< 1 week) or in 0.02% sodium azide PBS for long-term storage.

3.3 Immunohistochemistry

All incubation steps were performed on a horizontal shaker (Heidolph, Vibramax 100). Fixed brain slices of 50-100 μm thickness were permeabilized and blocked in blocking solution (5% normal goat serum [Jackson Immuno Research, 005-000-121], 1% TritonX-100 [Sigma, T9284] in PBS) for 2 hours at room temperature. Primary antibody binding was performed at 4 °C overnight in PBS containing 1% normal goat serum and 0.2% TritonX-100. Brain slices were washed three times for 10 minutes at room temperature with PBS supplemented with 2% normal goat serum. Secondary antibodies were applied for at least 2 hours at room temperature in PBS containing 1% normal goat serum and 0.2% TritonX-100. Vibratome sections were washed three times for 15 minutes at room temperature with washing solution (1% normal goat serum in PBS) and afterwards rinsed three times in PBS for 10 minutes at room temperature. Brain sections were mounted on glass slides (Roth, H868) and embedded in Slow Fade Gold (Invitrogen, S36936) using 100 μm spacers to prevent the tissue from being squeezed by the coverslip (Roth, 1871). Specimens were sealed with commercially available nail polish and stored light protected at 4 °C. A list of used primary and secondary antibodies is summarized in Table 1. For staining of cell nuclei brainstem slices were incubated with DAPI (1:2000) during the last washing step and washed one time thereafter in PBS for 10 minutes.

Table 1. Primary and secondary antibodies for immunohistochemistry of PFA fixed brainstem slices.

Primary antibodies

Antigen	Developed in	Clonality	Clone	Dilution	Source
Sec6	mouse	mono	9H5	1:250	Abcam (ab12235)
Sec8	mouse	mono	8S2E12	undiluted	S.C. Hsu
Sec15	mouse	mono	15S14H1	undiluted	S.C. Hsu
Bassoon	mouse	mono	SAP7F407	1:1000	Stressgen (VAM-PS003)
VGlut1	rabbit	poly	not indicated	1:1000	Synaptic Systems (135303)

Secondary antibodies

Against	Developed in	Dye	Dilution	Source
mouse	goat	Alexa 488	1:1000	Invitrogen (A11001)
mouse	goat	Alexa 647	1:1000	Invitrogen (A21235)
rabbit	goat	Alexa 647	1:1000	Invitrogen (A21244)
rabbit	goat	Alexa 350	1:1000	Invitrogen (A11046)

3.4 Molecular biology

3.4.1 Restriction digestion of DNA

All restriction enzymes were purchased from New England Biolabs and employed according to manufacturers recommendations.

3.4.2 Agarose gel electrophoresis

Agarose (Invitrogen, 15510-027) was dissolved in TAE buffer (40 mM Tris [Roth, 4855.2], 0.1% acetic acid [J.T.Backer, 6052], 1 mM EDTA [AppliChem, A3553] in H_2O) and nucleic acids were separated with the PerfectBlue Gelsystem from Peqlab.

3.4.3 Recovery of DNA fragments from AGE

DNA fragments were recovered from agarose gels by means of the MinElute Gel Extraction Kit from Quiagen.

3.4.4 Replication of DNA plamids in bacterial culture

Liquid bacterial cultures were grown in lysogeny broth (LB)-medium at 37 °C on a horizontal shaker at 180 rpm. Ampicilin was employed in a final concentration of 100 µg/ml, whereas kanamycin was used in a final concentration of 50 µg/ml.

LB-medium:
10 g NaCl
10 g bacto trypton
5 g yeast extract
(15 g Agar for plates)

Deoxyribonucleic acid (DNA) plasmids were isolated from bacteria host strains in small scale using the QIAprep Spin Miniprep Kit from Quiagen. If large DNA amounts were desired, bacterial pellets were processed with the Plasmid Giga Kit from Quiagen.

3.4.5 Ligation

The backbone to insert base pair (bp) ratio was calculated and molar amounts of the two DNA fragments employed accordingly (with a maximal ratio of 10) so that a total amount of 100 ng DNA was present in the enzyme reaction. DNA fragments were ligated with T4-ligase (New England Biolabs) according to the pipetting scheme given to the right. The mixture was incubated at room temperature (RT) for 2 hours or overnight at 16 °C. 10 µl of the mixture were transformed into the respective bacterial host strain.

Backbone	calculated
Insert	calculated
T4-ligase [ul]	1
T4-buffer [ul]	2
ad H2O [ul]	20

3.4.6 Transformation

Competent cells were purchased from Stratagene and stored at -80 °C. Cells were thawed on ice and 100 ng of DNA added to the melting bacterial suspension. After 30 minutes of incubation, cells were subjected to a heat shock at 42 °C for 45 seconds and afterwards chilled on ice for 2 minutes. LB medium (900 µl) was added and cells incubated at 37 ° for 1 hour while shaking. 50 and 500 µl of the cell suspension were plated on agar plates and incubated over night at 37 °C.

3.4.7 Plasmids and bacterial host strains

Bacterial host strains for the individual plasmids are depicted in Table 2 along with a comprehensive description and the antibiotic resistance, which is encoded by the plasmid.

Table 2. List of received and generated DNA plasmids and their individual bacterial host strains together with antibiotic resistance and a comprehensive description.

Plasmid name	Plasmid #	Host strain	Resistance	Description
pAcGFP1-C3-sec3	267	hb101	kanamycin	GFP-fusion expression vector for Sec3
pAcGFP1-C3-sec6	268	hb101	kanamycin	GFP-fusion expression vector for Sec6
pAcGFP1-C3-sec8	269	hb101	kanamycin	GFP-fusion expression vector for Sec8
pAcGFP1-C3-sec15	270	hb101	kanamycin	GFP-fusion expression vector for Sec15
pAcGFP1-C3-exo70	271	hb101	kanamycin	GFP-fusion expression vector for Exo70
pAM-DCA-GFP-sec3	296	TOP10	ampicilin	rAAV vector encoding GFP-sec3
pAM-DCA-GFP-sec6	297	TOP10	ampicilin	rAAV vector encoding GFP-sec6
pAM-DCA-GFP-sec8	298	TOP10	ampicilin	rAAV vector encoding GFP-sec8
pAM-DCA-GFP-sec15	299	TOP10	ampicilin	rAAV vector encoding GFP-sec15
pAM-DCA-GFP-exo70	300	TOP10	ampicilin	rAAV vector encoding GFP-exo70
FUGW-GFP-sec3	312	TOP10	ampicilin	lentiviral vector encoding for GFP-sec3
FUGW-GFP-sec6	313	TOP10	ampicilin	lentiviral vector encoding for GFP-sec6
FUGW-GFP-sec8	314	TOP10	ampicilin	lentiviral vector encoding for GFP-sec8
FUGW-GFP-sec15	315	TOP10	ampicilin	lentiviral vector encoding for GFP-sec15
FUGW-GFP-exo70	316	TOP10	ampicilin	lentiviral vector encoding for GFP-exo70
pAcGFP1-C3-exo70 aa 1-384	319	hb101	kanamycin	GFP-fusion expression vector for Exo70Nter
pAcGFP1-C3-exo70 aa 384-653	320	hb101	kanamycin	GFP-fusion expression vector for Exo70Cter
pAM-DCA-GFP-exo70Nter	330	TOP10	ampicilin	rAAV vector encoding GFP-exo70Nter
pAM-DCA-GFP-exo70Cter	331	TOP10	ampicilin	rAAV vector encoding GFP-exo70Cter

3.4.8 Sequencing

Newly received or generated DNA plasmids were sequenced by performing a polymerase chain reaction (PCR) with BigDye Terminator Mix (Applied Biosystems, 4337455) and primers, which were ordered from MWG-Biotech AG. The amount of compounds and the standard PCR program for the sequencing reaction is shown below.

Pipetting scheme for sequencing reaction

Primer [10 µM]	1 µl
DNA [1 µg/µl]	0.5 µl
BigDye Terminator Mix	4 µl
H_2O	4.5 µl

Polymerase chain reaction program

Melting	96 °C	1 minute	
Melting	96 °C	15 seconds	25 cycles
Annealing	60 °C	15 seconds	
Elongation	65 °C	4 minutes	
End	4 °C	∞	

In some cases the annealing and elongation temperatures had to be adjusted for individual primer/plasmid pairs in order for the sequencing reaction to work. PCR was performed in a Thermocycler from Biometra. Afterwards, 25 µl (3M NaAc 1:21 ethanol) was added to the sequencing reaction, the solution transferred to a fresh 1.5 ml tube and centrifuged at ~ 15000 g for 15 minutes. Two washing steps with 800 µl 70% ethanol removed remaining salt traces before the invisible DNA pellet was air dried and handed

over to an in-house MPImf sequencing facility. The DNA sequence trace chromatograms were assembled with the Seqman software from the Lasergene package (DNASTAR Inc.) and controlled for correct insertion of the cloned fragments. Plasmid maps were generated in Seqbuilder (DNASTAR Inc.) and Strider (CEA, France) software.

3.5 Cultivation of human embryonic kidney cells

3.5.1 Passaging

Cultivation medium:
DMEM (Gibco #41965-039), per 500 ml:
50 ml fetal bovine serum (Gibco #10500-064)
10 ml 100x non-essential amino acids (Gibco #11140-035)
10 ml 100x sodium pyruvate (Gibco #11360-039)
5 ml penicillin/streptomycin (Gibco #15140-122)

Human embryonic kidney (HEK) cells (Agilent Technologies, 240073) were grown in the medium specified to the right and cultivated at 37 °C in humified 5% CO_2 atmosphere. When cells reached ~80% confluence, the cell culture medium was aspirated and cells were washed with 37 °C PBS. Trypsin (Gibco, 15400) was added to the cells and plates were stored in the incubator for 2 minutes. Prewarmed DMEM medium was added to the cells to stop trypsin digestion. Cells were centrifuged at 200 g for 5 minutes and the supernatant aspirated to remove residual trypsin traces. The cell pellet was resuspended in prewarmed DMEM until a single cell suspension was obtained and cells were seeded at desired density.

3.5.2 Freezing and thawing

HEK cells were collected in log-phase at ~50% confluence to prepare liquid nitrogen stocks. Cells were harvested (see above) and the cell pellet resuspended to a cell density of 1 x 10^6 cells/ml in freezing medium (80% fetal bovine serum, 20% dimethylsulfoxide). The suspension was transferred into cryovials and slowly (1 °C/min in Nalgene cryo container) frozen to -80 °C. The day after, cryovials were stored in liquid nitrogen.

Frozen cells were quickly thawed in a 37 °C waterbath by gentle agitation. As soon as the last ice crystal dissolved, the cell suspension was transferred to 10 ml prewarmed cultivation medium. Cells were pelleted at 200 g for 5 minutes and resuspended in cultivation medium before seeding.

3.6 Calcium phosphate transfection

For transfection of DNA into HEK cells, the cells were seeded the day before transfection at a density of 6500 cells/cm^2. HeBS Buffer (280 mM NaCl, 50 mM HEPES, 1.5 mM Na_2HPO_4, pH adjusted to 7.05 with NaOH) and 2.5 M $CaCl_2$ was warmed to 37

°C and DNA amounts of 0.25 μg/cm^2 plate were employed. Volumes of the reagents were used according to Table 3.

Table 3. DNA, HeBS and $CaCl_2$ amounts for transfection of DNA plasmids into HEK cells. Volumes and concentrations of the reagents are calculated according to the area of the cell culture plate.

Diameter [cm]	Area [cm^2]	Format	DNA [μg]	CaCl2 [μl]	HeBS [μl]	ad H2O [μl]
1.2	1.1	24 well	0.3	0.7	7.3	15
1.8	2.5	12 well	0.6	1.7	16.5	33
3.5	9.6	6 well	2.3	6	63	125
5.5	23.8	dish	5.8	15	154	309
10	78.5	dish	19.1	51	510	1021
14	153.9	dish	37.5	100	1000	2000

$CaCl_2$ was added to adjusted DNA concentrations, mixed and incubated for 1 minute. HeBS buffer was added and the solution mixed vigorously by pipetting up and down. After 90 seconds of incubation, the precipitate was added to the cells in a drop wise fashion. The cell culture plates were returned to the incubator and medium was replaced 8-16 hours afterwards.

3.7 Adeno-associated virus production

A helper free plasmid system was employed for generation of recombinant adeno-associated virus (rAAV) preparations. The system consists of the vector plasmid (pAM) in which the expression cassette is flanked by adeno-associated virus 2 (AAV2) inverted terminal repeats. Expression of genes was driven by the cytomegalovirus enhancer/chicken β-actin promoter and increased by a downstream woodchuck post regulatory element, which was followed by the bovine growth hormone polyA signal. Ten 14 cm plates of AAV 293T cells were cotransfected with equimolar amounts using calcium phosphate precipitation of pAM plasmid and two helper plasmids, which carry all genes essential for packaging of pAM plasmids into capsids in AAV-293 HEK cells (Grimm et al., 2003). One helper plasmid (pDP1) encodes for the *cap* gene from AAV serotype 1 and the other (pDP2) for the *cap* gene of AAV serotype 2. The medium was exchanged the day after transfection and cells were collected with a cell scraper (Costar, 3008) 72 hours post transfection. The cell suspension was centrifuged at 200 g for 10 minutes and the cell pellet resuspended in 10 ml lysis buffer (150 mM NaCl, 50 mM Tris-HCl, pH 8.5). Cells were lysed via three freeze/thaw cycles between dry ice ethanol bath and 37 °C waterbath and vortexed briefly after each thaw cycle. Genomic DNA was digested with 500 units of benzonase endonuclease (Sigma E1014) for 2 hours at 37 °C. Cell debris was removed by centrifugation at 3600 g for 15 min and the supernatant

collected by means of a needle and syringe. The supernatant was pushed through a filter (Millex, SLHV013SL) to retrieve the crude lysate. Columns (Biorad, 732-1010) were rinsed with 10 ml equilibration buffer (1 mM $MgCl_2$, 2.5 mM KCl in PBS) and afterwards filled with 5 ml heparin agarose (Sigma, H6508) and 10 ml equilibration buffer. The agarose was allowed to sediment before equilibration buffer was released through the nozzle. The crude lysate was added to the column and incubated at 4 °C with heparin agarose on a shaker for 2 hours. Unbound crude lysate was eluted and the column washed with 20 ml equilibration buffer. AAV particles were released from the column by addition of 15 ml elution buffer (500 mM NaCl, 50 mM Tris-HCl, pH 7.2) and collected in filter tubes (Millipore, UFC9 100 24). The eluate was concentrated by centrifugation at 4500 rpm until less than 1 ml was left. The filter tube was refilled with PBS to 15 ml and centrifuged again to remove high salt concentrations until the filter retained less than 1 ml. This step was repeated once more and the last centrifugation continued until less than 500 µl of virus stock were left in the filter tube. The suspension was collected in a syringe and filtered (Millex, SLGV004SL) to retrieve the final virus stock. AAV particles were aliquoted and either stored at 4 °C or frozen in dry ice ethanol bath and stored at -80 °C.

3.8 Lentiviral vector production

HEK 293T cells seeded in five 10 cm petri dishes were grown to 70-80% confluence. Lentivirus production was based on three plasmids (Lois et al., 2002; Naldini et al., 1996): the transfer vector plasmid FUGW containing the gene of interest, the HIV-1 packaging vector Δ8.9 and the VSVG envelope encoding vector. Equimolar amounts of all three plasmids were transfected into HEK cells with polyethyleneimine (Sigma). Along those lines, a final volume of 5 ml Optimem (Invitrogen) was supplemented with 340 µl polyethyleneimine (Sigma, 1 mg/ml) before DNA (125 µg in total) was added. The mixture was vortexed and incubated for 30-45 minutes on the bench at RT. The transfection solution was added drop wise to the HEK cells and the medium exchanged with fresh cultivation medium 4 hours later. Two days later, the cell culture supernatant containing the viral particles was harvested and subjected to ultracentrifugation (90 minutes, 25 000 rpm in a SW32Ti rotor). The supernatant was discarded ant the pellet soaked in 200 µl (20 mM HEPES-Tris pH 7.4 in PBS) for 2 hours at 4° C to prepare the viral particles for careful resuspension. Aliquots were shock frozen using liquid nitrogen and stored at -80 °C until further use.

3.9 Primary hippocampal neuronal culture

3.9.1 Coverslips

Coverslips were baked at 180 °C for 4 hours and afterwards distributed in 24 well plates. Glass slides were covered with poly-l-lysine (20 µg/ml) and incubated at 37 °C for at least 1 hour. The coating solution was removed and coverslips washed three times with PBS before they were stored in Hank's Buffered Salt Solution (HBSS, Gibco) at 37 °C.

3.9.2 Preparation

Pregnant Wistar rats were ordered from Charles River and sedated with isofluran when embryos reached E19. All embryos were removed from the mother without breaking the amniotic sac. Then, embryos were decapitated close to the skull and heads placed on an ice chilled petri dish. Heads were fixed with forceps close to the eyes under a binocular. One blade of a fine scissor was pushed through the medulla towards the rostrum and a horizontal cut through on half of the brain performed. The same step was repeated for the other side. A second forceps was used to lift the skullcap from the medulla towards the rostrum. The dissected dorsal brain part containing the hippocampus was transferred on an ice chilled petri dish. The meninges were removed before the cortical hemispheres were bent to the side to reveal the banana-shaped hippocampus. Hippocampal tissue was dissected with two fine forceps from attached brain regions and transferred to ice cold HBSS. The hippocampal tissues from all embryos were pooled.

3.9.3 Cultivation

Hippocampal tissue was transferred in 2 ml of HBSS into a 15 ml conical tube and digested by addition of 200 µl trypsin solution for 20 minutes at 37 °C. Excess trypsin solution was removed and tissue washed two times with 12 ml plating medium without glutamine. The hippocampi were transferred to a 2 ml tube and resuspended 3x with a syringe and injection needle (BD, 301300) and 3x with a smaller needle (BD, 300400). A cell filter (BD, 352360) was placed on a 50 ml conical tube and wetted with 2 ml plating medium without glutamine. The tissue suspension was filtered into the conical tube and filled to 10 ml plating medium. Cells were counted and cell density adjusted with plating medium to 25 000 – 60 000 cells per well (500 µl). HBSS was aspirated from the coverslips before cells were seeded. The plating medium was replaced the next day or after at least 3

Plating medium:	
DMEM (PAA, E15-810)	50 ml
Sodium pyruvate (PAA, S11-003)	1 ml
Fetal bovine serum (PAN, 1902-K003628D)	5 ml
Penicilline/streptomycine (PAA, P11-010)	0.5 ml
Glutamine [200 mM] (PAA, M11-004)	500 µl
Growth medium:	
Neurobasalmedium (PAA, U15-023)	50 ml
B27 (PAN, P07-07210)	1 ml
Penicilline/streptomycine (PAA, P11-010)	0.5 ml
Glutamine [200 mM] (PAA, M11-004)	125 µl

hours with growth medium. One half of the growth medium was replaced ~once per week for prolonged cultivation.

3.9.4 *Transduction with viral particles*

Hippocampal cells were transduced with viral particles by addition of 0.2 – 5 µl of virus stock solution.

3.9.5 *Fixation and embedding*

The medium of hippocampal neuronal cultures was aspirated and cells washed with PBS two times. 4% paraformaldehyde solution was added and cells fixed for 15 minutes at RT. The fixative was aspirated and remaining traces washed away with PBS. Coverslips were embedded (Polysciences, 18606) upside down and stored at 4 °C in the dark.

3.10 Western blot

Protein samples were derived from 6-well plate hippocampal cultures, which had been infected with adeno-associated virus at DIV5 and incubated for another 12 days. The cultured cells were washed with 2 ml PBS and collected afterwards with a cell scraper in 300 µl of SDS-PAGE sample buffer. The suspension was heated for 10 minutes at 95 °C and centrifuged at 14 000 rpm for 5 minutes to remove cell debris. Supernatants were transferred into a fresh tube and stored at -20 °C.

SDS-PAGE sample buffer:
3.55 ml H2O
1.25 ml 0.5 M Tris-HCl p_H 6.8
2.5 ml Glycerol
2.0 ml 10 % SDS (w/v)
0.2 ml 0.5 % bromphenolblue (w/v)
stored at RT - add 50 µl β-mercaptoethanol to 950 µl sample buffer before use

Chemicals to fabricate 10% SDS gels using the mini protean 3 system from Biorad are shown to the right. The resolving gel was overlayed with isopropanol during polymerization. Protein samples were loaded onto SDS gels together with molecular weight standards (Biorad, 161-0319). Proteins were usually separated at a voltage of 120 V for ~80 minutes in running buffer. After SDS-PAGE proteins were transferred to PVDF membranes (Millipore, IPVH00010) by means of the Trans-Blot semi-dry system from Biorad according to manufacturer instruction at 15 V for 20 minutes. All following incubation and washing steps were performed on a horizontal shaker. Membranes were blocked in 5% milkpowder (Roth, T145.1) in TTBS (150 mM NaCl, 25 mM Tris-HCl p_H 7.5, 0.1 %

Chemical volumes for 10% SDS gels:
4.1 ml H_2O
3.3 ml 30% acrylamid/bis
2.5 ml Gel buffer*
0.1 ml 10% SDS (w/v) in H_2O
*Resolving gel buffer: 1.5 M Tris-HCl p_H 8.8
*Stacking gel buffer: 0.5 M Tris-HCl p_H 6.8
mix and add 50 µl of 10% APS and 5 µl of TEMED to initiate polymerization

Running buffer (10x):
30.3 g Tris base
144 g Glycine
10g SDS
ad 1 l H_2O

(v/v) Tween 20) for 1 hour at room temperature and washed 2 times with TTBS thereafter for 5 minutes. Primary antibodies against GFP (Santa-Cruz, sc-9996) were diluted 1:5000 in 1% milkpowder in TTBS and incubated with the membrane overnight at 4 °C. Membranes were washed 2 times with TTBS for 15 minutes before incubation with secondary antibodies (horseradish peroxidase conjugated, 1:20 000 in 1% milkpowder in TTBS) was performed for 1 hour at room temperature. Unbound secondary antibodies were removed from the membrane by washing the membranes 3 times with TTBS for 10 minutes. Upstate Visualizer Spray (Millipore, 17-373SP) was used to detect signal on photofilm (Amersham, 90136).

3.11 Stereotaxic injection

Pregnant Sprague Dawley rats were ordered from Charles River and cared for according to German animal law. Pubs were placed on a heating pad (35 °C, Watlow) and sedated with 5% isofluran (Baxter, HDG9623 – vaporizer: Surgivet, Isotec4) for 5 minutes with medical oxygen as carrier gas. Breathing rate of pubs was optically observed throughout the whole surgery procedure and isofluran levels adjusted accordingly. If eyes were open, they were covered with eye cream (Bayer, Bepanthen Augensalbe) to prevent them from drying out during stereotaxic injection. Approximately 30 µl lidocain (DeltaSelect, Licain) were injected subcutaneously between bregma and lambda before pubs were positioned in the stereotaxic apparatus. When animals did not respond to reflex tests, the skin was opened with a scalpel blade from a position rostral to bregma and caudal to occiput. Tissue was wetted and cleaned with normal rat ringer (135 mM NaCl, 5.4 mM KCl, 1.8 mM $CaCl_2$, 1 mM $MgCl_2$, 5 mM Hepes) throughout the whole surgery. The dura was removed with forceps and bregma positioned in the centre of the stereotax. Bregma and lambda was oriented parallel to the y-axis of the stereotax before a square of 3 x 4 mm was drilled into occiput with a dentist drill (Osada, EXL-40 – drill: Komet, 1104005). The skull was positioned with a eLeVeLeR (Sigmann Elektronik) so that bregma, lambda, x- and y-Axis are in a parallel plane to the ground plate of the stereotax. Micropipettes (Brand GmbH, 708707) were shaped with a horizontal puller (Sutter instrument, P-97) and mounted in an injection adapter (Wimmer et al., 2004). The pipette was connected to a 50 ml syringe with a silicon tube and filled with virus solution by applying negative pressure. The tip of the virus filled injection needle was positioned on bregma and all coordinates reset to 0. Injection coordinates were chosen according to the distance between bregma and lambda and are depicted in Table 6 in the results part. Approximately 200 nl of virus solution were injected per injection site and the needle was retracted 30 seconds after injection of the virus to allow

spread of particles in the tissue. The skin opening was sutured (BBraun, Dafilon DSMP11) and the pub gassed with pure medical oxygen to end anaesthesia. Pubs recovered within minutes after surgery and were returned to their mother.

3.12 Confocal imaging and data analysis

Confocal image stacks were acquired on a Leica SP2 with glycerol immersion objectives (63x (Leica, 506194), 10x (Leica, 506293)). The gain of photomultiplier tubes was kept constant at 750V and laser power as well as offset was adjusted to account for the whole dynamic range of 8-bit TIFF-files. Linear interpolation of laser intensity was employed to compensate for weaker light penetration in deeper imaging planes. The sampling rate of acquired images was below the resolution limit of the microscope with a usual voxel size of 93 nm, 93 nm and 162 nm in x-, y- and z- direction, respectively.

Image processing was performed in Amira software (Visage Imaging). First, images were cropped to reduce computation time for further post processing. 3D median filtering was used to remove noise and to smooth fluorescence signal. Manual thresholding was conducted afterwards to select for positive fluorescence signal and labelled regions were smoothed with a 3D median filter. Axons and neighbouring calyces, which were also selected in the previous procedure, but did not belong to the calyx of interest, were identified and removed manually. In case imaging data was acquired along with a second label, the imaging data was multiplied with the second label field to isolate signal from within the second label field. Retrieved label fields were quantified in Amira and evaluated statistically in Prism (GraphPad).

3.13 Electrophysiology

Virus injected animals were decapitated at day 13±1 and brains dissected in ice-cold, carbogen saturated slicing solution (in mM: 125 NaCl, 25 $NaHCO_3$, 2.5 KCl, 1.25 NaH_2PO_4, 3 myoinositol, 2 sodium pyruvate, 0.4 vitamin C, 0.1 $CaCl_2$, 3 $MgCl_2$, 25 glucose). Brainstem slices of 300 μm thickness were prepared with a vibratome (Leica, VT1200S) and stored in carbogenized extracellular solution (in mM: 125 NaCl, 25 $NaHCO_3$, 2.5 KCl, 1.25 NaH_2PO_4, 2 $CaCl_2$, 1 $MgCl_2$, 25 glucose) at 37°C for 45 minutes, and thereafter at room temperature. Whole cell patch clamp recordings were made at -70 mV holding potential from visually identified postsynaptic principal cells of the medial nucleus of the trapezoid body no longer than 3 h after decapitation with an EPC9 patch-clamp amplifier (Heka) at room temperature. Fluorescent calyces were visualized by isolating excitation light at 488 nm with a monochromator (Visitron Systems,

Polychrome II) and observed using an Axioskop (Zeiss) with a 60x objective (Olympus) coupled to a 1.6x pre magnification (Zeiss) and a CCD camera (Diagnostic Instruments Inc., Spot RT monochrome). Afferent presynaptic axons were stimulated close to midline of the brainstem with a bipolar electrode (FHC, PBSA0275). Recording electrodes were pulled from 2 mm thick-walled glass (Hilgenberg, 1807515) using a horizontal puller (Sutter Instruments, P97). Patch-pipettes had an open tip resistance of 1.6-2.5 MΩ. Access resistance (R_s) ranged from 3.2-6 MΩ for electrodes filled with intracellular solution containing (in mM): 130 Cs-gluconate, 10 CsCl, 5 Na_2-phosphocreatin, 10 HEPES, 5 EGTA, 10 TEA-Cl, 4 Mg-ATP, 0.3 GTP. Current traces were recorded with Pulse software (Heka) and analysed with custom written Igor (Wavemetrics) routines.

4 Results

4.1 Immunlocalization of exocyst subunits in the calyx of Held

We wanted to investigate the distribution of exocyst subunits Sec6, Sec8 and Sec15 in the presynaptic compartment. Initial immunocytochemistry experiments, which addressed the localization of exocyst subunits in hippocampal neurons, showed colocalization of Sec8 with the synaptic vesicle marker synaptotagmin (Hsu et al., 1996). A similar result was obtained from immunocytochemistry experiments with differentiated PC12 cells for the exocyst subunit Sec6 (Kee et al., 1997). In both studies no perfect colocalization of exocyst subunits and vesicle markers was observed, but the subunits were also detected outside synaptic vesicles positive areas. Hazuka et al. addressed the function of exocyst subunits at active synapses by analyzing the presence of Sec6 in conjunction with FM1-43 uptake experiments in hippocampal neurons. While 16% of the overall Sec6 signal was present in functional synapses, which were scored by the presence of synapsin and FM1-43, only 33% of active synapses were positive for Sec6 suggesting that this exocyst subunit is not essential in mature synapses for synaptic vesicle cycling (Hazuka et al., 1999). However, recent findings revealed that the antibodies used in the before mentioned studies do not label the whole exocyst complex population. Yeaman *et al.* showed that different antibodies against the same subunit reveal positive signal in varying compartments suggesting that epitopes are masked by subunit assembly or binding of interaction partners, which results in false-negative antibody signal (Yeaman et al., 2001). Hence, open questions regarding the function of exocyst subunits in mature synapses remain. The generation of new antibodies against Sec8 and Sec15, which are suited for immunocytochemistry in methanol fixed tissue, prompted us to investigate the distribution of these subunits in the presynaptic compartment again (Wang et al., 2004b). Apart from new antibodies, the giant size and clear compartmentalization of the calyx of Held comprise advantages for localization studies of the presynaptic compartment, which can lead to new findings about exocyst localization and might deliver hints to exocyst function in the nerve ending. This study is the first characterization of monoclonal antibody 8S2E12 against Sec8 and monoclonal antibody 15S14H1 against Sec15 in paraformaldehyde fixed brain tissue. Monoclonal antibody 9H5 against Sec6 was used for labelling of paraformaldehyde fixed brain tissue before (Vik-Mo et al., 2003).

For immunohistochemistry (IHC) of exocyst subunits in brain tissue rats were anaesthetized at postnatal day 21 (P21) and transcardially perfused with 4%

paraformaldehyde. Brainstem slices of ~80 µm thickness were prepared on a vibratome and subjected to immunohistochemistry. The MNTB of the embedded sections was imaged with a confocal microscope and the image stacks reconstructed and analysed with Amira.

4.1.1 *Immunolocalization of Sec6*

Immunohistochemistry with the monoclonal antibody 9H5 against Sec6 results in a sparse, punctuate staining pattern throughout the MNTB (Figure 13). Signal is detectable both in the principle cell and the calyx of Held, but almost no overlap between Sec6 and the vesicle marker VGlut1 can be observed. Instead, Sec6 is found close to synaptic vesicle clouds but opposite to the presynaptic membrane. In rare cases Sec6 signal is also detectable inside synaptic vesicle clouds and juxtaposed to the presynaptic side of the plasma membrane.

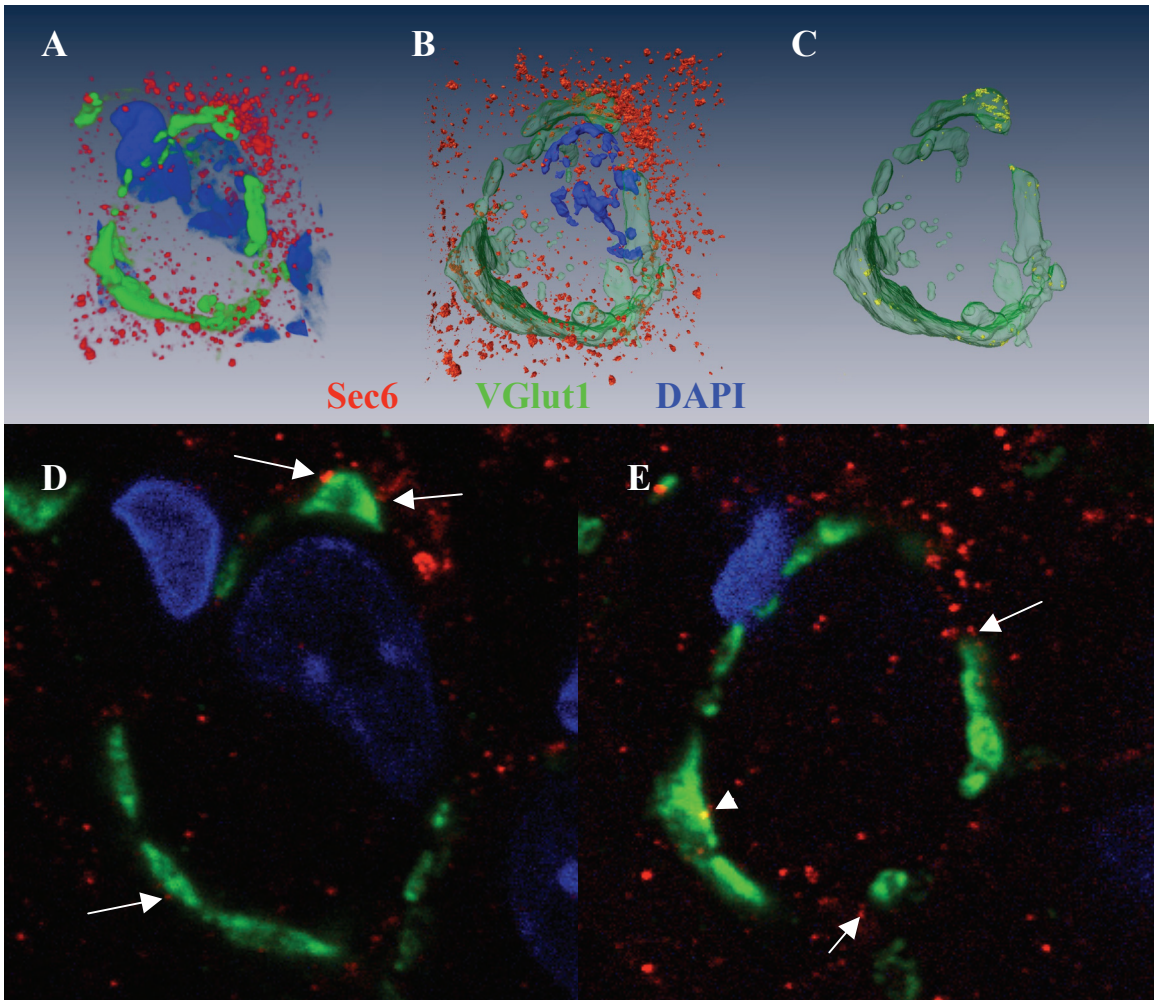

Figure 13. Sec6 is present in the calyx of Held and shows marginal overlap with the vesicle marker VGlut1. Paraformaldehyde fixed brainstem slices of P21 rats were subjected to immunohistochemistry and image stacks acquired with a confocal microscope. **(A)** Intensity based three-dimensional overview of tissue staining displays a punctuate **Sec6 (red)** pattern throughout the tissue, whereas **VGlut1 (green)** outlines the synaptic vesicle clusters of the calyx of Held. The uncondensed nucleus of the principle cell is stained with **DAPI (blue)**. **(B)** Binarized surface reconstruction of all three channels in which nuclei and synaptic vesicles, which do not refer to the central principle cell, have been removed. **(C)** Removal of Sec6 signal outside synaptic vesicle clusters reveals that only little Sec6 signal resides inside vesicle clusters **(yellow)**. Lower two images **(D)** and **(E)** show single confocal sections of the image stack. **(D)** Arrows in the orthoslice indicate Sec6 in close proximity to synaptic vesicles, whereas in **(E)** an arrowhead points towards a rare example of Sec6 in synaptic vesicle clouds and juxtaposed to the presynaptic membrane.

4.1.2 Immunolocalization of Sec8 and Sec15

In contrast to the sparse labelling observed for Sec6, the entire MNTB was immunoreactive for the monoclonal antibody 8S2E12 against Sec8 and the monoclonal antibody 15S14H1 against Sec15 (Figure 14). For both antibodies immunofluorescence is found in the whole cytoplasm of the principle cell and some of the signal is found in the nucleus. Similarly, no preference of the antibodies for a certain compartment inside the calyx of Held is detectable. Immunoreactivity is found towards the presynaptic membrane, in vesicle clouds labelled with VGlut1 antibody, in the cytosol and towards the membrane, which is directed away from the postsynaptic cell. Thus, subunits Sec8 and Sec15 seem to be present in the whole presynaptic compartment. It has to be stressed that the specificity of these antibodies in paraformaldehyde fixed tissue was not tested before. Therefore, we also tried to perfuse animals with a methanol-based fixative (Carnoy's solution) in order to compare the staining patterns for differently fixed tissue. When transcardial perfusions with Carnoy's fixative were performed, blood vessels constricted immediately upon contact with the solution and prevented the fixative from perfusing the brain homogeneously. In addition, the solution caused heavy shrinkage of brain regions but other brain regions, which have had no contact with the fixative, retained the normal size. Thus, brain sections and nuclei were deformed and therefore not suited for localization studies. Taken together, it cannot be excluded that the signal acquired from the IHC with antibodies 8S2E12 against Sec8 and 15S14H1 against Sec15 is false positive.

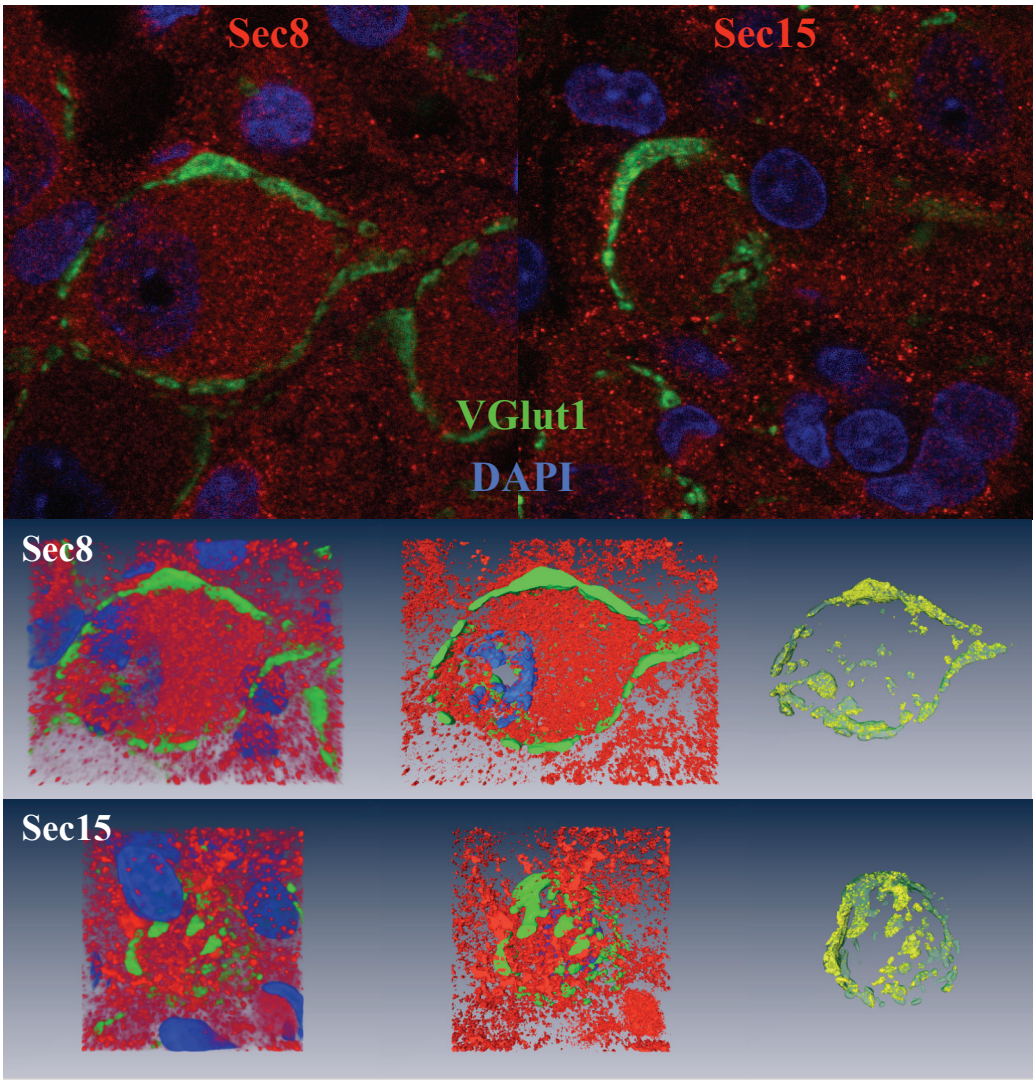

Figure 14. Immunohistochemistry of brainstem slices with antibodies against Sec8 (8S2E12) and Sec15 (15S14H1). P21 rats were perfused with paraformaldehyde and subjected to IHC with antibodies against **Sec8 (top left and center, red)**, **Sec15 (top right and bottom, red)** and **VGlut1 (green)**. DNA was stained with **DAPI (blue)**. **(Top)** Single confocal sections show intense immunoreactivity in the MNTB for antibodies 8S2E12 (Sec8, left) and 15S14H1 (Sec15, right). Both antibodies show colabelling with VGlut1 positive areas and are also found in the nucleus. No preference towards any compartment inside vesicle clusters is detectable for both antibodies. **(Middle)** 3D view of antibody staining against Sec8. Intensity based overview on the left and surface reconstruction in the centre reveal ubiquitous immunoreactivity in the MNTB. The left side shows only Sec8 signal inside VGlut1 positive areas and reveals abundant presence of Sec8 in this compartment **(Bottom)** 3D view of Sec15 immunoreactivity. Left image shows intensity based overview of Sec15 signal found throughout the MNTB, whereas the centre image represents binarized surface reconstruction and reveals that nuclei are slightly omitted. The right image illustrates only Sec15 immunoreactivity inside VGlut1 areas.

4.2 Cloning of GFP-fusion proteins into viral vectors

Since IHC experiments did not yield conclusive results about the localization of exocyst subunits in the calyx of Held, GFP-fusion constructs were cloned into an adeno-associated virus (AAV) vector to transduce GBCs with GFP-fusion transgenes of exocyst subunits and to localize them in the nerve terminal. It has not been proven so far whether GFP-fusion proteins of exocyst subunits localize like their endogenous proteins. Similarly no *in vitro* reconstitution assay of the exocyst complex has been performed in which one subunit was tagged with a fluorescent protein to test whether this tagged subunit can still incorporate into the complex. However, knockdown of Exo70 with siRNA can be rescued by the overexpression of GST tagged Exo70, which indicates that at least this subunit is functional when proteins of similar size like GFP are fused to its N-terminus (Liu et al., 2007). Also, binding partners of Exo70 like the Arp2/3 complex or Sec8 are able to bind to GFP-Exo70, which shows that the fluorescent protein tag allows binding of some interaction partners (Zuo et al., 2006). In addition, overexpression of GFP-Exo70 can induce the formation of actin-based membrane protrusions for which endogenous Exo70 is necessary indicating that the GFP-fusion protein of Exo70 is able to fulfil the function of the endogenous protein in this process.

Apart from localization studies of exocyst subunits, perturbation of exocyst function by means of viral vectors was also desired to elucidate the function of the multiprotein complex in the calyx of Held. In this regard, a truncation construct of Exo70, which was reported to act as a dominant-negative (Gerges et al., 2006; Inoue et al., 2003; Inoue et al., 2006; Liu et al., 2007; Pommereit and Wouters, 2007; Zuo et al., 2006), was also cloned into viral vectors.

N-terminal GFP-fusion genes of exocyst subunits Sec3, Sec6, Sec8, Sec15, Exo70 and the N-terminal fragment of Exo70 (Exo70Nter, aa 1-384) were excised from the pAcGFP1 vector and cloned into the AAV backbone (pAM). The restriction enzymes, which were employed for the cloning procedure, are shown in Table 4 for the individual plasmids. An exemplary map of the pAM vector is shown in Figure 15.

Table 4. Restriction enzymes used for cloning of exocyst subunit GFP-fusion proteins. GFP-fusion genes of exocyst subunits were excised from pAcGFP1 with the illustrated restriction enzymes. The AAV pAM vector was digested with the depicted enzymes to insert exocyst transgenes.

	GFP-Sec3	GFP-Sec6	GFP-Sec8	GFP-Sec15	GFP-Exo70	GFP-Exo70Nter
pAcGFP1	NheI/MfeI	NheI/MfeI	NheI/MfeI	BamHI/HindIII	NheI/MfeI	NheI/MfeI
pAM	SpeI/MfeI	SpeI/MfeI	SpeI/MfeI	BamHI/HindIII	SpeI/MfeI	SpeI/MfeI

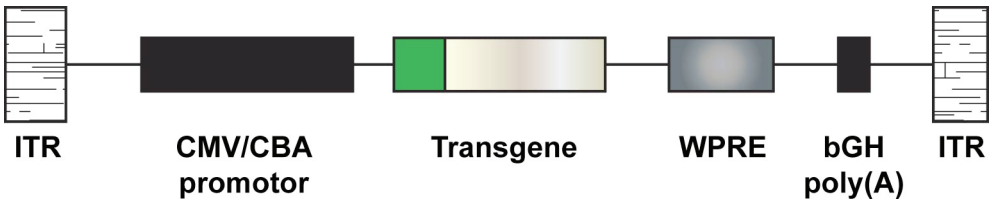

Figure 15. Schematic diagram of AAV vector (pAM). The expression cassette is flanked by adeno-associated virus 2 (AAV2) inverted terminal repeats (ITR). Expression of genes is driven by the cytomegalovirus enhancer/chicken β-actin (CMV/CBA) promoter and increased by a downstream woodchuck hepatitis B virus posttranscriptional element (WPRE), which is followed by the bovine growth hormone (bGH) poly(A) signal.

When GFP-fusion genes of exocyst subunits are introduced into the pAM vector, the size of the DNA strand from ITR to ITR exceeds the wildtype genome of AAV, which is 4.7 kb. To circumvent potential packaging problems of large DNA strands into AAV capsids, GFP-fusion proteins of excyst subunits were also cloned into the lentiviral vector FUGW, which has a larger packaging capacity of ~10 kb. Along those lines, a synthetic primer pair (Figure 16) was cloned between the AgeI and EcoRI site in the FUGW vector to create a cloning site for exocyst transgenes. The restriction enzymes, which were used for cloning of excoyst fusion genes from pAcGFP1 into FUGW-MCSI, are depicted in Table 5 for each individual plasmid pair. A schematic plasmid map of the FUGW vector is shown in Figure 17.

```
       NheI  MfeI    NdeI  HpaI
         ⌈     ⌈       ⌈     ⌈
5′-CCGGTGCTAGCCAATTGCATATGGTTAACG-3′
       ||||||||||||||||||||||||||||
       ACGATCGGTTAACGTATACCAATTGCTTAA
```

Figure 16. Primer pair DS83:DS84 used for creation of a multiple cloning site in the FUGW vector. FUGW was opened by digestion with AgeI and EcoRI and the hybridized primer pair was inserted to create FUGW-MCS1 for insertion of exocyst transgenes.

Table 5. Depicted restriction enzymes were used to clone GFP-fusion genes of exocyst subunits into the lentiviral FUGW-MCSI vector.

	GFP-Sec3	GFP-Sec6	GFP-Sec8	GFP-Sec15	GFP-Exo70
pAcGFP1	NheI/HpaI	NheI/HpaI	NheI/HpaI	NheI/HpaI	NheI/HpaI
FUGW-MCSI	NheI/HpaI	NheI/HpaI	NheI/HpaI	NheI/HpaI	NheI/HpaI

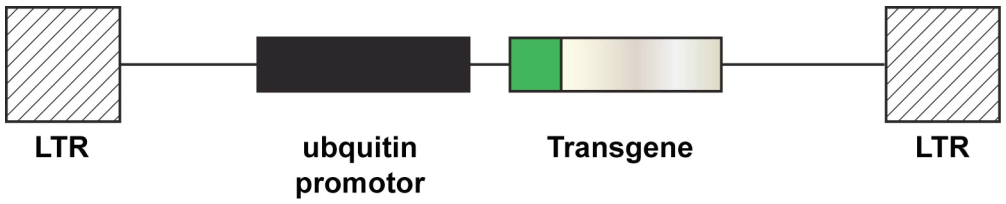

Figure 17. Schematic diagram of the lentiviral vector FUGW. The expression cassette is flanked by lentiviral long terminal repeats (LTR). Expression of the transgene is driven by an ubiquitin promoter.

4.3 Adeno-associated virus production

In order to transduce globular bushy cells (GBCs) with viral vectors and to localize GFP-fusion proteins of exocyst subunits in the calyx of Held, all generated pAM plasmids were used for production of recombinant adeno-associated viral (rAAV) particles. The standard protocol for generation of rAAV did not result in sufficiently high titters, which are necessary for stereotaxic injections into the ventral cochlear nucleus and acquisition of fluorescence signal in the calyx of Held. In many cases, hippocampal cells, which were used to test the infectivity of the virus stock, died within 2 days after the addition of virus solution and no fluorescence was detectable. Since other pAM plasmids, which encode for mOrange (monomeric Orange, i.e. cytosolic) or mGFP (myristoylated GFP, i.e. membrane targeted) and were processed in parallel or at least with identical reagents, yielded reliably sufficient infective particles, the reason for the absence or low number of infective particles most likely originates from the pAM plasmids, which encode for GFP-fusion proteins of exocyst subunits. Virus production was optimized for transfection efficiency of producer cells and molar relations of pAM plasmids to helper constructs were varied to obtain higher virus titters. Out of all pAM plasmids only GFP-Exo70 and GFP-Exo70Nter yielded a suitable virus stock, whereas all other pAM plasmids could not be used successfully to generate high numbers of rAAV particles for stereotaxic injections.

4.4 Lentivirus production

The experienced problems in the generation of rAAV particles might have been caused, because the packaging capacity of adeno-associated virus was exceeded by the insertion of GFP-fusion genes of exocyst subunits. Therefore generated FUGW vectors were used for production of lentiviral particles, which have a larger packaging capacity of ~10 kb. Only lentiviruses encoding for GFP-Sec15 could be generated, which satisfied the criterion for stereotaxic injection and transduced globular bushy cells in the VCN. Unfortunately, the number of lentiviral particles was not sufficient for any of the exocyst

GFP-fusion proteins to infect a sufficient number of GBCs in order to be able to acquire images of the presynaptic terminal in the MNTB.

4.5 Viral expression of exocyst subunits in cultured neurons

To control for correct expression of GFP-Exo70 and GFP-Exo70Nter from viral vectors, hippocampal neurons were transduced with rAAV particles at DIV3 (days in vitro) and resuspended 10 days later in SDS-sample buffer. Whole cell lysates were separated by SDS-PAGE and transferred onto membranes to verify expression of correctly sized proteins by Western Blot. Antibodies against GFP were used to detect GFP-fusion proteins and to analyse for potential cleavage of GFP from the fusion proteins.

Western Blot confirmed the correct size of GFP-Exo70 and GFP-Exo70Nter, which have a molecular mass of 98 (72+26) and 68 (42+26) kDa, respectively (Figure 18). Additionally, no cleaved GFP was detectable in whole cell lysates of neurons, which expressed the transgenes, suggesting that GFP-fusion proteins are expressed stably and are not degraded in neurons.

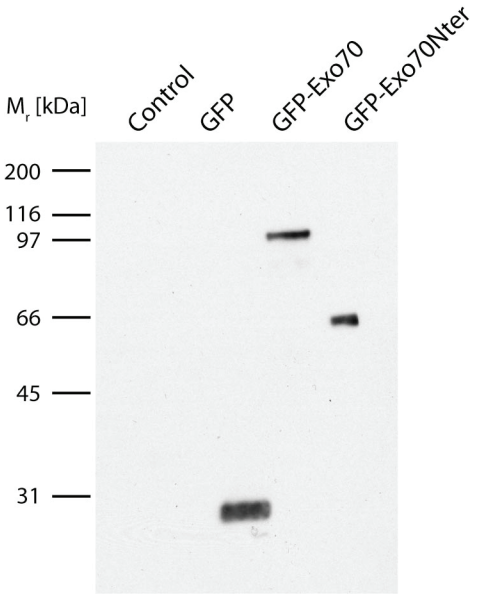

Figure 18. GFP-fusion proteins of exocyst subunits Exo70 and Exo70Nter are expressed correctly from viral vectors. Immunoblot of hippocampal whole cell lysates against GFP. Hippocampal cells were transduced with rAAV at DIV3 for 10 days and lysed with SDS sample buffer. Cell lysates were separated via SDS-PAGE an analysed by Western Blot using anti-GFP antibodies. Both transgenes show the correct size on the Western Blot of 98 and 68 kDa for GFP-Exo70 and GFP-Exo70Nter, respectively. No traces of cleaved GFP are detectable.

4.6 Transduction with GFP-Exo70 induces sprouting in hippocampal neurons

Earlier publications showed, that overexpression of GFP-Exo70 in NRK, HeLa or primary hippocampal cells induces the formation of actin-based membrane protrusions (Pommereit and Wouters, 2007; Wang et al., 2004b; Xu et al., 2005). The C-terminus of Exo70 binds to Arp2/3 complex and this interaction is crucial for induction of these actin structures since deletion or mutation of residues 571-572 and 628-630 abolishes the formation of membrane extensions and dramatically decreases the interaction with the Arp2/3 complex (Zuo et al., 2006). Thus, membrane protrusions were not observed upon overexpression of GFP-Exo70Nter, which lacks its C-terminus (Liu et al., 2007; Pommereit and Wouters, 2007; Zuo et al., 2006). To test the expression of GFP-Exo70 and GFP-Exo70Nter by viral vectors cultivated hippocampal neurons were transduced at DIV6 with rAAV. Cells were fixed at DIV20±1 with paraformaldehyde and imaged to analyse the expression pattern of GFP-fusion proteins. As control hippocampal neurons were infected with rAAVs, which encode for mGFP (myristoylated GFP, i.e. membrane targeted).

Some of the hippocampal cells, which had been infected with the full-length protein GFP-Exo70, showed abnormal sprouting when compared to only mGFP expressing cells (Figure 19 – A_i, B_i). Although this observation was not quantified in detail, GFP-Exo70 overexpressing neurons seem to have more dendritic spines compared to mGFP expressing cells on the dendrites and the cell body (Figure 19 - B_3, B_4). In some cases the cell body and dendrites were completely covered with spine like structures or long protrusions extended around the cell soma, when GFP-Exo70 was overexpressed (Figure 19 - B_2). Importantly, this phenotype is not observed upon overexpression of the dominant-negative truncation construct GFP-Exo70Nter (Figure 19 - C_i). Hence, virus mediated overexpression of GFP-Exo70 and GFP-Exo70Nter reproduced earlier findings in permanent cell culture and primary hippocampal neurons and further confirms correct expression of exocyst transgenes from generated rAAV particles.

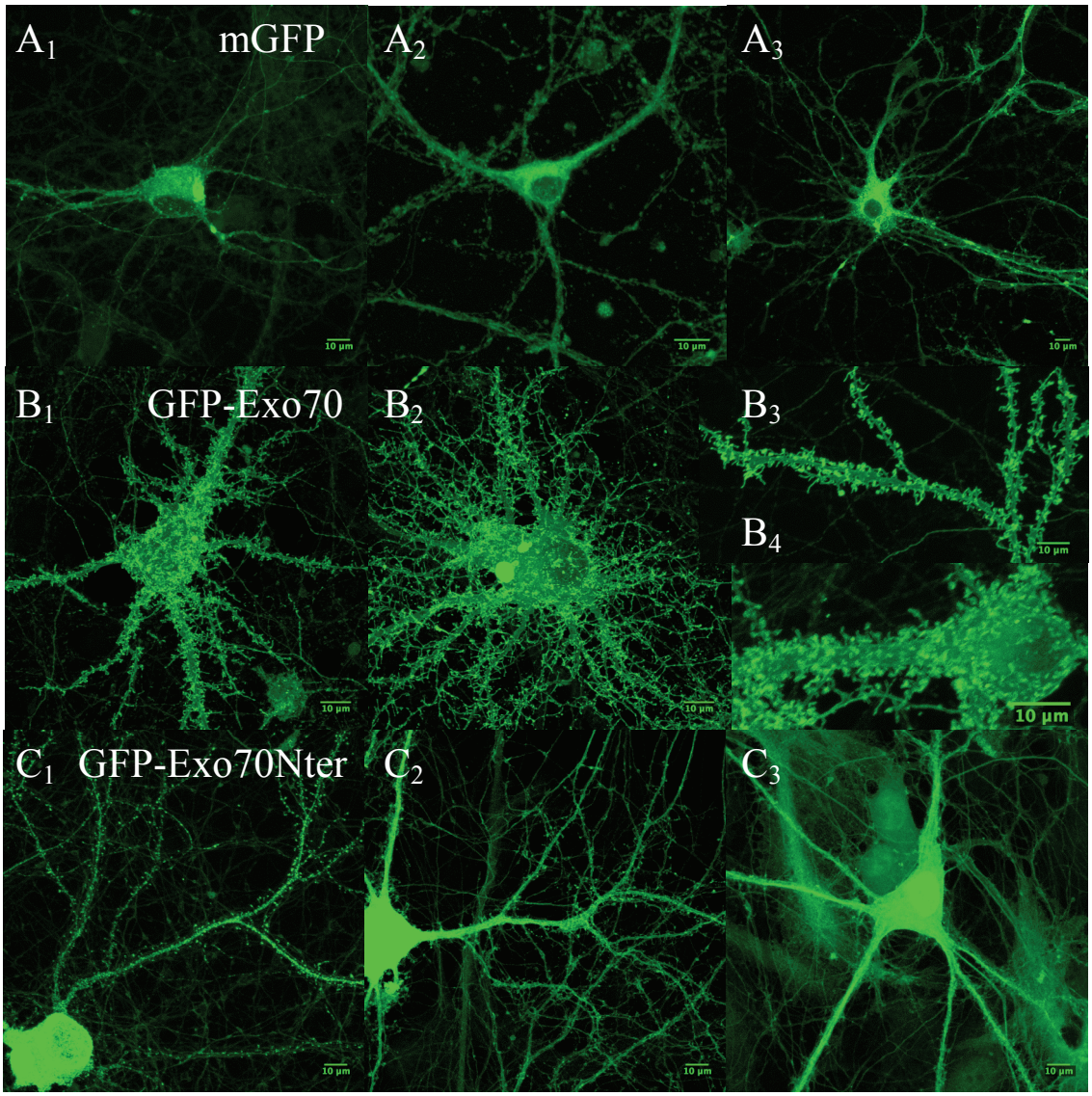

Figure 19. Transduction of hippocampal neurons with GFP-Exo70 but not with GFP-Exo70Nter induces formation of membrane protrusions. Cultivated hippocampal neurons were infected with rAAVs at DIV6 and fixed 14±1 days afterwards. Images represent maximum z-projections of confocal image stacks. While **(C_i) GFP-Exo70Nter** expressing neurons do not show evident increase in protrusive structures compared to **(A_i) mGFP** expressing cells, **(B_i) GFP-Exo70** overexpressing neurons show an increase in membrane structures on the surface of **(B_3) dendrites** or the **(B_4) cell soma**. For some GFP-Exo70 overexpressing cells dramatic sprouting can be observed which emanates from the cell soma and dendrites **(B_2).**

4.7 Overexpression of exocyst subunits by means of viral vectors *in vivo*

The generation of viruses, which encode for GFP-fusion proteins of exocyst subunits, enabled us to use stereotaxic injections to analyse the expression of these transgenes *in vivo*. First, we wanted to localize the GFP-fusion proteins in the nerve terminal to see whether the expression pattern suggests a particular function for the respective subunit in the presynaptic compartment. Likewise, we wanted to test whether overexpression of GFP-Exo70 or GFP-Exo70Nter provoke morphological phenotypes similarly to what we found in hippocampal cell cultures. In the second experiment, synaptic transmission was to be analysed by electrophysiological measurements to elucidate potential changes in synaptic vesicle cycling, when GFP-Exo70 or GFP-Exo70Nter are overexpressed.

4.7.1 Stereotaxic coordinates for the VCN of P2 rats

Since perturbations by overexpression of exocyst subunits in synaptic maturation and/or synaptic vesicle cycling were desired to happen as early as possible during development, a surgery procedure and stereotaxic coordinates for P2 rats had to be developed first. The variability in size between litters from different mothers and even between littermates requires a relative measurement to adopt injection coordinates according to the size of the brain. Therefore, the distance between bregma and lambda was noted for each individual pub and different coordinates were used to identify reliable coordinates for targeting the VCN with injection capillaries. Fluorescent nanobeads with a diameter of 40 nm were injected and animals sacrificed after surgery by decapitation. The brain was dissected and fixed overnight in paraformaldehyde before fluorescent beads were localized in vibratome sections of ~100 μm thickness. The coordinates for rats with a bregma to lambda distance of 2.8 – 3.3 mm is given on the left side of Table 6, whereas the coordinates for slightly larger pubs with a bregma to lambda distance of 3.4 – 4.0 are illustrated on the right side of Table 6.

Table 6. Injection coordinates into the ventral cochlear nucleus of Sprague Dawley rats. Coordinates are relative to bregma.

Bregma – Lambda: 2.8 – 3.3 mm			
X	**Y**	**Z**	**Depth**
0.9	-7.5	0.45	6.5-6.0
0.9	-7.1	0.45	6.5-6.0
0.9	-6.7	0.45	6.5-6.0
0.8	-7.3	0.45	6.5-6.0
0.8	-6.9	0.45	6.5-6.0
0.8	-6.5	0.45	6.5-6.0

Bregma – Lambda: 3.4 – 4.0 mm			
X	**Y**	**Z**	**Depth**
0.95	-8.0	0.45	6.5-6.0
0.95	-7.6	0.45	6.5-6.0
0.95	-7.2	0.45	6.5-6.0
0.85	-7.8	0.45	6.5-6.0
0.85	-7.4	0.45	6.5-6.0
0.85	-7.0	0.45	6.5-6.0

4.7.2 Localization of GFP-Exo70 and GFP-Exo70Nter in the calyx of Held

With the stereotaxic coordinates at hand a mixture of rAAV was injected into the VCN of 2-day-old rats. One virus encoded for cytosolic mOrange to label the whole presynaptic terminal, whereas the other virus encoded for the protein of interest, either GFP-Exo70 or GFP-Exo70Nter. With this combination of viruses it is possible to delineate the entire volume of the calyx of Held by means of the cytosolic mOrange staining and to locate GFP fluorescence of the protein of interest therein. To be able to correlate the findings from localization experiments with electrophysiological data we perfused virus injected rats at the same age of postnatal day 13±1 at which functional experiments were performed later on. Since we were also interested in potential effects on the maturation of the calyx of Held, which are provoked by overexpression of exocyst subunits, rats were also sacrificed at postnatal day 21 at which day the calyx has reached its mature morphological state. Hence, if overexpression of exocyst subunits interferes with the maturation of the presynaptic terminal, we should be able to reveal this effect by comparing the morphology of calyces, which are either only positive for mOrange or show a GFP signal in addition to the mOrange fluorescence in the terminal. After fixation of brain tissue, the brainstem was sliced into ~80 μm vibratome sections and images of the MNTB were acquired on a confocal microscope.

The expression pattern of GFP-Exo70 reveals an age dependent localization of the GFP-fusion protein. While GFP fluorescence is cytosolic in P13±1 animals, a prominent enrichment of GFP signal is detectable at the plasma membrane of GBCs from P21 rats (Figure 20). At both ages a uniform distribution of GFP fluorescence is noted throughout the cytoplasm, with no bright accumulations of GFP signal, which could indicate elevated presence of GFP-Exo70 at a certain compartment or single sites. Therefore, albeit the mere presence and the age dependent plasma membrane enrichment, the overexpression of GFP-Exo70 does not yield a hint towards a particular function of this subunit in the presynaptic terminal. Instead it suggests a rather general role for this subunit, which is related to the developmental stage of the presynaptic terminal since it seems to be redistributed to the plasma membrane only at later developmental stages.

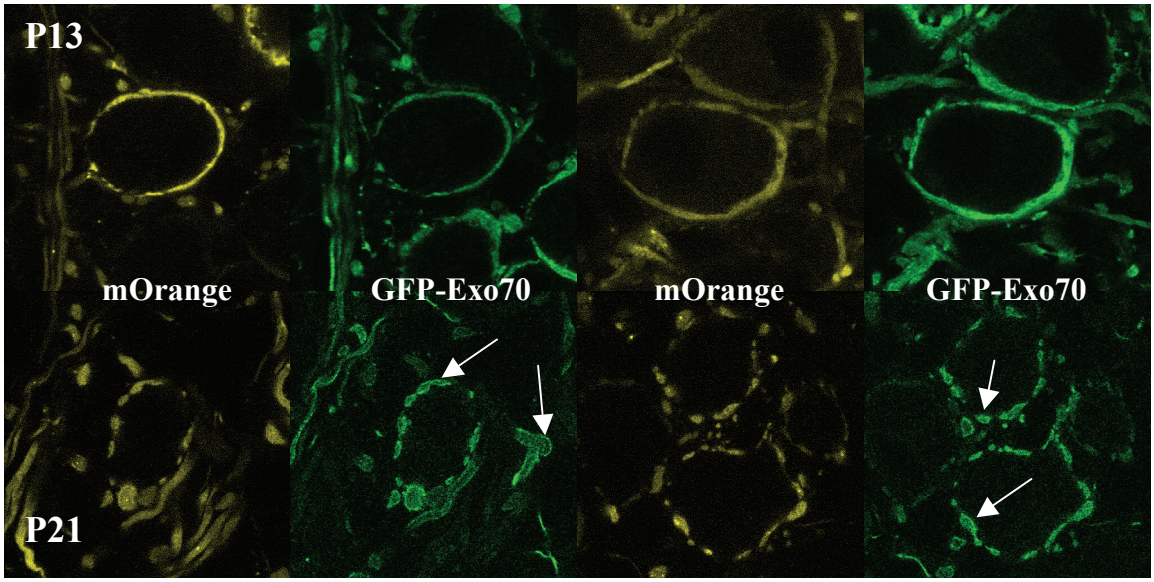

Figure 20. GFP-Exo70 is evenly distributed in the calyx of Held at P13±1 and P21 but only found on the plasma membrane at P21. rAAVs encoding for mOrange and GFP-Exo70 were injected into the VCN of P2 Sprague Dawley rats. Animals were sacrificed at **P13±1 (upper panels)** or at **P21 (lower panels)** and confocal image stacks of the MNTB were acquired. The images represent single confocal sections of either mOrange or GFP-Exo70 channel. **Arrows** indicate membrane enrichment of GFP-Exo70, which is only evident for calyces from P21 animals and absent in nerve terminals from P13±1 rats. At both ages the GFP signal is evenly distributed without exhibiting bright clusters, which could indicate elevated presence of the exocyst subunit or preference towards a presynaptic subcompartment.

In respect to 3D anatomy of the calyx of Held, no gross differences are detected between GBCs, which express mOrange alone or together with GFP-Exo70 (Figure 21). For younger animals of 13±1 days the calyx exhibits a closed spoon like shape, which is covering approximately one side of the postsynaptic cell. In contrast the mature morphological state of calyces from P21 animals is characterized by a fenestrated structure, which is engulfing the postsynaptic cell from all sides with finger like protrusions and swellings along those protrusion in unassigned intervals (Figure 21). For both ages, the characteristic developmental stage is recognized independently of whether GFP-Exo70 is coexpressed with mOrange. In addition, raw morphology is not strikingly altered at both ages indicating that the overexpression of GFP-Exo70 does not influence cellular processes, which govern the maturation of the calyx of Held.

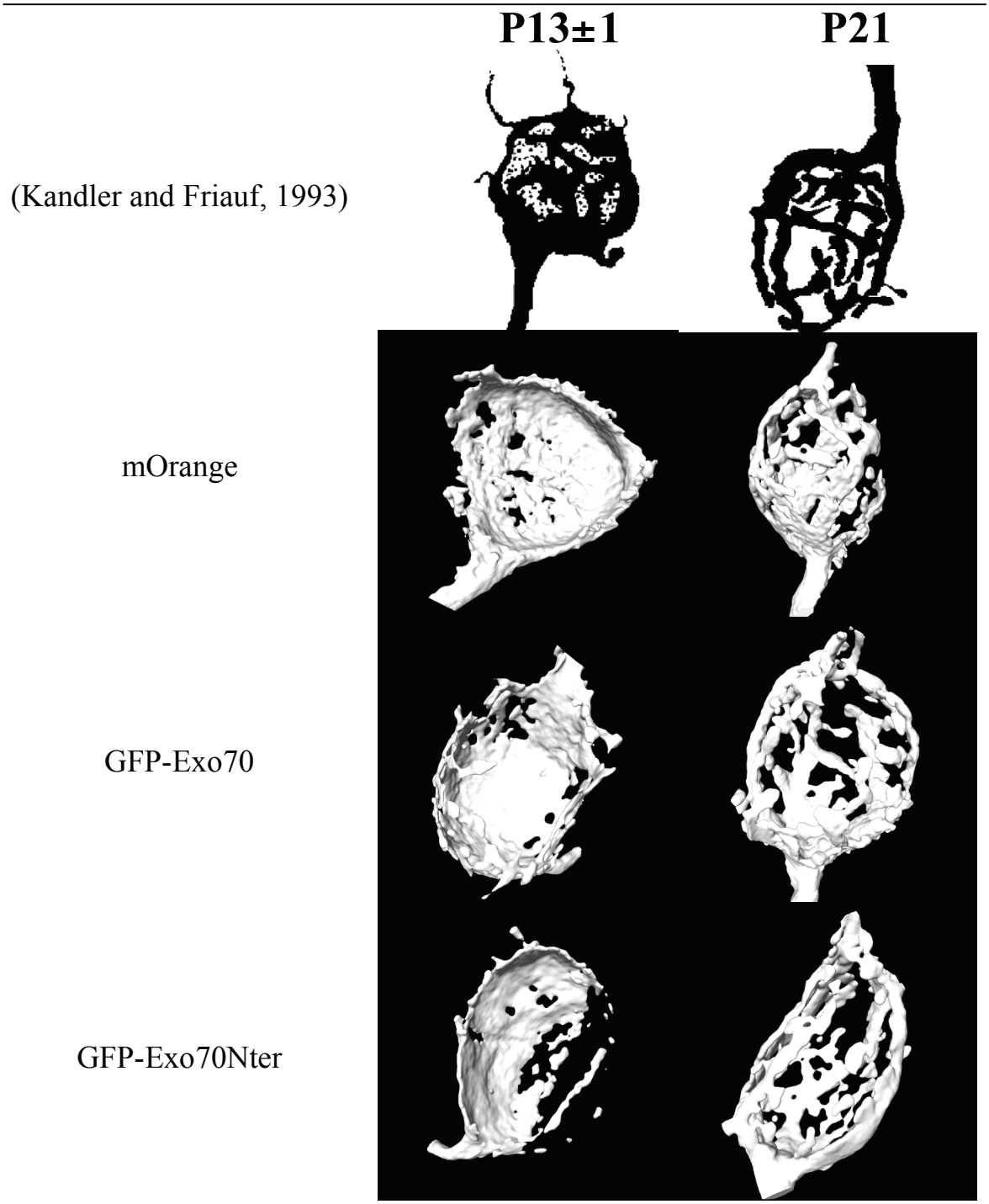

Figure 21. Overexpression of GFP-Exo70 or GFP-Exo70Nter in globular bushy cells allows for maturation of the calyx of Held. The upper two images are drawings of biocytin labelled calyces from (Kandler and Friauf, 1993) and represent developmental stages schematically. White calyces on black background are 3D reconstructions of the mOrange channel, which were conducted in Amira software. Text on the left side illustrates whether calyces only expressed mOrange or whether they were also positive for GFP-Exo70 or GFP-Exo70Nter. The calyx of Held undergoes maturation in all cases despite overexpression of exocyst transgenes in globular bushy cells. While calyces have a closed spoon like shape at P13±1 the development into a fenestrated structure with digitiform calycine collaterals is evident independently of the overexpression of exocyst subunits.

In contrast to the full-length fusion protein of Exo70 the dominant negative truncation construct GFP-Exo70Nter is not enriched at the plasma membrane neither for developing calyces in P13±1 animals nor in mature nerve terminals from P21 rats (Figure 22). At both ages fluorescence is detected throughout the cytosol of GBCs and the presynaptic compartment. As for the wildtype protein, no accumulation or absence of fluorescence signal is evident at a distinct compartment but fluorescence is rather uniformly distributed. Since the C-terminus of Exo70 is necessary for the interaction of this exocyst subunit with phosophatidylinositol 4,5-bisphosphate ($PI(4,5)P_2$), the lack of a membrane association of the truncation construct GFP-Exo70Nter was expected (Liu et al., 2007). The maturational state of calyces from P13±1 animals can readily be distinguished from nerve endings of P21 rats, if GFP-Exo70Nter is present in these nerve endings (Figure 21). The overall development from a spoon like closed shape into a fenestrated structure therefore seems unaffected by overexpression of GFP-Exo70Nter, which indicates that calyces can still mature when the dominant negative truncation construct of this exocyst subunit is overexpressed. Nevertheless, when calyces from wildtype cells were compared to GFP-Exo70Nter overexpressing ones, a morphological distortion was noticeable in calyces overexpressing GFP-Exo70Nter (Figure 23).

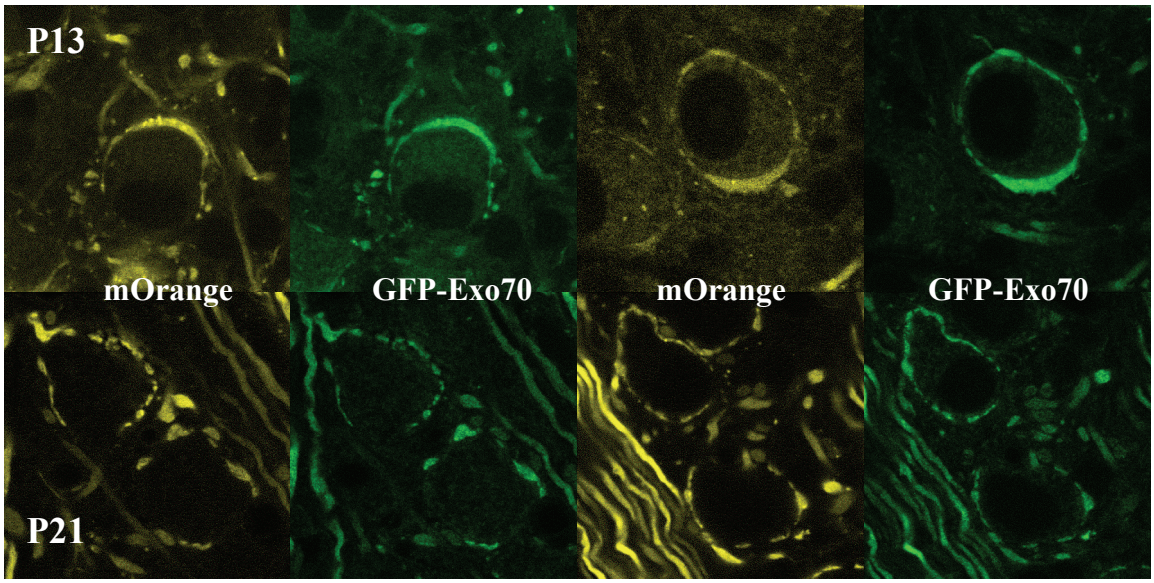

Figure 22. GFP-Exo70Nter is evenly distributed throughout the cytosol of calyces and does not localize to the plasma membrane like the full-length protein. The dominant-negative truncation construct GFP-Ex70Nter and mOrange were transduced into globular bushy cells via injection of rAAVs into the VCN of 2-day-old rats. Animals were sacrificed at **P13±1 (upper panels)** or at **P21 (lower panels)** and confocal image stacks of the MNTB were acquired. The images represent single confocal sections of either mOrange or GFP-Exo70Nter channel. GFP-Exo70Nter is distributed uniformly throughout the cytosol of P13±1 and P21 nerve terminals and is not enriched at plasma membranes. No preference towards a presynaptic compartment is detectable.

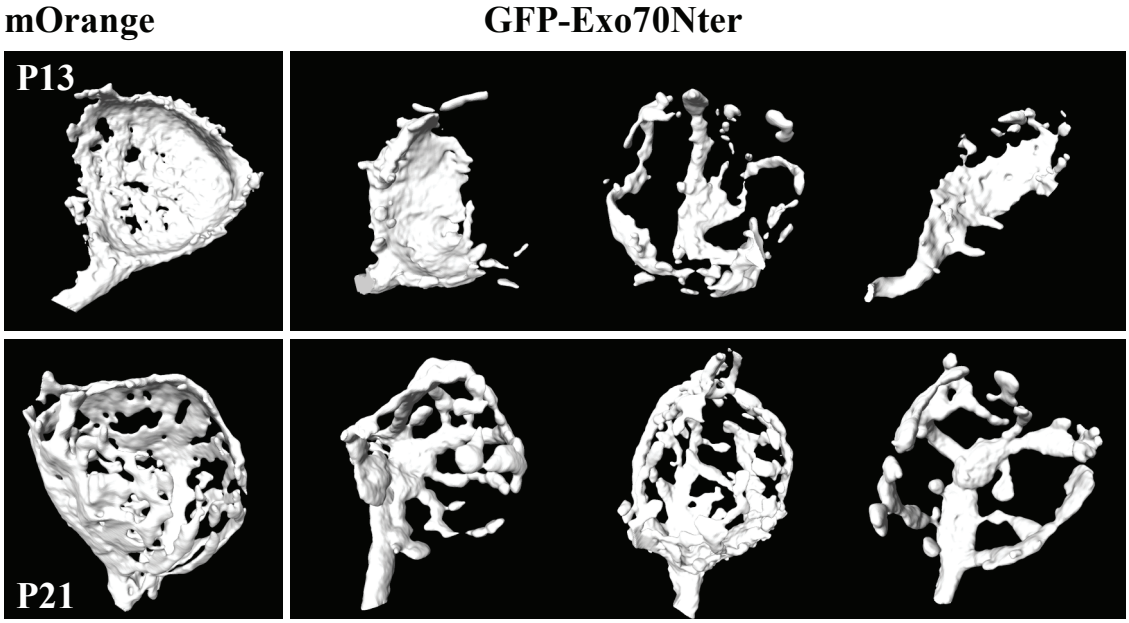

Figure 23. GFP-Exo70Nter overexpressing calyces exhibit a distorted morphology. Images represent 3D reconstructions of confocal image stacks. Only mOrange signal was used to perform reconstructions in Amira. The **left panel** shows reconstructions of calyces, which only expressed mOrange, while the **right panel** illustrates three examples of reconstructed calyces, which overexpressed GFP-Exo70Nter. Immature calyces at **P13±1 (upper row)** can readily be distinguished from adult nerve terminals at **P21 (lower row)** independently whether GFP-Exo70Nter is expressed. If wildtype calyces are compared to GFP-Exo70Nter overexpressing nerve endings (compare left and right panel) the later seem to be smaller and in some cases not equally fenestrated.

4.7.3 Determination of calyx volume

The observation that calyces exhibited a distorted morphology upon overexpression of GFP-Exo70Nter, prompted us to investigate this finding further. Since it was shown in earlier publications that overexpression of GFP-Exo70Nter impedes the incorporation of vesicle cargo into the plasma membrane (Gerges et al., 2006; Inoue et al., 2003; Inoue et al., 2006; Liu et al., 2007) a similar dysfunction might be provoked by the overexpression of GFP-Exo70Nter in the presynaptic compartment and lead to a distorted morphology of the nerve by impairing membrane-addition. To investigate the observation that GFP-Exo70Nter overexpressing calyces show a retarded morphology, the volume of the nerve terminal was taken as a measure. Therefore, confocal image stacks of mOrange labelled calyces from P13±1 and P21 animals were acquired. The animals were also injected with rAAV encoding for either GFP-Exo70 or GFP-Exo70Nter, but only mOrange fluorescence was used for 3D reconstruction. This restriction was necessary to avoid variability, which could arise from incomplete labelling of the nerve terminal or unlike expression patterns of exocyst GFP-fusion proteins and the characteristics of the different fluorescent proteins themselves, i.e. mOrange and GFP. The mOrange image stacks were

cropped to reduce computation time and subjected to a 3D median filter for noise reduction. Manual thresholding was applied to select for mOrange positive voxels and the obtained volume of interest (VOI) was smoothed with a 3D median filter. Structures like bypassing axons or neighbouring calyces, which were also labelled by manual thresholding, but did not belong to the analysed calyx, were identified and removed manually. The volume of the obtained VOI was computed and afterwards the calyx was analysed for the presence or absence of GFP fluorescence and assigned to the respective group, i.e. mOrange only, mOrange with GFP-Exo70, mOrange with GFP-Exo70Nter. Hence, the analysis of the acquired confocal image stacks was performed in a blind fashion. A scheme of the individual image processing steps is illustrated in Figure 24.

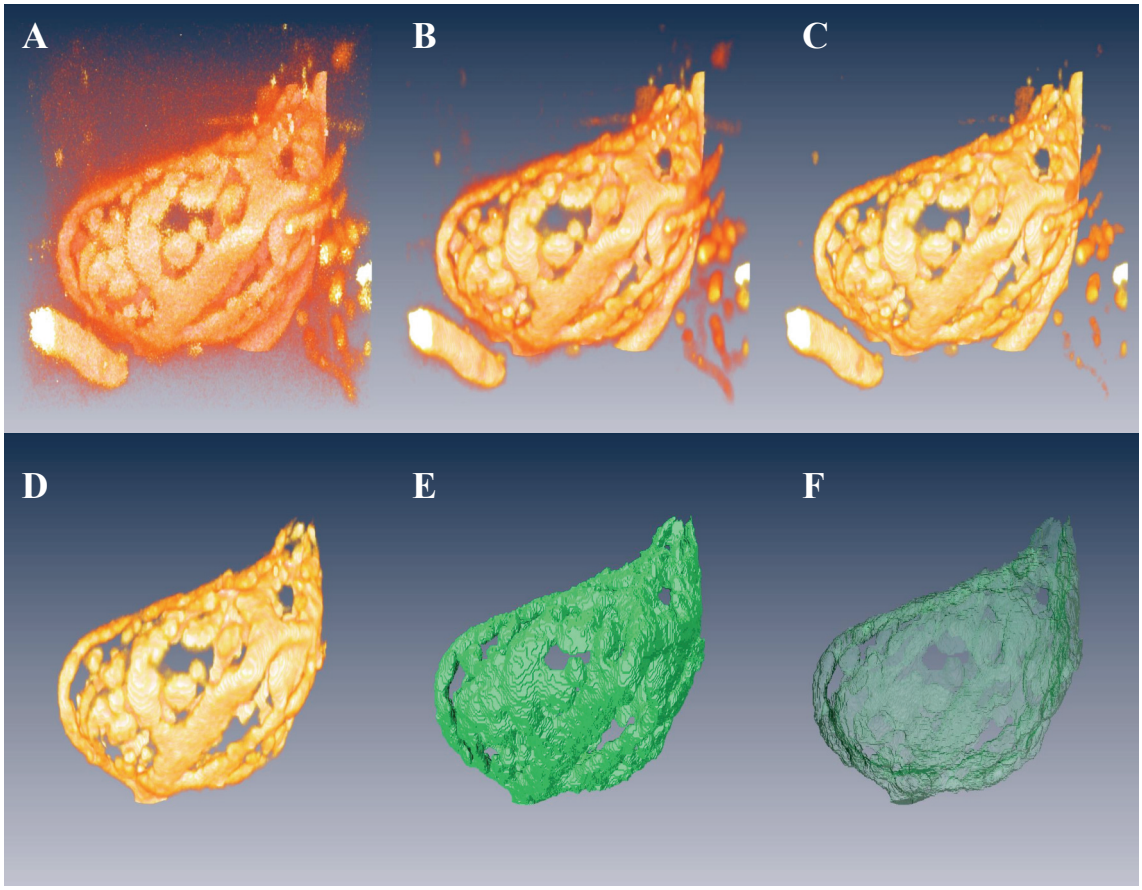

Figure 24. Representation of the image processing steps to determine the volume of the calyx of Held. **(A) Raw data** of confocal image stacks acquired on a Leica SP2 confocal microscope. **(B) 3D median filter** was applied to the raw data to remove noise and smooth the signal. **(C) Manual thresholding** was performed to select for mOrange positive signal and to binarize the image stack. **(D) Clipping**: structures, which were included in the thresholding procedure but did not belong to the calyx of interest, were removed by manual selection. **(E) Surface view** and **(F) transparent surface view** delineate the defined volume.

Results of calyx volume analysis for P13±1 animals are summarized in Figure 25. The volume of wildtype (WT, only mOrange expressing) calyces from P13±1 animals ranges from 319 μm^3 to 1028 μm^3 with a mean of 688 μm^3 and a standard deviation (SD) of 209 μm^3 (n = 22). Measured volumes of GFP-Exo70 positive calyces are more closely distributed with a standard deviation of 130 μm^3 and a minimal volume of 416 μm^3 and a maximal volume of 893 μm^3. The mean volume for 23 analysed calyces was calculated to 682 μm^3. For the dominant negative truncation construct GFP-Exo70Nter the volume of 22 calyces was determined. While the standard deviation of 140 μm^3 is similar to the other two groups the minimal and maximal volumes are lower with 181 μm^3 and 628 μm^3, respectively. Accordingly the mean volume is decreased compared to the other two groups to 422 μm^3. All groups are consistent with a normal distribution as determined by D'Agostino & Pearson omnibus K2 normality test. One-way ANOVA test suggest that it is unlikely that the differences in the mean volume of the three groups are observed due to random sampling ($P<0.0001$), i.e. the populations do not have the same means. The mean volumes of GFP-Exo70 and GFP-Exo70Nter overexpressing calyces were compared to the mean volume of WT terminals with Dunnett's multiple comparison test. This post-hoc test revealed that the mean volumes of WT and GFP-Exo70 positive calyces do not differ, whereas the mean volumes of WT terminals and GFP-Exo70Nter overexpressing terminals do ($P<0.001$). Thus, statistically it is unlikely that random sampling is responsible for the differences between the mean volumes of WT and GFP-Exo70Nter expressing calyces. Experimentally calyx images were acquired from altogether 7 animals with no preference for a particular subregion inside the MNTB, which could bias the samples towards smaller or larger volumes (Ford et al., 2009). Therefore, this result suggests that overexpression of GFP-Exo70Nter in globular bushy cells decreases the volume of immature calyces of Held.

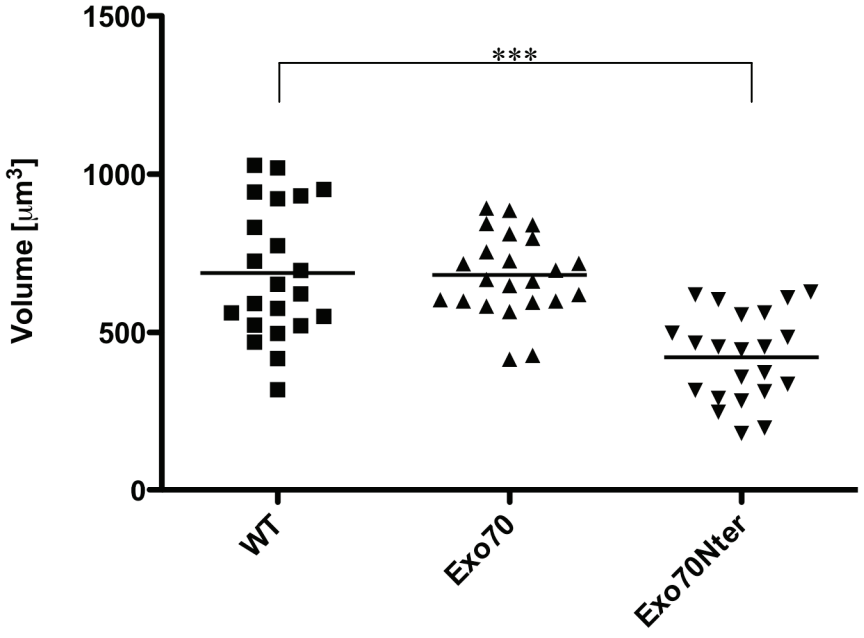

Figure 25. Overexpression of GFP-Exo70Nter decreases the volume of P13±1 calyces. GFP-fusion proteins of exocyst subunit Exo70 or Exo70Nter were transduced together with mOrange into globular bushy cells via stereotaxic injection of rAAVs into the VCN of 2-day-old rats. Animals were perfused with 4% paraformaldehyde at P13±1 and images stacks of calyces were acquired on a Leica SP2 confocal microscope in 100 μm vibratome brain slices. Volume of calyces was determined in a blind fashion as depicted in Figure 24 and data was acquired from 7 different animals. The average volume of GFP-Exo70Nter overexpressing calyces is statistically smaller compared to wildtype nerve endings as determined by one-way ANOVA and Dunnett's multiple comparison test ($P<0.0001$). Volumes of GFP-Exo70 positive calyces do not differ from wildtype distribution.

The volumes of adult calyces from P21 rats were also analyzed to address whether the effect seen in maturing calyces is carried on over age. Altogether 99 adult calyces from 7 animals were reconstructed manually and the mean volume of nerve terminals was calculated to 903 μm^3 for WT (SD: ±242 μm^3, n: 32, min: 455 μm^3, max: 1382 μm^3), 794 μm^3 for GFP-Exo70 (SD: ±195 μm^3, n: 35, min: 399 μm^3, max: 1176 μm^3) and to 820 μm^3 for GFP-Exo70Nter (SD: ±246 μm^3, n: 32, min: 331 μm^3, max: 1447 μm^3) overexpressing calyces. The volumes of nerve terminals from all three groups are distributed normally according to D'Agostino & Pearson omnibus normality test and no differences between the volumes of nerve terminals from WT, GFP-Exo70 and GFP-Exo70Nter overexpressing calyces can be detected (one-way ANOVA P value: 0.135). Thus, in contrast to maturing calyces at P13±1 overexpression of the dominant negative truncation construct GFP-Exo70Nter does not influence the volume of adult calyces of Held.

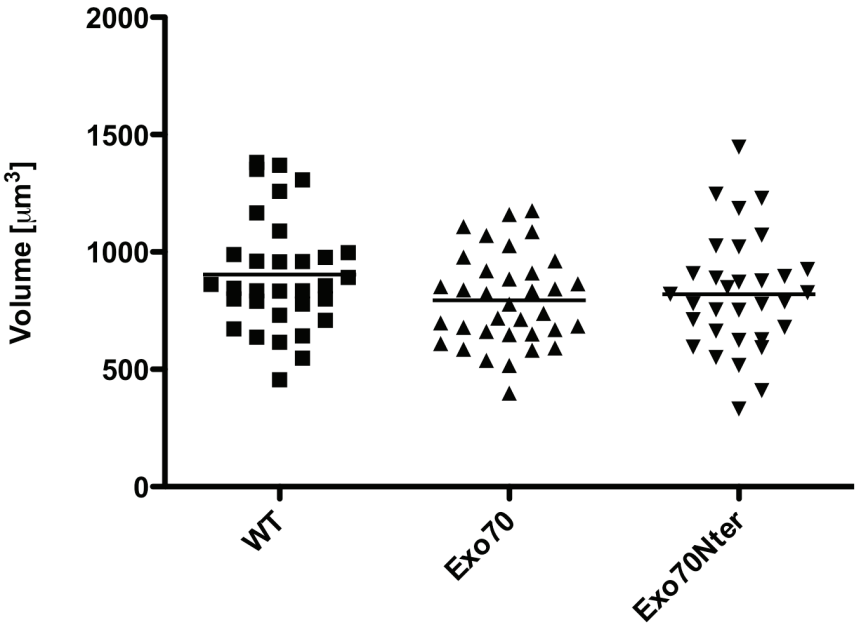

Figure 26. The volume of adult calyces (P21) is not influenced by overexpression of GFP-Exo70 or GFP-Exo70Nter. Rats were injected at P2 with rAAV encoding for mOrange and GFP-Exo70 or GFP-Exo70Nter into the VCN. Calyces were imaged at P21 in fixed brain slices of 100 μm thickness. mOrange signal was used to reconstruct calyces and measure volume of nerve terminals as depicted in Figure 24. Volume data was assigned to the respective group dependent on whether nerve terminals also showed GFP-signal and confocal image stacks were sampled from 7 different animals. No difference in volume distribution of calyces from the three groups is recognized by one-way ANOVA (P: 0.14).

Since measurement of nerve terminal volume is dependent on manual thresholding of image data, there might be an intrinsic bias of this analysis that brighter mOrange fluorescence is leading to larger volumes of the nerve terminal. Similarly, the effect of GFP-Exo70Nter might be dependent on the protein amount, which is present in globular bushy cells, because the dominant negative truncation construct has to bind to its interaction partners to block further downstream events. If this binding is incomplete, potential effects might be masked due to insufficient expression of the transgene from cells, which have been transduced by a smaller number of rAAVs.

To address whether volume determination of calyces is dependent on mOrange fluorescence intensity the volume of WT terminals was plotted against fluorescence intensity of mOrange for both ages (Figure 27). No correlation between volume of calyces and mOrange fluorescence intensity is evident for both ages (P13: $r^2 = 0.09$, P = 0.19; P21: $r^2 = 0.08$, P = 0.14), which means that the two variables do not vary together and suggests that the performed analysis does not include an intrinsic bias towards larger volumes for higher mOrange fluorescence intensities.

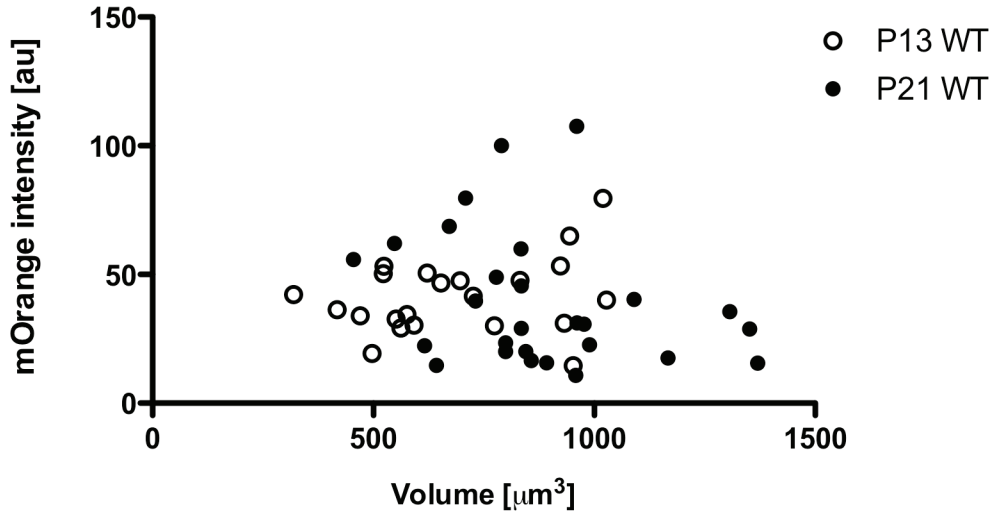

Figure 27. Volume analysis of calyces does not depend on mOrange fluorescence intensity. mOrange intensity of wildtype calyces is plotted against their respective determined volumes. **Open circles** represent wildtype calyces of P13±1 animals and **closed circles** depict calyces of P21 animals. Correlation between mOrange intensity and the determined volume was found to be 9% and 8% for P13±1 and P21 calyces, respectively.

The influence of transgene expression on the volume of mOrange labelled terminals was elicited by a correlation plot of calyx volume against GFP intensity of cells, which expressed either GFP-Exo70 or GFP-Exo70Nter (Figure 28). The results of the correlation analysis are summarized in Table 7 and indicate that GFP intensity of both transgenes is not related to the volume of calyces from within their own group neither at P13±1 nor at P21. In addition, GFP intensity distribution of GFP-Exo70Nter transduced calyces from P13±1 and P21 animals is similar between the two ages indicating that protein amounts, which were present in infected globular bushy cells, do not differ between the two ages (Figure 29). Therefore, the decrease in calyx volume of GFP-Exo70Nter overexpressing cells, which is observed in P13±1 animals, and the absence of a similar effect in P21 animals is unlikely caused by different expression levels of the transgenes at the two ages investigated.

In summary, analysis of nerve terminal volume indicates that overexpression of GFP-Exo70Nter in globular bushy cells decreases the volume of calyces from P13±1 animals but does not influence the volume of calyces from P21 rats. Overexpression of the full-length protein GFP-Exo70 does not lead to volume changes of the nerve terminal at any developmental stage. In conclusion, the observed findings suggest that while overexpression of the full length protein Exo70 does not perturb membrane addition *in vivo* the decrease of calyx volume at P13, which is observed upon overexpression of the dominant-negative truncation construct GFP-Exo70Nter, suggests that Exo70 is

necessary during pre-hearing maturation of the nerve terminal but dispensable at post-hearing onset maturational steps, since overexpression of GFP-Exo70Nter does not influence volume of calyces at P21.

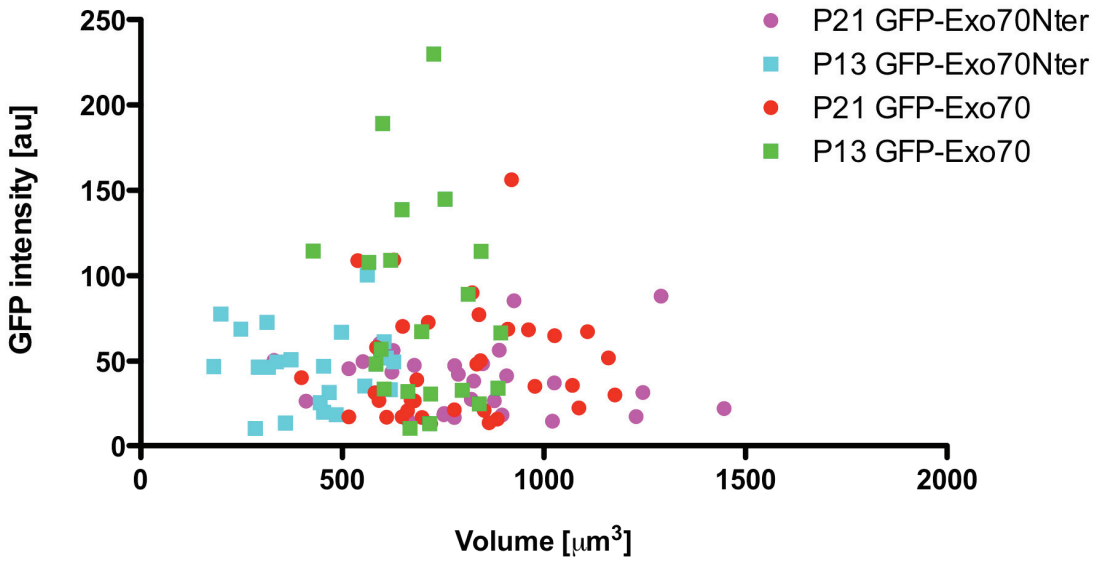

Figure 28. Expression levels of transgenes do not correlate with the volume of calyces of Held. GFP-intensities of analysed calyces are plotted against their measured volume. Symbols depict calyces from their corresponding group: **(magenta circles)** P21 GFP-Exo70Nter; **(cyan square)** P13±1 GFP-Exo70Nter; **(red circles)** P21 GFP-Exo70; **(green square)** P13±1 GFP-Exo70. Correlation analysis results are summarized in Table 7 and show no correlation between GFP-intensity and volume of calyces for any group.

Table 7. Correlation analysis between volume of nerve terminals and their GFP fluorescence intensity.

	Age	r^2	P value	Summary
GFP-Exo70	P13	0.04	0.42	ns
	P21	0.01	0.63	ns
GFP-Exo70Nter	P13	0.00	0.92	ns
	P21	0.01	0.65	ns

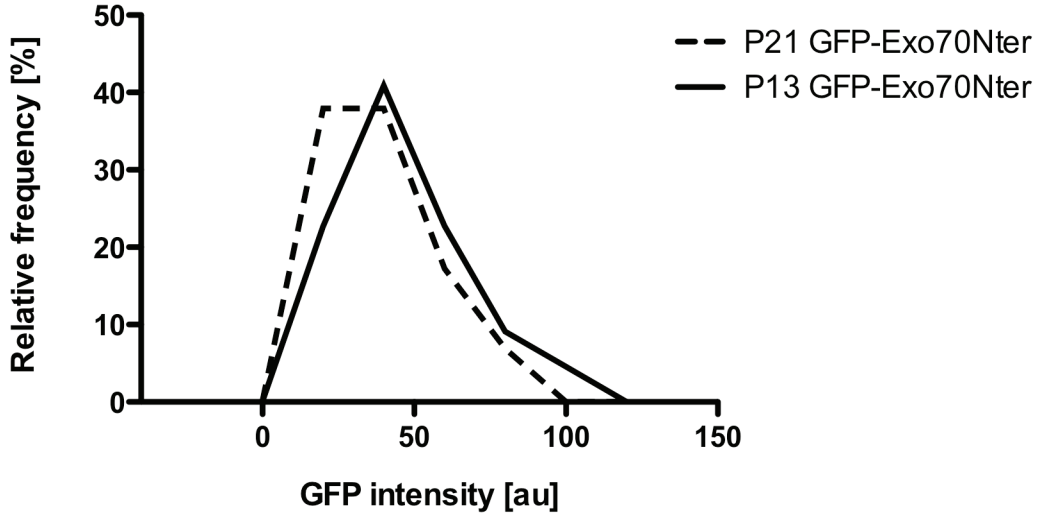

Figure 29. GFP intensity distribution of GFP-Exo70Nter infected calyces from P13±1 and P21 animals do not differ. GFP-intensities of calyces from **(open line) P21 GFP-Exo70Nter** and **(closed line) P13±1 GFP-Exo70Nter** expressing calyces are plotted against their relative frequency to control whether the population of investigated calyces at P13±1 differs from calyces analysed at P21 in terms of GFP-intensity. The relative frequency distribution of GFP-intensities does not differ considerably.

4.7.4 Distribution of active zone markers in the calyx of Held

The decreased volume of presynaptic nerve terminals from GFP-Exo70Nter overexpressing globular bushy cells points towards defects in membrane addition. To address whether the observed defects influence constitutive secretion or also impede more specialized secretory events like transport and incorporation of piccolo bassoon transport vesicles (PTV), the distribution of the active zone marker protein bassoon was examined in the calyx of Held to investigate whether the localization of this marker protein is altered by overexpression of GFP-fusion proteins of exocyst subunits. Along those lines rats were injected at postnatal day 2 with rAAV encoding for mOrange and transcardially perfused at P13±1 or P21. Vibratome brain sections of ~80 μm thickness were subjected to immunohistochemistry with bassoon antibodies and image stacks of the MNTB were acquired on a confocal microscope. To analyse potential effects by overexpression of exocyst GFP-fusion proteins on the distribution of bassoon immunoreactivity globular bushy cells were transduced in addition to mOrange with either GFP-Exo70 or GFP-Exo70Ner.

Antibody SAP7F407 against bassoon shows a punctuate pattern throughout the MNTB in which circular immunoreactivity around principle cells is evident (Figure 30). The presynaptic compartment of globular bushy cells from P13±1 and P21 animals, which did not overexpress exocyst subunits, exhibit concentrated clusters of bassoon immunoreactivity. While some of the antibody signal is found juxtaposed to the postsynaptic membrane other clusters are located inside the presynaptic compartment. The first population might reflect labelled active zones, while antibody signal, which is not found in close proximity to the plasma membrane, is likely to represent piccolo-bassoon transport vesicles (PTVs). Similarly, presynaptic terminals of cells, which had been infected with rAAV encoding for GFP-Exo70 or GFP-Exo70Nter, show a clear positive signal for bassoon in a comparable pattern, which is observed in uninfected cells. Thus, the distribution pattern of bassoon as determined by IHC does not change upon overexpression of exocyst subunit GFP-Exo70 or GFP-Exo70Nter. This result suggests that delivery of piccolo-bassoon transport vesicles (PTVs) and/or active zone assembly is not influenced by overexpression of the investigated exocyst subunits.

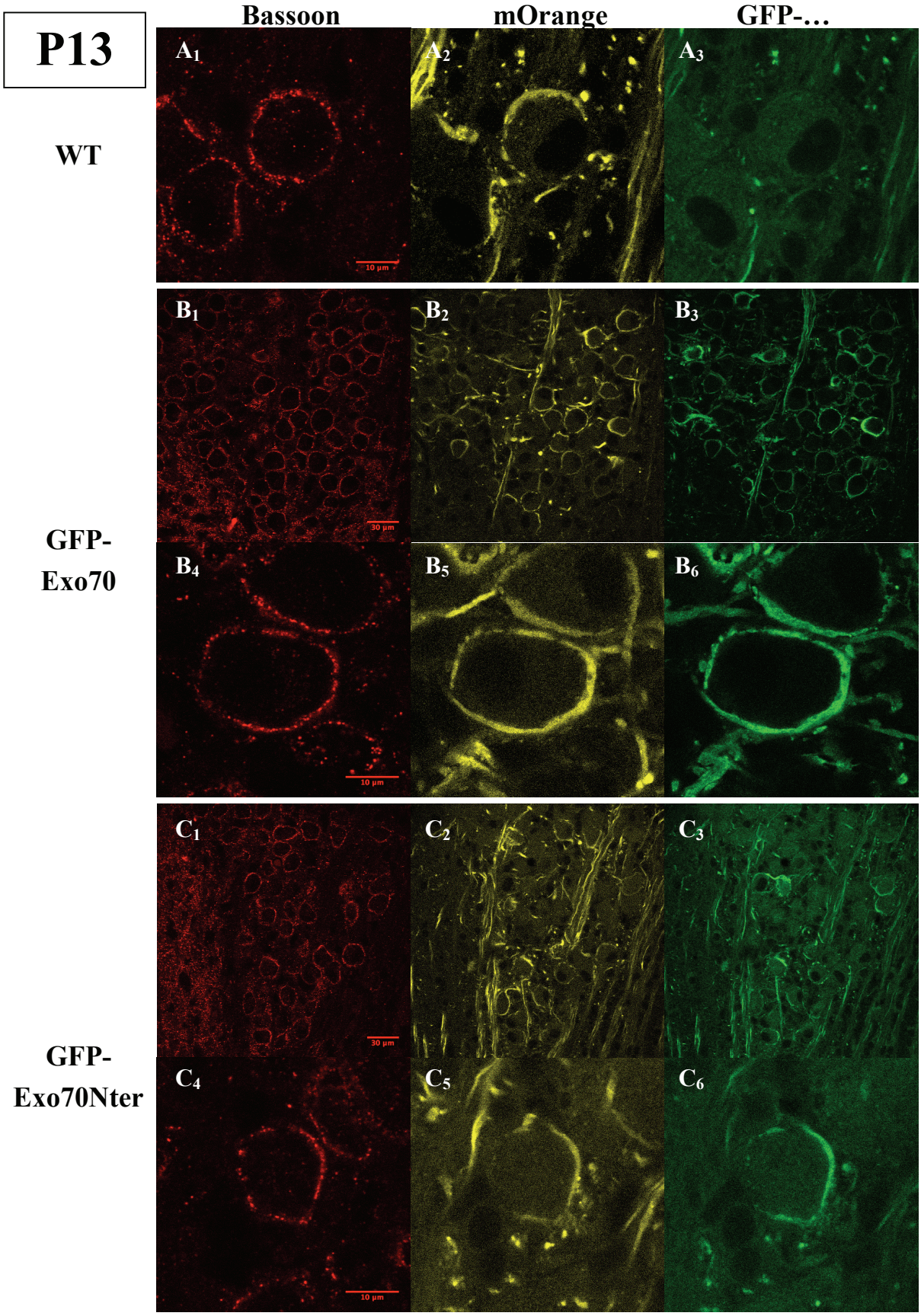
P13
Bassoon
mOrange
GFP-…
WT
GFP-Exo70
GFP-Exo70Nter
A1
A2
A3
B1
B2
B3
B4
B5
B6
C1
C2
C3
C4
C5
C6
10 µm
30 µm

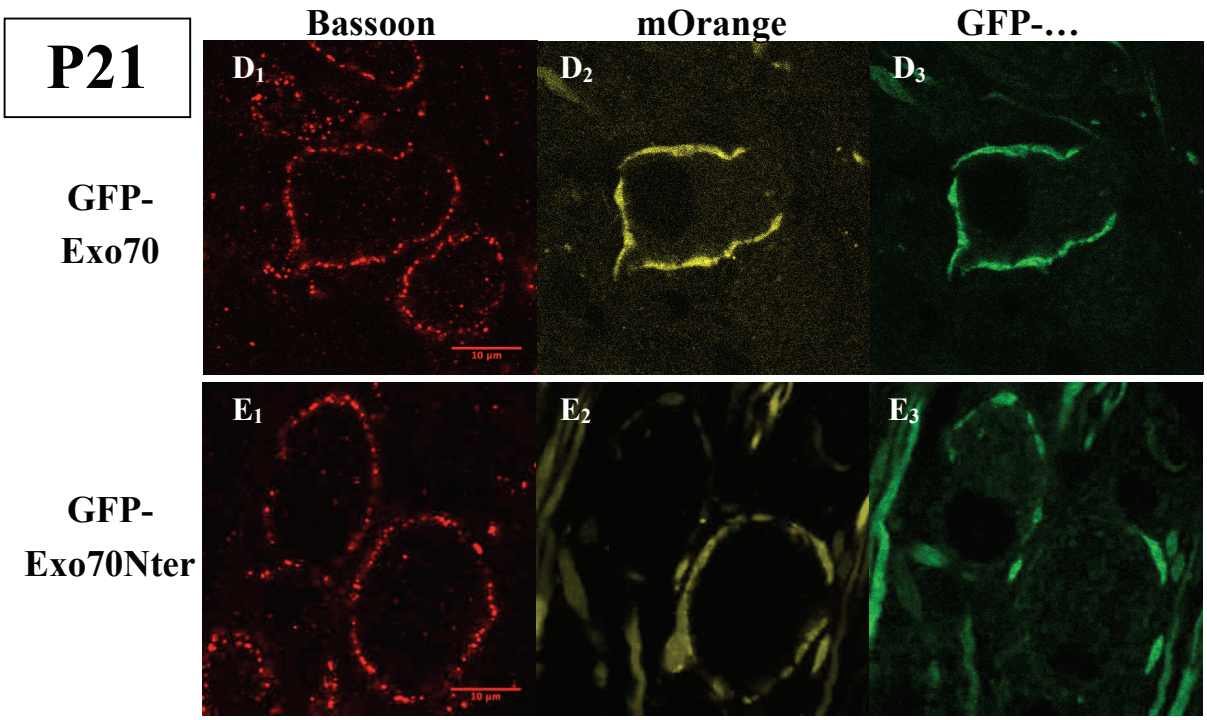

Figure 30. Bassoon localization is not influenced by overexpression of exocyst subunits. First three panels on the previous page **(A - C)** illustrate single confocal sections of the MNTB from **P13±1** animals, while the last two panels **(D and E)** on this page show orthoslices of calyces from **P21** animals. Globular bushy cells were transduced at P2 with **(A)** mOrange only or **(B and D)** together with GFP-Exo70 or **(C and E)** together with GFP-Exo70Nter. **(B_1 and C_1)** Bassoon antibody labelling exhibits a punctuate pattern throughout the MNTB, which clearly outlines principle cells. **(A_1 and D_1** – lower right cell**)** Calyces, which do not coexpress exocyst subunits, show prominent staining inside the nerve terminal at P13±1 and P21. Signal close to the presynaptic membrane most likely reflects active zones, whereas bassoon immunoreactivity inside the presynaptic compartment might reflect PTVs. **(B_1 and B_4, C_1 and C_4)** Cells, which overexpress exocyst subunits, exhibit bassoon localization, which is undistinguishable from uninfected cells. **(D_1 and E_1)** Also for mature calyces at P21 bassoon localization does not differ between exocyst overexpressing or wildtype cells.

4.7.5 Distribution of vesicle markers in the calyx of Held

To address whether overexpression of GFP-Exo70 or GFP-Exo70Nter has an influence on the presence and/or distribution of synaptic vesicles, immunohistochemistry against the synaptic vesicle resident glutamate transporter VGlut1 was performed. The experimental approach was identical to the protocol used for localization of bassoon immunoreactivity except that instead of antibody against bassoon antibody against VGlut1 was employed.

VGlut1 positive signal is found in the MNTB of P13±1 and P21 rats in a rim around principle cells, which is most abundant at regions, which are identified via mOrange signal as the calyx of Held. The distribution pattern of VGlut1 is not changed upon overexpression of GFP-Exo70 or GFP-Exo70Nter at either age. Hence, presence and localization of synaptic vesicles seems to be unaltered upon overexpression of the investigated exocyst subunits.

In conclusion, the staining pattern for all of the presynaptic markers investigated was indistinguishable between exocyst subunit overexpression and wildtype calyces at both developmental ages. Thus, interference in exocyst function by overexpression of GFP-Exo70 or GFP-Exo70Nter does not alter presence of synaptic vesicles and bassoon positive compartments. These findings suggest that the exocyst complex is not involved in transport and/or directed delivery of synaptic vesicles and active zone precursor vesicles to the nerve terminal.

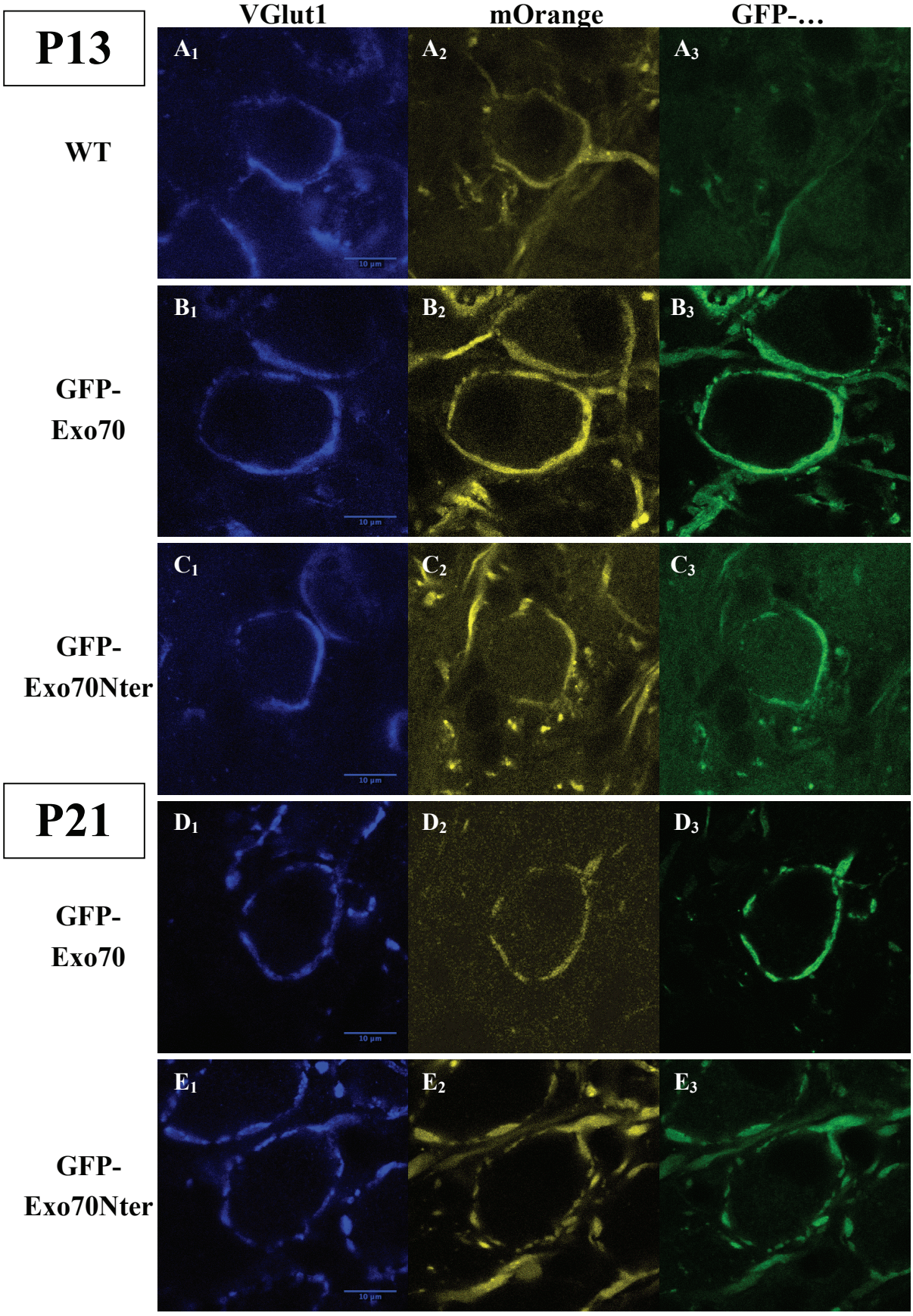
VGlut1
mOrange
GFP-…
P13
WT
GFP-Exo70
GFP-Exo70Nter
P21
GFP-Exo70
GFP-Exo70Nter
A1
A2
A3
B1
B2
B3
C1
C2
C3
D1
D2
D3
E1
E2
E3
10 µm

Figure 31. Localization of synaptic vesicle marker VGlut1 does not differ upon overexpression of exocyst subunits. Immunohistochemistry with antibodies against VGlut1 was performed on brainstem slices derived from **(A - C)** P13±1 and **(D and E)** P21 rats. VCN of rats was injected at P2 with rAAVs encoding for **(B and D)** mOrange and GFP-Exo70 or **(C and E)** mOrange and GFP-Exo70Nter. **(A)** VGlut1 immunoreactivity is found in the MNTB almost exclusively at sites, which are identified as calyceal inputs via fluorescence labelling. **(B - E)** Calyces, which overexpress exocyst subunits, cannot be distinguished from mOrange only expressing cells by looking at VGlut1 immunoreactivity at both ages investigated.

4.7.6 Involvement of the exocyst in synaptic vesicle cycle

The main goal of this study was to elucidate whether the exocyst complex is involved in the synaptic vesicle cycle. Generally, the synaptic vesicle cycle is divided into several steps: translocation of synaptic vesicles (SV) into close proximity of the active zone (AZ), tethering/docking of SV to the AZ, priming of SV, Ca^{2+}-triggered exocytosis of SV, endocytosis and refilling with neurotransmitters of SV. During this trafficking cycle each SV can be assigned to one of three different pools: the readily releasable pool (RRP), the recycling pool and the reserve pool. To elucidate potential changes in the synaptic vesicle cycle upon overexpression of GFP-Exo70 or GFP-Exo70Nter several aspects of the synaptic vesicle cycle were addressed by employing individual stimulation protocols, which will be explained in their respective subchapters. In this regard, Sprague Dawley rats were injected at postnatal day 2 with rAAV encoding for either GFP-Exo70 or GFP-Exo70Nter. After 11 days of expression animals were decapitated at P13, the brain dissected and the brainstem sliced into 300 μm thick sections. Afferent fibres of globular bushy cells were stimulated with a bipolar stimulation electrode close to midline and fluorescent calyces identified optically (Figure 32). Postsynaptic cells were patched at room temperature with low resistance pipettes (< 2.5 MΩ) and clamped at -70 mV holding potential with series resistance < 6 MΩ to record excitatory postsynaptic currents (EPSCs). The intracellular solution contained cesium gluconate to block potassium channels. No drugs were added to the external bath solution since desensitization is absent in calyces at this age (Taschenberger et al., 2002).

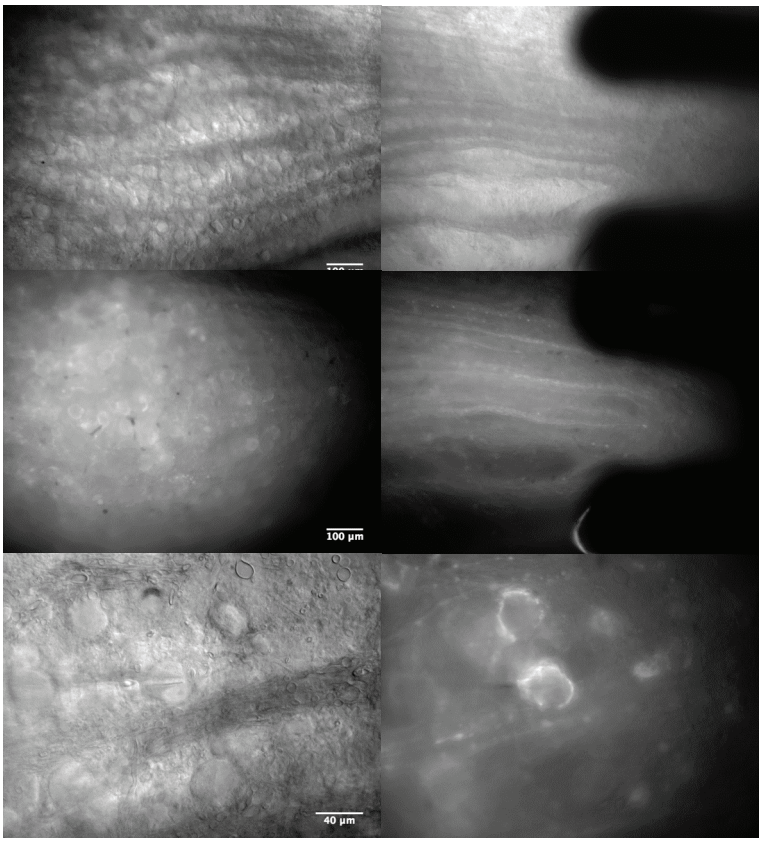

Figure 32. Afferent fibres of globular bushy cells were stimulated with a bipolar stimulation electrode and fluorescent calyces identified optically. Rats were injected with rAAV encoding for GFP-Exo70 or GFP-Exo70Nter at P2 and sacrificed at P13±1 for electrophysiology. **(Top)** Rat brains were sliced into 300 µm sections and morphology visualized by infrared light. Afferent fibres of globular bushy cells were stimulated with a bipolar stimulation electrode, which was placed close to midline. **(Middle)** Virus infected GBCs project their fluorescent axons towards the MNTB, where fluorescent calyces can be identified. **(Bottom)** Electrophysiological recordings were performed with a 63x objective and fluorescent calyces identified optically.

4.7.6.1 Spontaneous release

Synaptic vesicle fusion is either evoked by arrival of an action potential at the nerve terminal and subsequent opening of calcium channels or can also occur spontaneously in a calcium independent fashion. If the exocyst complex is involved in synaptic vesicle cycling, an alteration in the availability of SVs at the plasma membrane could occur, which would result in a frequency change at which spontaneous events appear. Also if the synaptic vesicle cycle is influenced by overexpression of exocyst subunits a change in the refilling process of SVs could occur, which would lead to a change in the quantal size of SV. Another possibility could be that upon interference in exocyst function SVs are not primed correctly, which would lead to a modification of the fusion kinetics of SVs. To address the before mentioned questions, miniature EPSCs (mEPSCs) of principal

cells, which are postsynaptic to either wildtype or exocyst subunit overexpressing calyces, were recorded.

Principal cells were patched in whole-cell mode and clamped at -70 mV holding potential to record mEPSCs over a time course of two minutes. mEPSCs were isolated from the recorded current traces by a custom written waveform recognition algorithm in Igor software and analysed for amplitude, charge and inter-event-time. Risetime of mEPSCs was defined as the time interval between 20% and 80% of amplitude and decay of mEPSC was fitted to a single exponential function to determine the time constant τ. Exemplary raw data current traces, aligned average mEPSCs and analysed parameters are shown in Figure 33. The parameters were averaged over all mEPSC events from one cell and these values were averaged over all cells from the same group and graphed in Figure 33. As can be inferred from the selected raw data current traces, the inter-event-time, with which mEPSCs occurred, did not change upon overexpression of exocyst subunits. While mEPSC from wildtype synapses are detected every 1.1 ± 0.2 seconds on average, GFP-Exo70 and GFP-Exo70Nter overexpressing calyces release vesicles spontaneously every 1.3 ± 0.3 and 1.6 ± 0.4 seconds, respectively. The quantal size of wildtype synapses was determined to 38 ± 5 pA and did not change upon overexpression of exocyst subunits (GFP-Exo70: 39 ± 3 pA, GFP-Exo70Nter: 33 ± 3 pA). Similarly mEPSC charge did not differ between the three groups with values of 24 ± 3, 28 ± 4 and 24 ± 3 fC for wildtype, GFP-Exo70 and GFP-Exo70Nter, respectively. Selected averaged mEPSCs of the three groups were aligned to 20% of amplitude and normalized to peak amplitude to compare fusion kinetics. All three mEPSC traces overlay without extensive deviation and no differences in risetime are detected between wildtype (152 ± 12 μs) and exocyst subunit overexpressing calyces (GFP-Exo70: 170 ± 11 μs, GFP-Exo70Nter: 168 ± 5 μs). Similarly, no differences in decay constants are observed between the three groups (wildtype: 417 ± 42 μs, GFP-Exo70: 424 ± 27 μs, GFP-Exo70Nter: 452 ± 23 μs). Hence, overexpression of exocyst subunits does not influence spontaneous release of synaptic vesicles and therefore Exo70 seems not to be involved in calcium independent release of neurotransmitters. Also loading of synaptic vesicles with neurotransmitters seems to be independent of Exo70 since quantal size of mEPSCs did not change upon overexpression of either GFP-Exo70 or GFP-Exo70Nter.

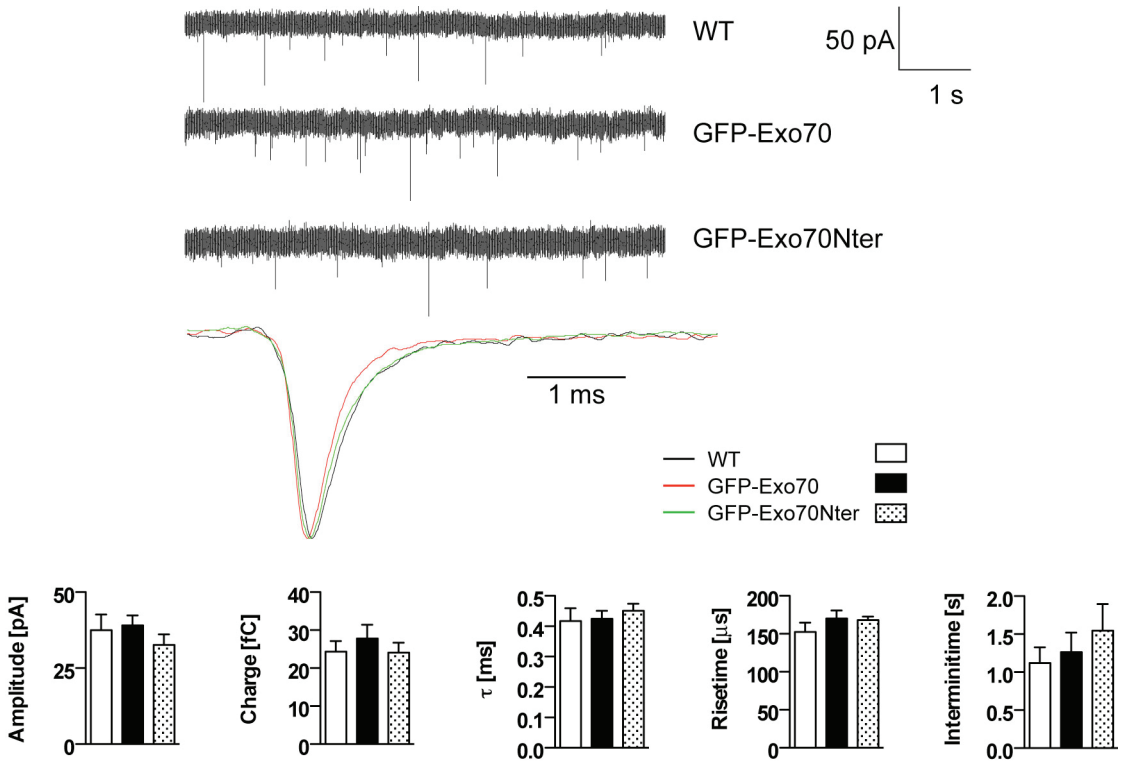

Figure 33. Spontaneous release is not influenced by overexpression of GFP-Exo70 or GFP-Exo70Nter. mEPSCs were recorded from principal cells voltage-clamped at -70mV, which were postsynaptic to **(— , white bar)** wildtype or **(— , black bar)** GFP-Exo70 or **(— , dotted bar)** GFP-Exo70Nter expressing calyces. **(Top)** Raw data current traces of mEPSC recordings. **(Center)** Averaged, aligned and normalized mEPSC of one cell from each group. The current traces overlay without significant deviations. **(Bottom)** mEPSC parameters were determined for each cell and the average over all cells is shown together with error bars representing SEM (n_{WT}: 5; $n_{GFP\text{-}Exo70}$: 7; $n_{GFP\text{-}Exo70Nter}$: 6). Risetime was defined as the time interval between 20% and 80% of amplitude and decay was fitted to a single exponential function to obtain the time constant τ. mEPSC parameters were analysed for differences with one-way ANOVA without detecting statistical significance between the groups in any parameter.

4.7.6.2 Evoked release

Next we wanted to address the involvement of exocyst in evoked release to determine whether Ca^{2+}-triggered fusion of synaptic vesicles proceeds normally at the active zone after the arrival of an action potential, when GFP-fusion proteins of exocyst subunits are overexpressed in globular bushy cells. By using low frequency stimulation (0.1 Hz) the calyx of Held is evoked from a resting state in which wildtype synapses are not depressed and therefore do have a readily releasable pool of synaptic vesicles available (see also Figure 34). Thus, low frequency stimulation addresses presence and fusion kinetics of primed synaptic vesicles, which release their content after arrival of an action potential.

Action potentials were evoked with a frequency of 0.1 Hz for 100 seconds and excitatory postsynaptic currents (EPSCs) were measured to this stimulus. As expected, the postsynaptic responses of wildtype cells are not depressed by low frequency stimulation of 0.1 Hz (Figure 34). Also principal cells, which received inputs from GFP-Exo70 or GFP-Exo70Nter transduced calyces, show no evident decrease in the EPSC amplitude over time at this stimulation frequency. The obtained current traces were offline corrected for differences in series resistance and averaged afterwards to analyse amplitude and charge of EPSCs. Decay of current traces was fitted to a single exponential function to obtain the decay time constant τ. Risetimes were measured between 10% and 90% of amplitude. One current trace from each group, which are normalized and aligned to 10% of amplitude, is shown exemplarily in Figure 35A. As can be seen from the selected examples, EPSC traces overlay with no evident difference between postsynaptic responses from WT nerve terminals and calyces, which are positive for GFP-Exo70 or GFP-Exo70Nter. Similarly, a comparison of all recorded cells does neither reveal differences in amplitude or charge of postsynaptic responses nor in their risetime or decay time constant between the three groups. The numeric mean values are shown in Table 8 for each parameter along with standard error of the mean (SEM) and number of recorded cells (n). The EPSC parameters were compared by one-way ANOVA. The results of the statistical test are given in Table 8 and suggest that there is no difference between postsynaptic responses from principal cells, which are innervated from WT nerve terminals or calyces, which were transduced with GFP-Exo70 or GFP-Exo70Nter. Hence, overexpression of GFP-Exo70 or GFP-Exo70Nter does not impede priming of synaptic vesicles, if the calyx of Held is innervated from a resting state, i.e. stimulated with low frequency of 0.1 Hz. The absence of deviations in risetime or decay time constant indicate that synchronous release of synaptic vesicles is not altered if globular bushy cells are transduced with rAAV encoding for GFP-Exo70 or GFP-Exo70Nter.

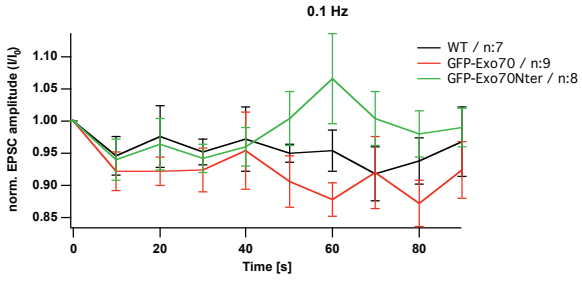

Figure 34. Low frequency stimulation does not induce short-term synaptic depression. Calyces from P13±1 animals were stimulated with 10 stimuli at 0.1 Hz. EPSC amplitudes (I) were normalized to the first EPSC amplitude (I_0) and graphed against time. Error bars represent SEM for number of cells depicted in the legend. Postsynaptic responses do not show considerable depression independently whether principal cells were postsynaptic to (—) wildtype or (—) GFP-Exo70 or (—) GFP-Exo70Nter expressing calyces.

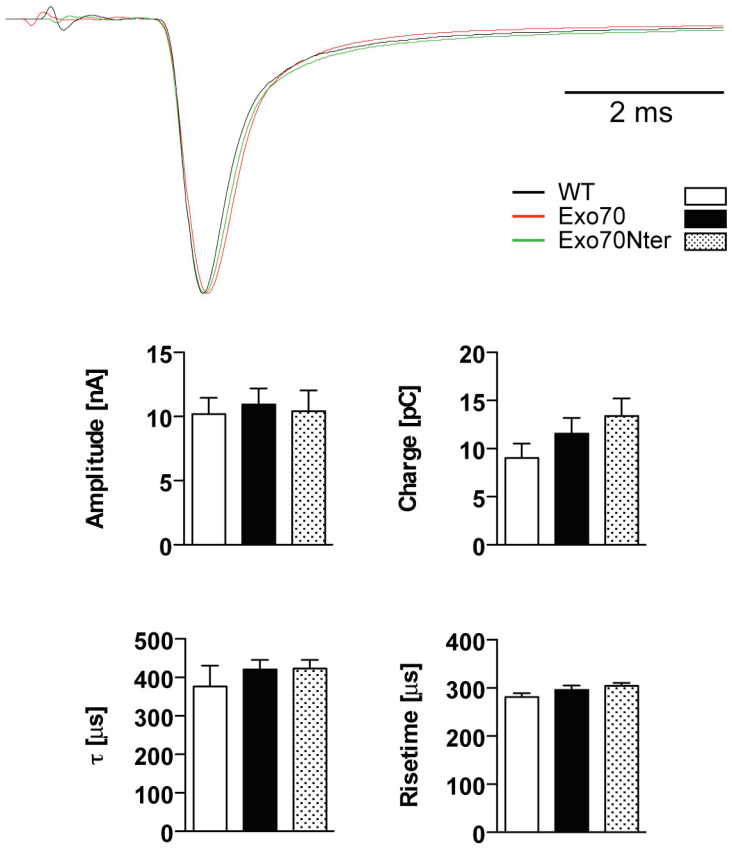

Figure 35. EPSC kinetics are not altered by overexpression of GFP-Exo70 or GFP-Exo70Nter. EPSC responses to 10 stimuli at 0.1 Hz were averaged to analyse EPSC parameters for **(— , white bar)** wildtype or **(— , black bar)** GFP-Exo70 or **(— , dotted bar)** GFP-Exo70Nter expressing calyces. **(Top)** Averaged and normalized EPSCs are aligned to 10% of amplitude. The current traces overlay without clear deviations. **(Bottom)** EPSC parameters were analysed for 7 wildtype, 9 GFP-Exo70 and 8 GFP-Exo70Nter expressing cells. Error bars represent SEM. One-way ANOVA did not detect any differences between the three groups for any parameter.

Table 8. One-way ANOVA analysis of EPSC parameters.

	wildtype	GFP-Exo70	GFP-Exo70Nter	one-way ANOVA
n [cells]	7	9	8	-
Amplitude [nA]	10.0±1.3	10.9±1.3	10.4±1.6	0.92
Charge [pC]	9.0±1.5	11.6±1.6	13.4±1.8	0.26
τ [µs]	376±54	419±26	422±23	0.60
Risetime [µs]	281±8	296±9	305±6	0.19

4.7.6.3 Readily releasable pool size

Since overexpression of exocyst subunits did not alter fusion kinetics of primed synaptic vesicles, we were interested to see whether overexpression of exocyst subunits alters delivery of synaptic vesicles to the readily releasable pool (RRP) and therefore results in a change of RRP size. This parameter can be estimated by calculating the cumulative EPSC amplitudes for time intervals that are short in respect to the time required from recovery after depression. Therefore, calyces were stimulated with a frequency of 100 Hz and cumulative EPSC amplitudes calculated by fitting a line to the steady-state region for times larger than 100 ms and back extrapolation to zero (Figure 36). This estimate takes into account the cumulative EPSC amplitudes reached within the first five to six stimuli, corresponding to a time interval of about 50 ms at which replenishment of SVs to the active zone is negligible (<5%) (Schneggenburger et al., 1999). The number of vesicles in the RRP can then be estimated by dividing the cumulative EPSC amplitude by the quantal size, which was determined already during analysis of spontaneous release.

By means of this analysis the cumulative EPSC amplitude of wildtype calyces was calculated to 29 ± 4 nA (n: 5) (Figure 37). While GFP-Exo70 overxpressing calyces exhibited a smaller average cumulative EPSC amplitude of 22 ± 1 nA (n: 8), GFP-Exo70Nter overexpressing calyces showed similar values of 28 ± 4 nA (n: 7) compared to uninfected nerve terminals. Statistical comparison of the three groups by one-way ANOVA did not reveal any significant differences between the values of cumulative EPSC amplitudes (P=0.26). Hence, overexpression of exocyst subunits does not change the size of the cumulative EPSC amplitude. Since no difference in quantal size was detected during analysis of spontaneous release between the three groups, this result suggests that the size of the readily releasable pool does not change upon overexpression of GFP-Exo70 or GFP-Exo70Nter.

The pool of readily releasable vesicles of wildtype cayces was calculated to 763 transmitter quanta, when the average value of the cumulative EPSC amplitude (29 ± 4 nA, n: 5) was divided by the average value of quantal size (38 pA). The RRP size of GFP-Exo70 overexpressing calyces was determined to 564 quanta (cum. EPSC= 22 ± 1 nA, n: 8; q= 39 pA), whereas GFP-Exo70 overexpressing calyces exhibit a RRP size of 848 synaptic vesicles (cum. EPSC= 28 ± 4 nA, n: 7; q= 33 pA).

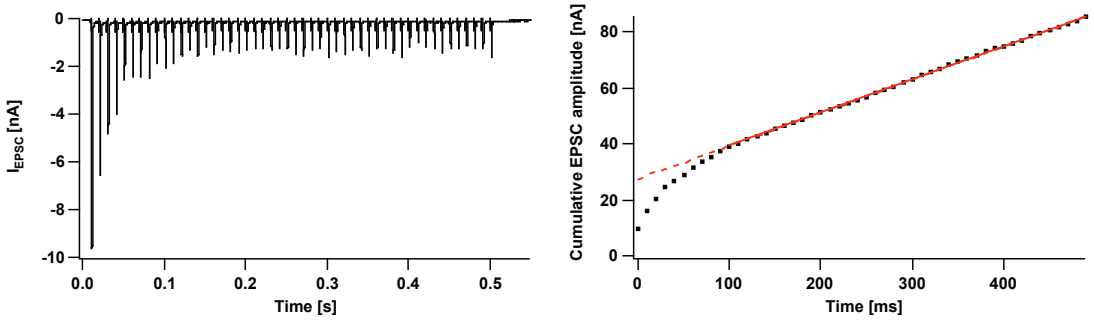

Figure 36. Determination of readily releasable pool (RRP) size. (Left) Calyces were evoked with 50 stimuli at 100 Hz and postsynaptic responses measured. **(Right)** Peak EPSC amplitude values of the stimulation train were extracted and graphed in a cumulative plot against time. To estimate the contribution of the RRP to this stimulus, a (—) line was fitted to the steady-state region for times larger than 100 ms and back-extrapolated (- -) to time 0. The y-axis intercept represents an estimate of the cumulative EPSC amplitudes before steady-state depression.

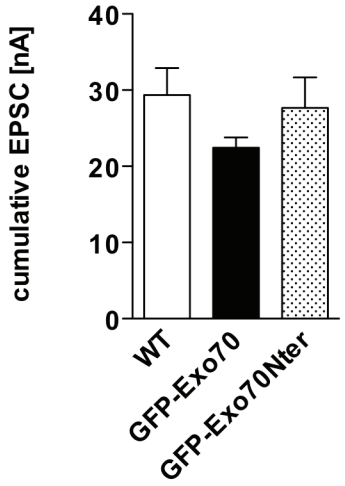

Figure 37. RRP size is not influenced by overexpression of exocyst subunits. Calyces were stimulated with 100 Hz trains to determine RRP size as shown in Figure 36. Although cumulative EPSC amplitudes of GFP-Exo70 expressing cells were slightly smaller, values of the three groups did not differ significantly (one-way ANOVA P value: 0.26). Error bars represent SEM from 5 for WT, 8 for GFP-Exo70 and 7 for GFP-Exo70Nter independent experiments.

4.7.6.4 Short-term depression

If wildtype calyces are stimulated with frequencies faster than 0.2 Hz at room temperature, EPSC amplitudes decrease exponentially after the first stimulus and decay to a new steady-state value (von Gersdorff et al., 1997). At the age at which electrophysiological measurements were performed (P13), this response behaviour is attributed mainly to the depletion of the readily releasable pool (RRP) up to a steady-state condition, at which the number of SVs, which are newly delivered to the active zone, equalizes the number of SVs, which are released upon a stimulus. If exocyst is involved in the mechanisms, which underlie synaptic short-term depression, a change in the steady-state value or the time course of short-term depression would be expected upon interference in exocyst function.

To induce short-term depression, axons of globular bushy cells were stimulated with frequencies from 0.3 – 100 Hz and postsynaptic responses recorded in whole cell mode. Normalized EPSC amplitudes during frequency trains were plotted versus time as shown in Figure 38. To estimate the time course of decaying postsynaptic responses a single exponential fit was performed to the EPSC amplitudes to obtain the time constant τ and the steady-state value I_{ss}.

When calyces were stimulated with frequencies higher than 0.3 Hz, robust short-term depression was evident for all recorded cells independently whether principal cells are postsynaptic to wildtype calyces or nerve terminals, which overexpress GFP-Exo70 or GFP-Exo70Nter (Figure 39). The extent of short-term depression can be expressed by the ratio of the first EPSC amplitude I_0 devided by the steady-state value I_{ss}. As expected from the normalized EPSC amplitude plots in Figure 39, no differences in the extent of short-term depression nor in its time course were detected upon overexpression of exocyst subunits at any frequency investigated (Figure 40). Thus, overexpression of exocyst subunit GFP-Exo70 or GFP-Exo70Nter does not alter short-term depression in the calyx of Held.

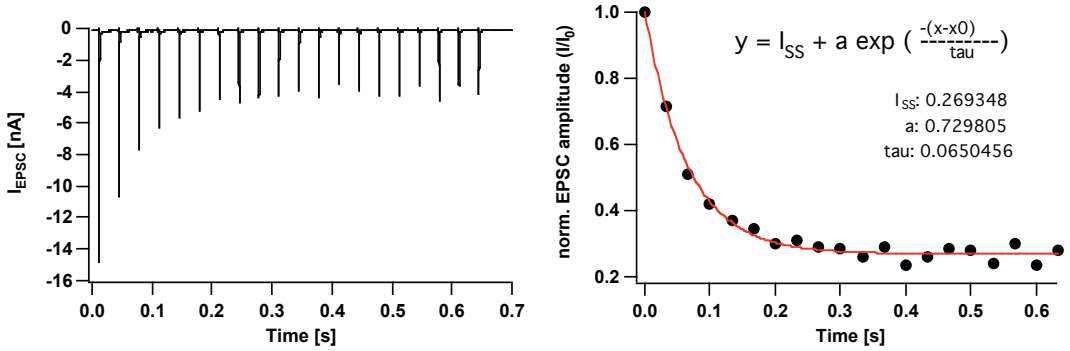

Figure 38. Analysis of short-term depression. (Left) Axons of calyces were stimulated with frequencies > 0.3 Hz and postsynaptic responses measured. **(Right)** The peak EPSC amplitude values (I) are extracted and normalized to the first amplitude (I_0). The ratio is plotted against time and the time course fitted with a single exponential function to obtain the time constant τ and the steady-state value I_{ss}.

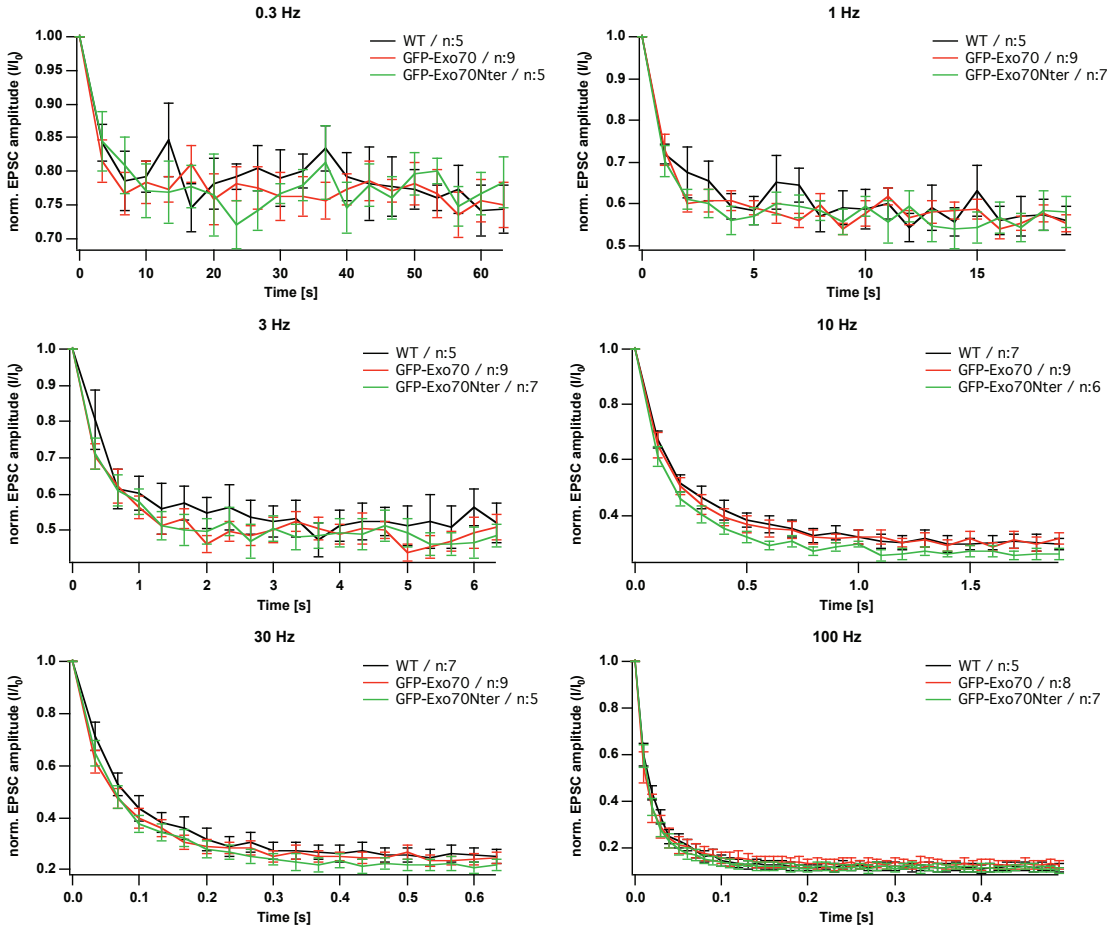

Figure 39. Short-term depression at frequencies from 0.3 – 100 Hz. Afferent fibres of globular bushy cells were stimulated with depicted frequencies to measure postsynaptic responses. Peak EPSC amplitudes (I) were normalized to the first peak EPSC amplitude (I_0) and plotted against time. Error bars represent SEM from (—) wildtype, (—) GFP-Exo70 and (—) GFP-Exo70Nter expressing cells, whereas the number of cells for each frequency train is given in the panel legend.

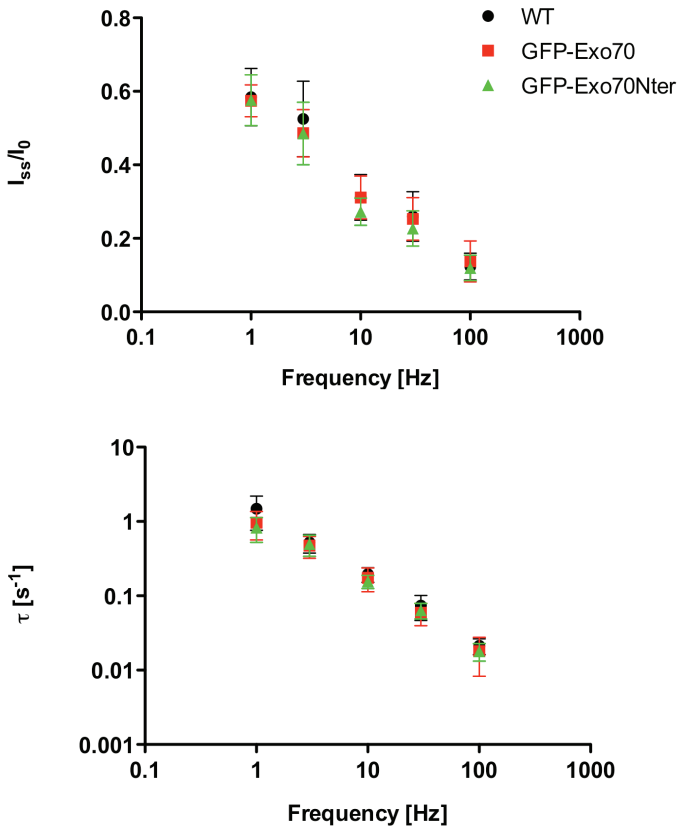

Figure 40. Short-term depression is not influenced by overexpression of exocyst subunits. Normalized peak EPSC amplitude values of frequency trains were analysed as shown in Figure 38 and parameters are plotted for (●) wildtype (■) GFP-Exo70 and (▲) GFP-Exo70NTer. **(Top)** The extent of short-term depression as expressed by the ratio of I_{ss}/I_0 decreases equally with increasing stimulation frequency for wildtype, GFP-Exo70 and GFP-Exo70Nter expressing cells. **(Bottom)** Time course of short-term depression is measured by the time constant τ, which decreases for faster frequency trains, i.e. depression occurs more rapidly. Exocyst subunit overexpressing cells depress with the same kinetics as observed for wildtype cells for all frequencies investigated. Error bars represent SEM from the number of cells shown in **Figure 39** for each individual frequency and group.

4.7.6.5 Replenishment of the readily releasable pool

While short-term depression is mainly induced by depletion of synaptic vesicles from the RRP, the response behaviour of the postsynaptic cell to high frequency trains is a sum of events, which cannot be distinguished by the previous stimulation protocol. To address a potential involvement of the exocyst complex in delivery of SVs to the RRP directly, the RRP of calyces was depleted with 50 stimuli at 100 Hz and recovery after depression measured by applying a second stimulus (recovery stimulus) with increasing time intervals after the depletion train. The amplitude of the recovery stimulus was plotted versus time to measure the time course of recovery by performing a single exponential fit and extracting the time constant τ (Figure 41).

Recovery stimulus amplitudes from wildtype, GFP-Exo70 and GFP-Exo70Nter overexpressing calyces overlaid with no evident differences between the three genotypes (Figure 42). Wildtype calyces recovered from the depletion train with time constants τ of 2.8±0.94 seconds (n: 5), while GFP-Exo70 and GFP-Exo70Nter overexpressing calyces refilled the RRP with time constants of 2.4±1.1 (n: 5) and 2.9±0.7 seconds (n: 4), respectively. Hence, the results from the recovery after depression stimulation protocol show, that overexpression of GFP-Exo70 or GFP-Exo70Nter does not alter the kinetics with which the readily releasable pool is refilled with synaptic vesicles.

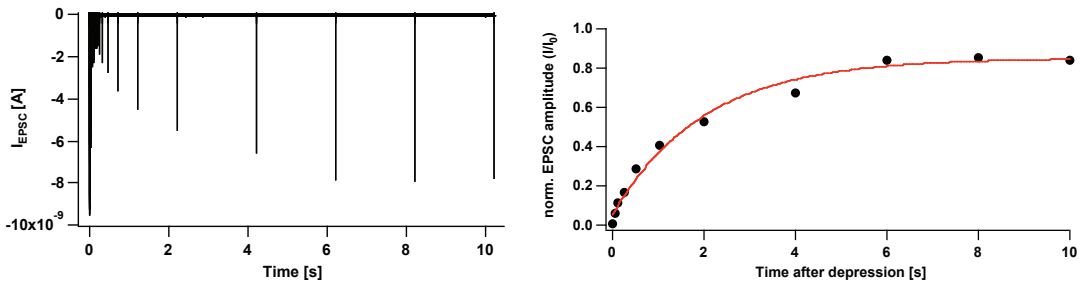

Figure 41. Recovery after depression stimulation protocol and analysis. (Left) Axons are depolarized with a depletion train comprising 50 stimuli at 100 Hz. A second stimulus (recovery stimulus) is applied after the depletion train with increasing time intervals to measure the time course of recovery. **(Right)** The steady-state value of the depletion train is subtracted from the peak EPSC amplitudes of recovery stimuli (I) and values are normalized to the first stimulus of the depletion train (I_0). Values are plotted against time and fitted to a single exponential function to obtain time constant τ.

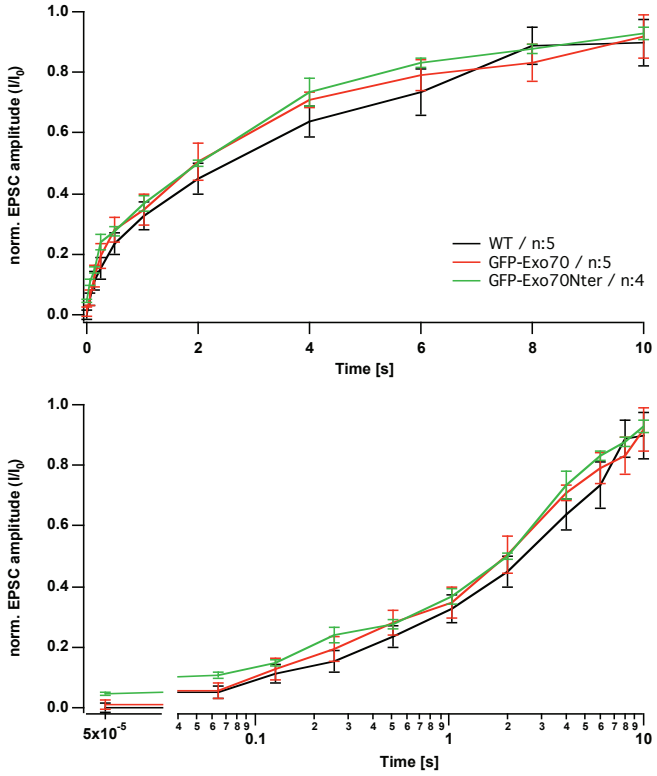

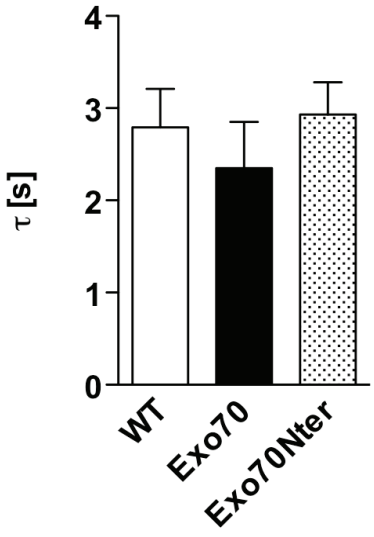

Figure 42. Recovery from short-term depression is unchanged upon overexpression of exocyst subunits in the calyx of Held. Stimulation protocols and data processing was performed as illustrated in Figure 41. Error bars represent SEM from (—) 5 wildtype, (—) 5 GFP-Exo70 and (—) 4 GFP-Exo70Nter expressing cells. **(Top and center)** Normalized recovery stimuli plotted against time. The second graph shows the identical dataset as the first one, but with a logarithmic time axis for clarity of especially the early recovery stimuli. **(Bottom)** Time constant τ as determined by single exponential fit to the time course of recovery stimuli does not differ between the three genotypes.

In conclusion, all of the employed stimulation protocols did not reveal differences between exocyst subunit overexpressing and wildtype calyces. These results clearly show that acute targeted genetic perturbation of exocyst function by overexpression of GFP-Exo70 or GFP-Exo70Nter does not lead to alterations in the synaptic vesicle cycle. More specific, our experimental approach suggests that the exocyst complex is not involved in immediate fusion of synaptic vesicles for both evoked and spontaneous release. An

unaltered quantal content of synaptic vesicles points out that the exocyst complex does not contribute to the refilling of SV with glutamate. Determination of miniature event frequency and size of the RRP revealed that the exocyst does not transport vesicles to sites of SV fusion for both evoked and spontaneous release of neurotransmitter. The tethering complex is also not involved in the events underlying refilling of the RRP since kinetics for recovery after depression were indistinguishable between the three groups. Finally, exocyst does not contribute to the molecular mechanisms underlying short-term depression because kinetics as well as extent of short-term depression were unaltered in exocyst subunit overexpressing calyces.

5 Discussion

In this study, the involvement of the exocyst complex in the calyx of Held was addressed *in vivo*. Recently developed and published antibodies were tested in paraformaldehyde fixed brain slices of the MNTB to reveal the distribution pattern of exocyst subunits Sec6, Sec8 and Sec15 in relation to the synaptic vesicle marker VGlut1. Recombinant adeno-associated and lentiviral particles encoding for N-terminal GFP-fusion proteins of exocyst subunits Sec3, Sec6, Sec8, Sec15 and Exo70 were generated and tested in hippocampal cultures together with a reported dominant-negative truncation construct of Exo70 (Exo70Nter, aa 1-384). Stereotaxic coordinates for the injection of viral particles into the ventral cochlear nucleus of 2-day-old rats were established to transduce globular bushy cells with recombinant adeno-associated viral particles. Virus mediated overexpression was used to localize GFP signal in the calyx of Held and/or to provoke phenotypes by overexpression of GFP-Exo70 and GFP-Exo70Nter. Three forms of vesicle trafficking were assessed: (1) general membrane addition by measuring the volume of the presynaptic nerve terminal; (2) delivery of synaptic precursor vesicles by immunlocalization of the active zone marker protein bassoon; (3) the synaptic vesicle cycle by means of electrophysiological recordings.

5.1 Immunlocalization of exocyst subunits in the calyx of Held

The exocyst was suggested to specify synapse-assembly domains (Hazuka et al., 1999) but its function in mature nerve terminals is poorly understood. Only one study concentrated on exocyst function in adult brain tissue by localizing subunit Sec6 and Sec8 with immunohistochemistry (Vik-Mo et al., 2003). The authors reported high immunoreactivity for both antibodies in adult rat brain and found Sec6 partially colocalized with but virtually independent from the synaptic vesicle marker synaptophysin. Therefore, they assumed that “the function of the exocyst complex is required also in mature brain, indicating a role beyond synaptogenesis”. Sec6 colocalized to a higher extent with secretograninII containing vesicles in this study and was found at the cytoplasmatic side of the plasma membrane outside active zones indicating an association of the exocyst with transport of cargo vesicles rather than synaptic vesicles. Sec8 did not colocalize with Sec6 but whether this finding indicates either incomplete labelling because of epitope inaccessibility or the presence of independent exocyst subcomplexes was not addressed any further.

Here, we used the same antibody against Sec6 (mAb 9H5) and two recently characterized antibodies against Sec8 (mAb 8S2E12) and Sec15 (mAb 15S14H1) (Wang et al., 2004b) to address the distribution of these exocyst subunits in the calyx of Held. We reasoned that the staining pattern in relation to other marker proteins could yield some hints towards the function of these subunits in the mature nerve terminal. It was also of interest whether the individual immunoreactivities of the antibodies would give rise to the existence of subcomplexes of these subunits inside the presynaptic compartment or whether they would preferentially colocalize.

We observed a sparse punctuate staining pattern in paraformaldehyde fixed brainstem slices for Sec6, which is comparable to the before mentioned study from (Vik-Mo et al., 2003). The overlap between Sec6 and the synaptic vesicle marker VGlut1 was marginal and in few cases we observed immunoreactivity towards the presynaptic side. In contrast, antibodies against Sec8 and Sec15 showed ubiquitous immunoreactivity throughout the entire MNTB yielding no clear hint towards a preferred cell compartment. It is doubtful whether the signal, which we obtained for Sec8 and Sec15, reflects the real presence of these subunits. It cannot be excluded that the antibodies exhibit cross reactivity in paraformaldehyde tissue, without testing them in tissue derived from knockout animals. Unfortunately, animals with a gene deletion of Sec8 do not pass gastrulation phase excluding such a control experiment (Friedrich et al., 1997). Similarly, knockout of Sec15 in drosophila leads to growth arrest at the second instar larvae stage and a similar phenotype could be anticipated in mammals (Mehta et al., 2005). Taken together, we did not gain new insights about exocyst subunit distribution in the presynaptic compartment of the calyx of Held. Without further knowledge about the protein loci involved in subunit interaction it remains a matter of speculation whether different localization patterns for antibodies against exocyst subunits reflect individual subcomplexes or are simply a consequence of incomplete labelling. This situation is further complicated by the possibility that interactions with proteins outside the complex might also shield antigens from antibody recognition. Therefore, immunlocalization studies of exocyst subunits can only serve as hints, which need to be further confirmed by additional experiments, which are able to revise a postulated hypothesis. In this study, we could not infer a new function from immunohistochemistry results about exocyst function in the presynaptic compartment.

Since immunohistochemistry against exocyst subunits in paraformaldehyde fixed brainstem slices did not lead to clear results, we also did not pursue the initial aim to down regulate exocyst subunits by RNAi and to monitor the decrease in protein levels by IHC any further.

5.2 Viral particles for transgene delivery *in vivo*

Investigation of exocyst function *in* or *ex vivo* was hampered by the lethal phenotype, which is induced upon gene deletion of exocyst subunits in mammals. Only one knockout study (Sec8) was performed in mammals (Friedrich et al., 1997) but the lethal phenotypes observed in drosophila for Sec5, Sec6, Sec10 and Sec15 suggest that a similar phenotype might display in mammals or at least discouraged scientist to generate knockout mice (Andrews et al., 2002; Beronja et al., 2005; Mehta et al., 2005; Murthy et al., 2003). The design of replication-deficient viral vectors in conjunction with stereotaxic injections now allows for acute genetic modification of a locally confined brain region. This experimental paradigm enabled us to provide the first study about exocyst function *in vivo*.

However, the unreliable production of recombinant adeno-associated and lentiviral particles encoding for exocyst subunits posed severe constraints on our initial experimental strategy. Only rAAV encoding for GFP-Exo70 and GFP-Exo70Nter could be purified to high virus titer stocks, which are necessary for stereotaxic injections. After several rounds of production, in which we altered number of producing cells, molar relations of helper and vector plasmids and transfection strategies, it still was not possible to increase the titer of virus stocks. Transgenes not related to exocyst, like fluorescent proteins, which were processed in parallel, were packaged reliably in viral particles. Since transfection of viral vector alone resulted in stable expression of transgenes in producer cells, toxic effects of exocyst subunit overexpression are unlikely. Also lentiviruses, which can package up to 10 kb and therefore offer enough sequence capacity to encode GFP-fusion proteins of exocyst subunits, could not be refined to a high number of viral particles indicating that packaging capacity alone is not responsible for inefficient virus production. It might be that secondary DNA structures adopted by exocyst transgenes are the cause for packaging problems into viral capsids but we do not have further proof for this assumption. According to personal communication with D. Grimm, who devised the rAAV production protocol used here, some transgenes do not package efficiently into rAAV for unknown reasons, suggesting that the virus production problems encountered here are a general rather than an exocyst specific characteristic of rAAV production.

Nevertheless, the two rAAVs harbouring GFP-Exo70 and GFP-Exo70Nter transgenes could be used to infect hippocampal neurons and to validate expression of correctly sized GFP-fusion proteins by Western Blot. These viruses were used in this study to overexpress GFP-fusion proteins of exocyst subunits in globular bushy cells in order to analyse exocyst function *in vivo*.

5.3 Overexpression of exocyst subunits *in vivo*

Virus mediated overexpression of GFP-Exo70 and GFP-Exo70Nter in globular bushy cells enabled us to describe the GFP-signal inside the calyx of Held under *in vivo* conditions. Both proteins showed an ubiquitous distribution similar to what has been reported in different permanent cell lines for GFP- or Myc-tagged proteins (Bao et al., 2008; Liu et al., 2007; Matern et al., 2001; Pommereit and Wouters, 2007; Zuo et al., 2006). Also in line with previous publications, GFP-Exo70 had a preference towards the plasma membrane in P21 animals, whereas GFP-Exo70Nter did not localize to this cell compartment. This observation was expected since GFP-Exo70Nter misses the C-terminal amino acids which are required for its interaction with $PI(4,5)P_2$ (Liu et al., 2007). Interestingly, GFP-Exo70 was not enriched in the plasma membrane of calyces from P13 animals. The difference between the localization of GFP-Exo70 in maturing and adult calyces might reflect a function of this subunit that is dependent on the maturational stage of the nerve terminal. Based on the localization data we cannot conclude in exactly which process Exo70 is acting during maturation.

5.4 Differences between *in vitro* and *in vivo*

Overexpression of GFP-Exo70 was shown to induce the formation of membrane protrusion in permanent cell lines and hippocampal cell culture (Liu et al., 2007; Pommereit and Wouters, 2007; Wang et al., 2004b; Xu et al., 2005; Zuo et al., 2006). We also observed the occurrence of membrane protrusion in cultured hippocampal cells, when neurons were transduced with GFP-Exo70. In contrast, a similar effect upon overexpression of GFP-Exo70 in globular bushy cells was not evident *in vivo*. Neither was the dendritic tree abnormally fenestrated nor did we detect an increased number of collaterals at the presynaptic nerve terminal or any membrane protrusions along the cell perimeter.

During neuronal development, neurite outgrowth is controlled by cell-cell interactions. This signalling can occur via secreted factors, which act over distance, and is also regulated by surface expressed cell-adhesion molecules (CAM), which are incorporated into the plasma membrane and therefore signal in immediate proximity. In cultured cells, the later signalling event can only occur if cells have contact with each other. This criterion is rarely met in hippocampal preparations and could explain the different sprouting behaviour between cultured hippocampal cells and neurons in intact tissue: while neurite extension is negatively regulated in neurons in intact tissue, cultured hippocampal neurons do not receive such a negative feedback from (not existing) neighbouring cells. This explanation would also imply that the exocyst complex is

involved in a signalling pathway that is acting via cell-adhesion molecules and regulates neuronal outgrowth. A similar mechanism was elucidated by Pommereit and Wouters, (2007), who showed that NGF sensation induces binding of TC10 and Exo70 in PC12 cells and formation of this complex is necessary for the occurrence of membrane protrusions. This pathway was shown to counteract Cdc42 mediated N-WASP activation in a locally controlled manner by the presence of Exo70 at the plasma membrane. The authors therefore proposed that the Exo70-TC10 pathway activates the Arp2/3 complex in locally controlled manner, which would represent an intriguing link between actin dynamics and vesicle transport that is required for membrane extension.

5.5 Exocyst is necessary for growth of nerve terminals

In the process of neurite elongation, secretory vesicles are secreted at the neuronal growth cone and this process requires a multitude of cellular machineries like actin and microtubule dynamics, protein synthesis, protein modification, lipid synthesis and directed transport (Futerman and Banker, 1996). The exocyst complex was suggested to be involved in neurite outgrowth by delivering secretory vesicles to the growth cone of differentiating neurons. This was inferred from the observation that exocyst subunits are enriched at sites of neurite extension in hippocampal neurons (Hazuka et al., 1999) and are recruited to the growth cone of differentiating PC12 cells. Furthermore, neurite outgrowth is repressed by expression of a dominant-negative form of Sec10 in PC12 cells (Vega and Hsu, 2001) and by Sec5 deletion in drosophila neuronal cultures (Murthy et al., 2003). Here, we investigated the involvement of the exocyst complex in neuronal maturation of mammals *in vivo* with a focus on the maturation of the presynaptic compartment. This was accomplished by virus mediated perturbation of exocyst function in globular bushy cells at P2 and subsequent analysis of calyx volume at two different developmental stages, i.e. maturing (P13) and adult (P21) calyces.

Exocyst function was perturbed in our experimental approached by overexpression of GFP-Exo70Nter. The dominant-negative truncation construct Exo70Nter employed here was used in several studies before. In these studies, it was shown that overexpression of Exo70Nter impedes surface expression of secretory proteins like VSV-G, Glut4 or AMPARs, but that the transport of these secretory proteins to the plasma membrane still persists (Gerges et al., 2006; Inoue et al., 2003; Inoue et al., 2006; Liu et al., 2007). This phenotype indicates that Exo70 is not responsible for trafficking of cargo to the plasma membrane, but for late fusion events of secretory vesicles that mediate the incorporation of proteins into the plasma membrane. Since Exo70Nter still interacts with other exocyst subunits (Sec8) (Liu et al., 2007; Zuo et al., 2006), the observed insertion defects most

likely arise from the deletion of amino acids K632 and K635, which are necessary for the direct interaction of Exo70 with the plasma membrane via $PI(4,5)P_2$ (Liu et al., 2007). This model proposes that Exo70 serves as a landmark for the remaining exocyst subunits at the plasma membrane. Therefore, we anticipated a strong perturbation in exocyst function by interfering in the most downstream event of exocyst mediated vesicle secretion.

The volume of mOrange expressing calyces of Held was determined from confocal image stacks and afterwards scored for the absence or presence of either GFP-Exo70 or GFP-Exo70Nter. Comparison of wildtype (only mOrange expressing), GFP-Exo70 and GFP-Exo70Nter expressing calyces revealed that overexpression of GFP-Exo70Nter leads to a decrease in calyx volume in P13 animals. Surprisingly, this effect was not observed in adult calyces at P21. This was unexpected at first since we anticipated that a dominant-negative effect in membrane addition would increase over time. It is possible that the blockade of exocyst function by overexpression of GFP-Exo70Nter is not complete, because endogenous protein amounts are still present in the transduced neurons. On the other side, protein amounts of the transgene increase over time as judged by GFP-fluorescence and are expected to minimize the effect of endogenous proteins. Thus, if protein amounts are sufficient to block exocyst function before P13, they should also be sufficient to perturb complex function afterwards. Either way, based on volume measurements and inspection of nerve terminal morphology calyces can mature to their adult state, if GFP-Exo70Nter is overexpressed. We do not provide clear evidence whether this is due to incomplete blockade of exocyst function, redundant mechanisms or a development specific function of Exo70. However, we also detected a switch from a cytosolic to a plasma membrane enriched localization of Exo70 for the two ages investigated. In conjunction with this observation and the presence of presumably higher protein amounts of Exo70Nter in older animals, the mismatch between the volume analysis of the two ages would rather argue towards a developmentally regulated function of Exo70.

Overexpression of full-length protein, GFP-Exo70, did not change the volume of calyces of Held at the two ages investigated. As discussed earlier, sprouting phenotypes were detected for several cultured cells, when GFP-Exo70 was overexpressed (Liu et al., 2007; Pommereit and Wouters, 2007; Wang et al., 2004b; Xu et al., 2005; Zuo et al., 2006). Therefore, an increase in nerve terminal volume due to a gain of function phenotype could have been expected. The discrepancy between the *in vitro* and *in vivo* observation is most likely based on differences in cell-cell interactions between these two environments. While signalling from neighbouring cells in tissue might stop neurite

outgrowth, this form of inhibition is not acting on singularized cells in a culture dish and therefore allows for the formation of membrane protrusions *in vitro*.

Based on the surface expression defects observed in cell culture upon overexpression of GFP-Exo70Nter (Gerges et al., 2006; Inoue et al., 2006; Liu et al., 2007), it is plausible to assume, that the decrease in calyx volume caused by our experimental approach impeded the incorporation of cargo vesicles into the plasma membrane of the nerve terminal. This defect most likely arises from the sequestration of other endogenous exocyst subunits by the dominant-negative truncation construct and the inability of this complex to interact with the plasma membrane since the necessary amino acids for plasma membrane anchorage are deleted (aa 632, 635). Another reason for the insertion defects observed upon overexpression of GFP-Exo70Nter could arise from the deletion of amino acids 628-630, which are necessary for interaction of Exo70 with the Arp2/3 complex (Zuo et al., 2006). The Arp2/3 complex is a core protein for actin polymerisation, which exerts its nucleation activity after activation of N-WASP, which in turn is activated by Rho-family GTPases (Pollard and Borisy, 2003). Zuo et al. (2006) showed that deletion of amino acids 628-630 is sufficient to abrogate the formation of actin based membrane protrusions, which are induced by an constitutively active form of Cdc42. Unfortunately, this mutant was not assayed for surface secretion defects of proteins. Membrane expansion involves both dynamic regulation of actin cytoskeleton and delivery of plasma membrane vesicles. The interaction of Exo70 with the plasma membrane (aa 632, 635) and its interaction with the Arp2/3 complex (aa 628-630) establish an intriguing link between those two processes. By overexpression of GFP-Exo70Nter (aa 1-384) both interactions will be affected and it cannot be inferred from the volume analysis whether one effect dominates over the other. Clearly, both pathways are necessary for growth and morphological modifications of the nerve terminal.

5.6 Exocyst and synaptogenesis

The volume analysis of calyces of Held, which overexpressed GFP-Exo70Nter, indicated defects in membrane addition. We were curious to see, whether the observed decrease in volume would be accompanied by a decrease in the number of active zones. This was of special interest since the molecular events, which lead to the formation of these highly specialized membrane areas, is not well characterized. Contact between pre- and postsynaptic partners are initialized by cadherins and members of the immunoglobulin (Ig) superfamilies (reviewed in Craig et al., 2006). Neurexins and neuroligins are surface molecules that can initialize synaptic contacts (reviewed in Dean and Dresbach, 2006). In addition, these neuron specific surface molecules have been

implicated in the recruitment of synaptic components. For example, presentation of neuroligins or synaptic cell-adhesion molecule (SynCAM) to axons induces the assembly of active zones and results in the formation of functional synapses (Biederer et al., 2002; Scheiffele et al., 2000). Also cadherins, which alone are not sufficient to induce synapse assembly, have been implicated to organize synaptic components (reviewed in Salinas and Price, 2005). For example, in β-catenin knockout animals synaptic vesicles are dispersed and the reserve pool of SV is reduced (Bamji et al., 2003). This loss of function is dependent on a C-terminal PDZ binding domain and interaction with an unknown protein. Neurexin, which is the heterologous presynaptic binding partner of neuroligin, and SynCAM also contain PDZ binding motifs on their C-terminal tails and interact with the PDZ domain of calcium/calmodulin-dependent serine protein kinase (CASK) (Biederer et al., 2002; Hata et al., 1996). CASK is a multi-domain scaffold protein that induces actin polymerisation together with protein 4.1 and spectrin on neurexins (Biederer and Sudhof, 2001). CASK also forms a tripartite complex with veli, Munc18-interacting-protein (Mint) and N-type calcium-channels (Biederer and Sudhof, 2001). One prediction of a presynaptic assembly cascade is therefore that postsynaptic neuroligin clusters presynaptic neurexins which would lead to actin activity and delivery of calcium-channels via CASK to the presynaptic specialization. Neurexins can also bind to Mint and to synaptotagmin providing a link to the fusion machinery (Biederer and Sudhof, 2000; Petrenko et al., 1991). Although these findings demonstrate an important role for neurexins in synaptogenesis, a link to the main components of the CAZ like bassoon, piccolo, RIM, Munc13 and ERCs is still missing. These proteins have been suggested to arrive at the active zone in so called piccolo, bassoon transport vesicles (PTVs) and serve as unitary building blocks for active zones (Shapira et al., 2003; Zhai et al., 2001). These vesicles comprise CAZ proteins and also proteins required for synaptic vesicle fusion like piccolo, bassoon, RIM, Munc13, Munc18, syntaxin, SNAP-25, N-type calcium channels, α-liprin and ERC. Thus, active zones could form after contact initiation between partner neurons via CAMs, which triggers the delivery of PTVs to active zones. At present, however, an understanding of these issues in molecular terms is still missing. What molecules are involved in axonal transport and targeting of precursor vesicles? How is transport arrested at particular sites? How are these processes related to the mechanisms of contact initiation?

The exocyst was suggested to specify sites for nascent synapses during synaptogenesis, since some of its subunits preceded the arrival of synaptic marker proteins at sites of active endocytosis (Hazuka et al., 1999). Therefore, the exocyst complex was considered an attractive candidate for the delivery of PTVs to sites of active zone formation. The experimental paradigm used here does not allow probing exocyst

function in synaptogenesis. The calyx establishes its contact with principal cells already at P3 (Kandler and Friauf, 1993), while in this study stereotaxic injections with viral particles were performed at P2. Taking an expression time of at least 5 days into consideration, potential interference will take place when the synaptic terminal has already matured considerably and is able to undergo neurotransmitter release (Taschenberger and von Gersdorff, 2000). Despite the existence of an active synapse at P7, the calyx of Held is continuously changing morphology up to its adult stage at P21. Therefore, new synaptic contacts have to be assembled at before non-existing sites and already established synaptic contacts might have to be disassembled due to membrane reorganization. Therefore, the mechanisms, which govern active zone assembly, are still required in the calyx of Held after partner neurons have contacted each other.

Here, we assessed the distribution of active zones in the calyx of Held at the maturational stage (P13) and at the adult stage (P21). This was accomplished by immunohistochemistry against the active zone resident protein bassoon. This active zone marker was detected in a punctuate pattern in the presynaptic terminal at both ages investigated. Immunoreactivity resided juxtaposed to the postsynaptic cell, whereas some signal could also be found inside the cytoplasm. While the first population reflects active zones, the later population most likely represents PTVs. Calyces, which overexpressed either GFP-Exo70 or GFP-Exo70Nter, were indistinguishable from wildtype nerve terminals. Hence, overexpression of exocyst subunits does not influence the distribution of the active zone marker protein bassoon on a light microscopical level. If the exocyst complex would be involved in the transport of PTVs, overexpression of GFP-Exo70Nter would be expected to stall the incorporation of the precursor vesicles into the plasma membrane. This could result in an increase in cytoplasmatically localized PTVs or in membrane attached but not incorporated vesicles. Membrane bound and membrane incorporated populations can hardly be separate by the resolution of the confocal microscope used here (194 nm for 633 nm wavelength). However, the qualitatively identical bassoon distribution pattern between wildtype and exocyst subunit overexpressing calyces argue against an involvement of the exocyst complex in the delivery of PTVs. In addition, electrophysiological recordings support the existence of functional active zones indicating that immunoreactivity in close proximity to the plasma membrane reflects incorporated active zones in exocyst subunit overexpressing calyces (see below). Thus, the exocyst complex does not contribute to active zone assembly by transport of active zone precursor vesicles *in vivo*. Since overexpression of GFP-Exo70Nter clearly decreased the volume of presynaptic terminals at P13 this finding also suggests that two independent pathways exist for active zone assembly and membrane extension and that exocyst would only be involved in the later.

5.7 Exocysts involvement in the synaptic vesicle cycle

Calcium-evoked release of neurotransmitter is restricted to a specialized membrane area called the active zone. During ongoing synaptic activity the readily releasable pool of synaptic vesicles is depleted and has to be refilled with synaptic vesicles from the recycling pool (Rizzoli and Betz, 2005). Active zone resident proteins like RIM and Munc13 bind to the synaptic vesicle specific Rab3 GTPase and this interaction was suggested to assist in directed docking of synaptic vesicles at the active zone (Dulubova et al., 2005). However, ultrastructural analysis of synapses from RIM or Munc13 knockout animals show that the active zones of these animals do exhibit docked synaptic vesicles (Augustin et al., 1999; Schoch et al., 2002). Thus, another mechanism has to exist, which brings synaptic vesicles in close proximity to the active zone. Additionally, RIM and Munc13 are active zone resident proteins and their interaction with Rab3 does not explain how synaptic vesicles are transported from more distant areas of the presynaptic compartment to the release site. In the cytoplasm, synaptic vesicles are encircled by an actin scaffold and are "glued" together by synapsin (Hilfiker et al., 1999; Sankaranarayanan et al., 2003). Phosphorylation of synapsins by calcium/calmodulin-dependent protein kinase II (CaMKII) reduces the affinity of synapsin to vesicles and unleashes them for transport to the active zone (Benfenati et al., 1992). Again, which proteins, molecular motors or cytoskeletons are involved in this translocation step is unknown.

Neurotransmitters are not only released by action potentials, but are also released spontaneously. Spontaneous release contributes to ambient levels of neurotransmitters in the extracellular space and therefore also contributes to information processing and cell-cell signalling (Wasser and Kavalali, 2009). There are indications that spontaneously released neurotransmitters are discharged by a population of synaptic vesicles, which is different from the one that is employed after arrival of an action potential. Differences between these populations include the release site as well as the fusion machinery and also the location of storage vesicles in the cytoplasm (Colmeus et al., 1982; Sara et al., 2005).

Subunits of the exocyst complex were found colocalized with synaptic vesicle markers, syntaxin-1 and Rab3, which lead to the hypothesis that the exocyst "mediates the delivery and docking of synaptic vesicles to the plasma membrane" (Ting et al., 1995). This was later on denied by the finding that sites of active exo- and endocytosis are only to a small extent positive for Sec6 (Hazuka et al., 1999). However, the antibody used in the FM-dye experiments was shown afterwards to bind only to a subpopulation of Sec6 further complicating conclusions about an involvement of the exocyst complex in

synaptic vesicle cycling (Yeaman et al., 2001). Since then, exocyst function in synaptic transmission was exclusively addressed in drosophila. Neurotransmission was not affected by genetic deletions or mutations of exocyst subunits Sec5, Sec6, Sec10 or Sec15 (Andrews et al., 2002; Beronja et al., 2005; Mehta et al., 2005; Murthy et al., 2003). These studies clearly suggest that exocyst is not involved in synaptic transmission in invertebrates, but they also highlight the different phenotypes, which are observed upon knockout of a single exocyst subunit suggesting that knockout of a single subunit might not affect the entire function spectrum of the whole complex. For example, interference in Sec8 and Exo70 function was shown to diminish AMPAR insertion into the plasma membrane of mammalian hippocampal neurons (Gerges et al., 2006). If these subunits would have been deleted in drosophila, synaptic transmission should have been altered in an ubiquitous genetic knockout, unless exocyst function relies on different interaction partners in vertebrates and invertebrates. Without further proof, the later case has to be assumed since findings about exocyst function in synaptic vesicle cycling cannot be copied one-to-one from drosophila to mammals, but can only serve as building blocks for hypotheses. Taken together, the exocyst complex has been suggested to supply synaptic vesicles to the active zone but experiments addressing this hypothesis in mammals were inconclusive so far. Studies in drosophila argue against an involvement of several exocyst subunits in synaptic transmission but extrapolating these findings to the function of the whole complex is in disagreement with defects observed in mammals.

Therefore, we decided to unequivocally address exocyst function in mammalian synaptic vesicle cycling by performing postsynaptic electrophysiological recordings to the calyx of Held. Exocyst function was perturbed in our experimental approach by virus mediated overexpression of the dominant-negative truncation construct GFP-Exo70Nter. Potential gain of function phenotypes were also assessed by overexpression of the full-length protein GFP-Exo70. Postsynaptic recordings were conducted at RT with brain slices from P13 rats, which had been injected at P2 with rAAVs encoding for the respective exocyst subunit.

Electrophysiological recordings revealed that frequency, quantal size and fusion kinetics of spontaneous miniature events was unchanged upon overexpression of exocyst subunits. Similarly, low-frequency (0.1 Hz) stimulation did not reveal differences in quantal content, charge and EPSC kinetics of evoked postsynaptic responses from wildtype and exocyst subunit overexpressing calyces. Thus, overexpression of GFP-Exo70 or GFP-Exo70Nter does not influence the fusion machinery of both spontaneous and evoked synaptic vesicle fusion since fusion kinetics are unchanged. A comparable quantal size between the three groups indicates that refilling of synaptic vesicles with neurotransmitters is not influenced by our perturbation approach. Consecutively, an

unchanged quantal content and miniature frequency suggests that the product of release probability and number of primed vesicles remains the same, if exocyst subunits are overexpressed. To differentiate between these two possibilities, we estimated the readily releasable pool size and found it to be unchanged between the three groups suggesting that release probability is also unaltered. Synaptic short-term depression was analysed for a set of stimulation frequencies (0.3-100 Hz) to investigate exocysts involvement in the molecular mechanisms underlying this from of synaptic plasticity. Again, wildtype responses were indistinguishable from exocyst subunit overexpressing calyces. In conjunction with an unchanged RRP size this result strongly suggests that depletion and replenishment of the RRP is independent from exocyst function. Finally, recovery after depression was assessed and also found to be unaltered supporting the independence of RRP recovery from exocyst function. In summary, our electrophysiological recordings clearly show that overexpression of GFP-Exo70 or GFP-Exo70Nter does not influence synaptic transmission.

The remaining question is to which extent the findings from our experimental approach can be related to the function of the entire complex in synaptic transmission. This involves two aspects: (1) how efficiently was exocyst function perturbed by overexpression of GFP-Exo70 or GFP-Exo70Nter? (2) Is the function of the whole complex affected by interfering with Exo70 or do other exocyst subunits exert their function on their own without the need of a functional Exo70?

The strongest evidence for a successful interference in exocyst function in our *in vivo* model is presented by the reduction in calyx volume for P13 animals upon overexpression of GFP-Exo70Nter. Electrophysiological recordings were conducted at the same age as the volume analysis and if exocyst is involved in the synaptic vesicle cycle effects should have been evident. As discussed earlier, it has to be assumed that endogenous protein levels of Exo70 account for remaining exocyst activity, but if protein levels of the introduced transgene are high enough to perturb one function of the complex, i.e. membrane addition, they most likely should also affect other processes in which the complex is involved. Thus, our electrophysiological measurements in conjunction with calyx volume analysis strongly argue for a successful interference in exocyst function by overexpression of GFP-Exo70Nter and consecutively deny an involvement of the complex in synaptic vesicle cycling.

Overexpression of GFP-Exo70 induces excessive membrane protrusions in cultured cells and thus displays a gain of function phenotype (see above). *In vivo*, this phenotype does not highlight most likely due to negative feedback from neighbouring cells (see above). In our electrophysiological measurements, we also did not observe an increase in mEPSC frequency or EPSC amplitudes upon overexpression of GFP-Exo70, which could

result from amplification of synaptic vesicle transport or tethering capacity. Therefore, overexpression of GFP-Exo70 *in vivo* does either not display a gain of function phenotype or these negative results further confirm the independence of the synaptic vesicle cycle from exocyst function.

Can subunits other than Exo70 compensate for overexpression of GFP-Exo70Nter and thus mask an involvement of the exocyst complex in synaptic vesicle cycling? Principally, it is possible that exocysts influence on the synaptic vesicle cycle is mediated by a subunit different than Exo70 and thus remains undetected in our experiments. Since our understanding of subunit assembly, especially in mammals, is very limited, this possibility cannot be excluded. However, we disfavour this explanation for our results for several reasons: (1) Exo70 is has been shown to be the membrane anchor for the remaining exocyst subunits and therefore the most downstream subunit at which exocyst mediated vesicle secretion converges (Gerges et al., 2006; Liu et al., 2007). Hence, every exocyst mediated secretion event most likely requires functional Exo70. (2) Other subunits like Sec5, Sec6, Sec10 and Sec15 have been investigated in drosophila and were found to be dispensable for synaptic transmission (Andrews et al., 2002; Beronja et al., 2005; Mehta et al., 2005; Murthy et al., 2003). Although these findings cannot be extrapolated without further confirmation to mammals they argue against the possibility, that a subcomplex composed of the remaining subunits Sec3, Sec8 and Exo84 or a combination of those are involved in exocyst mediated synaptic vesicle fusion. (3) We observed defects in membrane addition by overexpression of GFP-Exo70Nter and experiments in cell culture dealing with several different forms of secretion were also affected by knockdown of the full-length protein Exo70 or by overexpression of GFP-Exo70Nter (Bao et al., 2008; Gerges et al., 2006; Inoue et al., 2006; Liu et al., 2007; Pommereit and Wouters, 2007; Xu et al., 2005; Zuo et al., 2006). Thus, it seems that Exo70 is necessary for several different forms of exocyst mediated secretion and a very atypical subcomplex would therefore be required for an exocyst mediated but Exo70 independent form of synaptic vesicle fusion. Taken together, it is possible that an Exo70 independent subcomplex of exocyst subunits is involved in transport and/or tethering of synaptic vesicle but due to the before mentioned reasons we consider this scenario very unlikely. Thus, we postulate that the exocyst complex is not contributing to synaptic vesicle cycling or fusion in mammals *in vivo*.

5.8 Exocyst – quo vadis?

The mammalian exocyst complex was discovered 14 years ago (Hsu et al., 1996; Kee et al., 1997; Matern et al., 2001; Ting et al., 1995). Since then this complex has been

associated with a bewildering array of cellular processes starting from protein synthesis, specific targeting of post Golgi vesicles, actin, microtubule and septin dynamics, oncogenic transformation (Chien et al., 2006; Lim et al., 2005), cytokinesis, polarized outgrowth, synaptic transmission, endocytosis (Chen et al., 2006; Prigent et al., 2003; Zhang et al., 2004) and was shown to be an effector for several GTPases of the Ras superfamily (see Introduction for references if not indicated). This long list of involvements is contrasted by a very limited understanding of subunit interaction. Although initial experiments aimed to unravel the interactions of subunits inside the complex these findings received little attention (Matern et al., 2001; Moskalenko et al., 2003). Instead, interaction partners of single subunits and their effectors have been identified leading to the long list of involvements presented above. Thus, today we are confronted with a vast amount of pathways, in which single subunits are involved, but we are far from understanding complex assembly and hierarchy, if there is any. This situation poses many questions. Does the complex always assemble before it generates a certain output? Does exocyst serve as a central integrator in this regard by receiving information from different cellular processes? Is complex formation necessary or are single subunits independent? If complex formation is necessary, where do we find it in the cell? How important is the complex for the function of single subunits after all? Is the dependency of a single subunit on the complex related to a certain pathway? From an energetic point of view it would be surprising if seven “passive” subunits are awaiting binding of the last subunit to exert a function. Similarly, it is hard to imagine that all eight subunits are always found in one complex and that they would only become active after whole complex formation. A dynamic behaviour of single subunits is both from the theoretical and the experimental point of view more likely. This hypothesis would suggest that single subunits or smaller subcomplexes are at first independent from the whole complex. After activation of a pathway via GTPases from the Ras superfamily, subunits would assemble into a larger subcomplex or the entire complex, which would enable this complex to trigger some kind of response, i.e. transport of vesicles, induction of changes in cytoskeleton dynamics, integration of another pathway or membrane anchorage. However, these schemes are highly speculative since a cascade that is based on more than two exocyst subunits has never been presented. To a major part the uncertainty about the composition of exocyst complexes is related to the unreliable localization of single subunits. Immunlocalization suffers from epitope inaccessibility after subunit assembly and genetic labels could sterically avoid complex formation or result in false-positive signal due to protein overexpression. In addition, it represents an experimental as well as a technical challenge to monitor eight subunits at the same time. *In vitro* biochemical studies of truncation constructs might provide answers to the

location of intersubunit binding sites to finally arrive at an exocyst complex assembly map. This map would not answer which complexes exist where in the cell since the possibility of binding does not include necessity. But it might serve to isolate single subunits and their pathways from the action of the remaining complex in the cell to allow further conclusions about the importance of single subunits and complex assembly in specific cellular responses. In any case, such a map would substantially increase our understanding of the complex and serve as a baseline to exploit the importance and action of different subcomplexes to establish a coherent picture of exocyst function.

Here, we addressed three longstanding hypotheses for the exocyst complex: first, we confirmed the involvement of the exocyst complex in neuron outgrowth *in vivo* by showing that overexpression of a dominant-negative subunit decreases the volume of the calyx of Held. Second, immunohistochemistry against the active zone marker protein bassoon argues against an influence of the exocyst in transport of synaptic precursor vesicles. This finding suggests that exocyst is not involved in synaptogenesis by delivering of active zone precursor vesicles as suggested before. Third, synaptic vesicle cycling is completely unaffected by our experimental approach excluding the initial assumption that exocyst is contributing to synaptic vesicle tethering.

With this study, we provide new insights about this exciting eight-subunit protein complex and hope that it will assist future studies to unravel the many remaining mysteries, which need to be addressed. It will require many years of research to understand the function of all eight single subunits and especially how they become integrated locally and functionally into the complex. Every bit of information will be curiously awaited and necessary to deprive exocyst of its secrets.

6 Summary / Zusammenfassung

6.1 Summary

Synaptic vesicles have to be constantly transported to the active zone to ensure ongoing synaptic transmission. Although some proteins which mediate docking and priming of synaptic vesicles have been identified (Munc13, RIM, SNAREs) the molecular mechanisms that mobilize synaptic vesicles from the recycling or reserve pool to the active zone are not well understood. Here, we investigated the involvement of the exocyst complex, a multiprotein tethering complex involved in directed transport of vesicle cargo, in the trafficking of synaptic vesicles. By means of stereotaxic injection of recombinant adeno-associated viral particles into the ventral cochlear nucleus of 2-day-old Sprague Dawley rats we performed acute genetic perturbation of exocyst function by overexpression of a dominant-negative truncation construct of Exo70, a subunit of the exocyst complex, in globular bushy cells to analyze potential changes in synaptic transmission at the calyx of Held. Additionally, the morphology of presynaptic terminals was reconstructed from confocal image stacks to investigate the influence of exocyst perturbation on synaptic architecture and maturation.

Manual reconstruction of 166 calyces of Held and subsequent volume analysis revealed that overexpression of the dominant-negative truncation construct of Exo70 results in a statistically significant decrease in nerve terminal volume at P13 indicating induced defects in membrane addition by acute genetic perturbation. Surprisingly, calyces, which overexpressed the truncation construct of Exo70 (Exo70Nter), had comparable volumes to wildtype cells at a matured state in P21 rats. These findings suggest that while exocyst function is necessary during early maturation of calyces of Held it seems to be dispensable at later developmental stages.

The developmental stage dependent function of Exo70 is further supported by the observation of a localization shift of the full-length GFP-fusion protein Exo70 between the two ages investigated. While adult calyces in P21 rats display plasma membrane localization for GFP-Exo70, this plasma membrane association is not evident for maturing calyces from P13 animals.

Despite the hypomorphic nature of P13 calyces overexpressing Exo70Nter, low frequency (0.1 Hz) stimulation did not affect EPSC kinetics, suggesting that the fusion machinery of synaptic vesicles remained unaffected. Decay of EPSC amplitudes upon repetitive stimulation (0.3 – 100 Hz) was indistinguishable from wildtype, suggesting that exocyst is not involved in the molecular mechanisms underlying short-term depression. Similarly, readily releasable pool size and kinetics of recovery from depression,

frequency of spontaneous release, quantal size and mEPSC kinetics remained unaffected by Exo70Nter overexpression. Thus, perturbation of exocyst function by overexpression of a dominant-negative truncation construct of Exo70 did not affect synaptic transmission, suggesting that exocyst does not contribute to the synaptic vesicle cycle and neurotransmitter release.

In summary, our findings show that the exocyst complex is required for presynaptic membrane addition at early stages of calyx maturation, while a role as a tethering factor of synaptic vesicles in local vesicle recycling remains unlikely. Thus, the exocyst complex may be required for the delivery of cargo from the cell soma to synaptic terminals, but not for trafficking steps in the synaptic vesicle cycle.

6.2 Zusammenfassung

Synaptische Vesikel müssen fortlaufend zur aktiven Zone transportiert werden, um eine anhaltende synaptische Transmission sicherzustellen. Obwohl einige Proteine, die das Andocken und *priming* von synaptischen Vesikeln vermitteln, bereits identifiziert wurden (Munc13, RIM, SNAREs), sind die molekularen Mechanismen, die synaptische Vesikel vom Recycling- oder Reservepool zur aktiven Zone befördern, nicht vollständig verstanden. In dieser Studie haben wir die Beteiligung des Exozystkomplexes, einem Multiproteinkomplex der zum gerichteten Transport vesikulärer Fracht beiträgt, am Zyklus synaptischer Vesikel *in vivo* untersucht. Durch die stereotaktische Injektion von rekombinanten adeno-assoziierten viralen Partikeln in den ventralen kochleären Kern von 2 Tage alten Ratten konnten wir ein dominant negatives Konstrukt von Exo70, einer Untereinheit des Exozystkomplexes, in *globular bushy cells* überexprimieren. Dadurch wurde eine akute genetische Störung der Exozystfunktion hervorgerufen, anhand welcher mögliche Veränderungen der synaptischen Transmission in der Heldschen Calyx untersucht werden konnten. Zusätzlich wurde die Morphologie der präsynaptischen Endigung anhand konfokaler Bildsequenzen rekonstruiert, um den Einfluss des Exozystkomplexes in Hinblick auf Architektur und Reifung der Synapse zu untersuchen.

Manuelle Rekonstruktion von 166 Heldschen Calyces und darauf folgende Volumenbestimmung ergab, dass die Überexpression des dominant negativen Konstruktes von Exo70 in einer statistisch relevanten Verminderung des Volumens von reifenden (P13) Nervenendigung resultiert. Dieser Befund deutet darauf hin, dass die akute genetische Perturbation Defekte im Membranaufbau hervorruft. Überraschenderweise zeigten Calyces von P21 Ratten im maturierten Stadium, welche das verkürzte Konstrukt von Exo70 (Exo70Nter) überexprimieren, ein mit Wildtypzellen vergleichbares Volumen. Dieser Befund deutet darauf hin, dass die Exozystfunktion für

die frühe Reifung der Heldschen Calyx notwendig, in späteren Entwicklungsstadien allerdings verzichtbar ist.

Die funktionelle Abhängigkeit von Exo70 zum Entwicklungsstadium wird weitergehend durch die Beobachtung gestützt, dass die Lokalisation des Wildtyp-Exo70 Proteins zwischen den beiden Entwicklungsstadien (P13 und P21) einer Veränderung unterliegt. Während GFP-Exo70 in adulten Calyces (P21) an der Membran auftritt, ist dieses Lokalisationsmuster in heranreifenden Calyces (P13) nicht zu beobachten.

Ungeachtet des hypomorphen Phänotyps der P13 Calyces, welche Exo70Nter überexprimieren, blieb die EPSC Kinetik bei der Stimulation mit niedrigen Frequenzen (0,1 Hz) zum Wildtyp vergleichbar. Dies deutet darauf hin, dass die Fusionsmaschinerie für synaptische Vesikel durch den experimentellen Ansatz unbeeinflusst bleibt. Die Abnahme der EPSC Amplitude durch repetitive Stimulation (0,3 – 100 Hz) war identisch zum Wildtyp, was darauf hindeutet, dass der Exozyst bei den molekularen Mechanismen, die der *short-term depression* zugrunde liegen, keine Rolle spielt. Ebenso blieb durch die Überexpression von Exo70Nter die Größe des *readily releasable pools*, die Kinetik der Erholung nach Depression, die Frequenz der spontanen Freisetzung, die Quantengröße und mEPSC Kinetik unverändert. Die Perturbation der Exozystfunktion durch die Überexpression eines dominant negativen verkürzten Konstruktes von Exo70 führte folglich nicht zur Veränderung der synpatischen Transmission. Dies deutet darauf hin, dass Exozyst weder an dem synaptischen Vesikelzyklus noch an der Neurotransmitterfreisetzung beteiligt ist.

Zusammenfassend zeigen unsere Daten, dass der Exozystkomplex für den präsynaptischen Membranaufbau im frühen Stadium der Calyxreifung notwendig ist. Die Funktion des Exozyst als *tethering*-Faktor von synaptischen Vesikeln im lokalen Vesikelrecycling erscheint dagegen unwahrscheinlich. Folglich könnte der Exozystkomplex beim Transport vesikulärer Fracht vom Zellsoma zu den synaptischen Endigungen notwendig sein, nicht aber in Transportprozessen des synaptischen Vesikelzyklus.

7 Abbreviations

β-PE	β-phorbol ester
AAV	adeno-associated virus
Ab	antibody
AMPAR	α-amino-3-hydroxy-5-methyl-4-isoxazolepropionic acid receptor
aPKC	atypical protein kinase C
AZ	active zone
bGH	bovine growth hormone
bp	base pair
CAM	cell-adhesion molecule
CaMKII	calcium/calmodulin-dependent protein kinase II
CASK	Ca^{2+}/calmodulin-dependent serine protein kinase
CBA	chicken β-actin
Cdc	cell division cycle
CMV	cytomegalovirus
DAG	diacylglycerol
DIV	days *in vitro*
DNA	deoxyribonucleic acid
EM	electron microscopy
EPSC	excitatory postsynaptic current
ER	endoplasmatic reticulum
FM(-dye)	Fei Mao (the developer name)
GBC	globular bushy cell
GFP	green fluorescent protein
GLYT1	glycine transporter 1
HBSS	Hanks buffered salt solution
HEK	human embryonic kidney
HeLa	Henrietta Lacks
Ig	immunoglobulin
IHC	immunohistochemistry
IP_3R1	1,4,5-trisphosphate receptors
ITR	inverted terminal repeat
LB	lysogeny broth
LTR	long terminal repeats

mAb	monoclonal antibody
MAGUK	membrane-associated guanylate kinases
mEPSC	miniature excitatory postsynaptic current
mGFP	myristoylated green fluorescent protein
Mint	Munc18-interacting protein
MNTB	medial nucleus of the trapezoid body
MTOC	microtubule organizing center
Munc	mammalian uncoordinated
NCAM	neuronal cell adhesion molecule
NGF	nerve growth factor
NMDAR	N-methyl D-aspartate receptor
NRK	normal rat kidney
NSF	N-ethyl maleimide-sensitive factor
N-WASP	neural Wiskott-Aldrich syndrome protein
P	postnatal day
pAb	polyclonal antibody
PBS	phosphate buffered saline
PCR	polymerase chain reaction
PDZ	PSD95/Discs/zona occludence-1 binding domain
$PI(3,4,5)P_3$	phosphatidylinositol 3,4,5-trisphosphate
$PI(4,5)P_2$	phosphatidylinositol 4,5-bisphosphate
PSD	post-synaptic density
PTP	post-tetanic potentiation
PTV	piccolo bassoon transport vesicle
RIM	Rab3-interacting protein
RRP	readily releasable pool
R_S	series resistance
RT	room temperature
SAP	synapse-associated protein
SD	standard deviation
SDS	sodium dodecyl sulfate
SDS-PAGE	sodium dodecyl sulfate polyacrylamide gel electrophoresis
SEM	standard error of the mean
Sg	secretogranin
SNAP	soluble NSF attachment protein
SNARE	soluble NSF attachment protein receptor
STD	short-term depression

STE	short-term enhancement
SV	synaptic vesicle
SynCAM	synaptic cell-adhesion molecule
TGN	trans-Golgi network
TTBS	tween tris-buffered saline
v/v	volume per volume
VCN	ventral cochlear nucleus
VOI	volume of interest
w/v	weight per volume
WPRE	woodchuck hepatitis B virus posttranscriptional element
WT	wildtype

Hiermit erkläre ich an Eides statt, dass ich die vorliegende Dissertation selbstständig und ohne unerlaubte Hilfsmittel durchgeführt habe.

Heidelberg, den 16.06.2009 ……

Darius Schwenger

8 References

Ahmari, S.E., J. Buchanan, and S.J. Smith. 2000. Assembly of presynaptic active zones from cytoplasmic transport packets. *Nat Neurosci*. 3:445-51.

Altrock, W.D., S. tom Dieck, M. Sokolov, A.C. Meyer, A. Sigler, C. Brakebusch, R. Fassler, K. Richter, T.M. Boeckers, H. Potschka, C. Brandt, W. Loscher, D. Grimberg, T. Dresbach, A. Hempelmann, H. Hassan, D. Balschun, J.U. Frey, J.H. Brandstatter, C.C. Garner, C. Rosenmund, and E.D. Gundelfinger. 2003. Functional inactivation of a fraction of excitatory synapses in mice deficient for the active zone protein bassoon. *Neuron*. 37:787-800.

Andrews, H.K., Y.Q. Zhang, N. Trotta, and K. Broadie. 2002. Drosophila sec10 is required for hormone secretion but not general exocytosis or neurotransmission. *Traffic*. 3:906-21.

Arikkath, J., and L.F. Reichardt. 2008. Cadherins and catenins at synapses: roles in synaptogenesis and synaptic plasticity. *Trends Neurosci*. 31:487-94.

Armstrong, N., J. Jasti, M. Beich-Frandsen, and E. Gouaux. 2006. Measurement of conformational changes accompanying desensitization in an ionotropic glutamate receptor. *Cell*. 127:85-97.

Augustin, I., C. Rosenmund, T.C. Sudhof, and N. Brose. 1999. Munc13-1 is essential for fusion competence of glutamatergic synaptic vesicles. *Nature*. 400:457-61.

Bain, A.I., and D.M. Quastel. 1992. Multiplicative and additive Ca(2+)-dependent components of facilitation at mouse endplates. *J Physiol*. 455:383-405.

Bamji, S.X., K. Shimazu, N. Kimes, J. Huelsken, W. Birchmeier, B. Lu, and L.F. Reichardt. 2003. Role of beta-catenin in synaptic vesicle localization and presynaptic assembly. *Neuron*. 40:719-31.

Bao, Y., J.A. Lopez, D.E. James, and W. Hunziker. 2008. Snapin interacts with the Exo70 subunit of the exocyst and modulates GLUT4 trafficking. *J Biol Chem*. 283:324-31.

Basu, J., N. Shen, I. Dulubova, J. Lu, R. Guan, O. Guryev, N.V. Grishin, C. Rosenmund, and J. Rizo. 2005. A minimal domain responsible for Munc13 activity. *Nat Struct Mol Biol*. 12:1017-8.

Becherer, U., and J. Rettig. 2006. Vesicle pools, docking, priming, and release. *Cell Tissue Res*. 326:393-407.

Benfenati, F., F. Valtorta, J.L. Rubenstein, F.S. Gorelick, P. Greengard, and A.J. Czernik. 1992. Synaptic vesicle-associated Ca2+/calmodulin-dependent protein kinase II is a binding protein for synapsin I. *Nature*. 359:417-20.

Benson, D.L., and H. Tanaka. 1998. N-cadherin redistribution during synaptogenesis in hippocampal neurons. *J Neurosci*. 18:6892-904.

Bentley, D., and M. Caudy. 1983. Pioneer axons lose directed growth after selective killing of guidepost cells. *Nature*. 304:62-5.

Beronja, S., P. Laprise, O. Papoulas, M. Pellikka, J. Sisson, and U. Tepass. 2005. Essential function of Drosophila Sec6 in apical exocytosis of epithelial photoreceptor cells. *J Cell Biol*. 169:635-46.

Betz, A., U. Ashery, M. Rickmann, I. Augustin, E. Neher, T.C. Sudhof, J. Rettig, and N. Brose. 1998. Munc13-1 is a presynaptic phorbol ester receptor that enhances neurotransmitter release. *Neuron*. 21:123-36.

Betz, A., P. Thakur, H.J. Junge, U. Ashery, J.S. Rhee, V. Scheuss, C. Rosenmund, J. Rettig, and N. Brose. 2001. Functional interaction of the active zone proteins Munc13-1 and RIM1 in synaptic vesicle priming. *Neuron*. 30:183-96.

Betz, W.J. 1970. Depression of transmitter release at the neuromuscular junction of the frog. *J Physiol*. 206:629-44.

Biederer, T., Y. Sara, M. Mozhayeva, D. Atasoy, X. Liu, E.T. Kavalali, and T.C. Sudhof. 2002. SynCAM, a synaptic adhesion molecule that drives synapse assembly. *Science*. 297:1525-31.

Biederer, T., and T.C. Sudhof. 2000. Mints as adaptors. Direct binding to neurexins and recruitment of munc18. *J Biol Chem*. 275:39803-6.

Biederer, T., and T.C. Sudhof. 2001. CASK and protein 4.1 support F-actin nucleation on neurexins. *J Biol Chem*. 276:47869-76.

Boyd, C., T. Hughes, M. Pypaert, and P. Novick. 2004. Vesicles carry most exocyst subunits to exocytic sites marked by the remaining two subunits, Sec3p and Exo70p. *J Cell Biol*. 167:889-901.

Butz, S., M. Okamoto, and T.C. Sudhof. 1998. A tripartite protein complex with the potential to couple synaptic vesicle exocytosis to cell adhesion in brain. *Cell*. 94:773-82.

Calakos, N., S. Schoch, T.C. Sudhof, and R.C. Malenka. 2004. Multiple roles for the active zone protein RIM1alpha in late stages of neurotransmitter release. *Neuron*. 42:889-96.

Carter, A.G., and W.G. Regehr. 2002. Quantal events shape cerebellar interneuron firing. *Nat Neurosci*. 5:1309-18.

Cases-Langhoff, C., B. Voss, A.M. Garner, U. Appeltauer, K. Takei, S. Kindler, R.W. Veh, P. De Camilli, E.D. Gundelfinger, and C.C. Garner. 1996. Piccolo, a novel 420 kDa protein associated with the presynaptic cytomatrix. *Eur J Cell Biol*. 69:214-23.

Charron, F., E. Stein, J. Jeong, A.P. McMahon, and M. Tessier-Lavigne. 2003. The morphogen sonic hedgehog is an axonal chemoattractant that collaborates with netrin-1 in midline axon guidance. *Cell*. 113:11-23.

Chen, X.W., M. Inoue, S.C. Hsu, and A.R. Saltiel. 2006. RalA-exocyst-dependent Recycling Endosome Trafficking Is Required for the Completion of Cytokinesis. *J Biol Chem*. 281:38609-16.

Chen, X.W., D. Leto, S.H. Chiang, Q. Wang, and A.R. Saltiel. 2007. Activation of RalA is required for insulin-stimulated Glut4 trafficking to the plasma membrane via the exocyst and the motor protein Myo1c. *Dev Cell*. 13:391-404.

Chien, Y., S. Kim, R. Bumeister, Y.M. Loo, S.W. Kwon, C.L. Johnson, M.G. Balakireva, Y. Romeo, L. Kopelovich, M. Gale, Jr., C. Yeaman, J.H. Camonis, Y. Zhao, and M.A. White. 2006. RalB GTPase-mediated activation of the IkappaB family kinase TBK1 couples innate immune signaling to tumor cell survival. *Cell*. 127:157-70.

Colmeus, C., S. Gomez, J. Molgo, and S. Thesleff. 1982. Discrepancies between spontaneous and evoked synaptic potentials at normal, regenerating and botulinum toxin poisoned mammalian neuromuscular junctions. *Proc R Soc Lond B Biol Sci*. 215:63-74.

Colon-Ramos, D.A., M.A. Margeta, and K. Shen. 2007. Glia promote local synaptogenesis through UNC-6 (netrin) signaling in C. elegans. *Science*. 318:103-6.

Craig, A.M., E.R. Graf, and M.W. Linhoff. 2006. How to build a central synapse: clues from cell culture. *Trends Neurosci*. 29:8-20.

Cubelos, B., C. Gimenez, and F. Zafra. 2005. The glycine transporter GLYT1 interacts with Sec3, a component of the exocyst complex. *Neuropharmacology*. 49:935-44.

de Lange, R.P., A.D. de Roos, and J.G. Borst. 2003. Two modes of vesicle recycling in the rat calyx of Held. *J Neurosci*. 23:10164-73.

Dean, C., and T. Dresbach. 2006. Neuroligins and neurexins: linking cell adhesion, synapse formation and cognitive function. *Trends Neurosci*. 29:21-9.

Dean, C., F.G. Scholl, J. Choih, S. DeMaria, J. Berger, E. Isacoff, and P. Scheiffele. 2003. Neurexin mediates the assembly of presynaptic terminals. *Nat Neurosci*. 6:708-16.

Deguchi-Tawarada, M., E. Inoue, E. Takao-Rikitsu, M. Inoue, T. Ohtsuka, and Y. Takai. 2004. CAST2: identification and characterization of a protein structurally related to the presynaptic cytomatrix protein CAST. *Genes Cells*. 9:15-23.

Del Rio, J.A., B. Heimrich, V. Borrell, E. Forster, A. Drakew, S. Alcantara, K. Nakajima, T. Miyata, M. Ogawa, K. Mikoshiba, P. Derer, M. Frotscher, and E. Soriano. 1997. A role for Cajal-Retzius cells and reelin in the development of hippocampal connections. *Nature*. 385:70-4.

Dick, O., S. tom Dieck, W.D. Altrock, J. Ammermuller, R. Weiler, C.C. Garner, E.D. Gundelfinger, and J.H. Brandstatter. 2003. The presynaptic active zone protein bassoon is essential for photoreceptor ribbon synapse formation in the retina. *Neuron*. 37:775-86.

Dresbach, T., A. Hempelmann, C. Spilker, S. tom Dieck, W.D. Altrock, W. Zuschratter, C.C. Garner, and E.D. Gundelfinger. 2003. Functional regions of the presynaptic cytomatrix protein bassoon: significance for synaptic targeting and cytomatrix anchoring. *Mol Cell Neurosci*. 23:279-91.

Dresbach, T., A. Neeb, G. Meyer, E.D. Gundelfinger, and N. Brose. 2004. Synaptic targeting of neuroligin is independent of neurexin and SAP90/PSD95 binding. *Mol Cell Neurosci*. 27:227-35.

Dresbach, T., V. Torres, N. Wittenmayer, W.D. Altrock, P. Zamorano, W. Zuschratter, R. Nawrotzki, N.E. Ziv, C.C. Garner, and E.D. Gundelfinger. 2006. Assembly of active zone precursor vesicles: obligatory trafficking of presynaptic cytomatrix proteins Bassoon and Piccolo via a trans-Golgi compartment. *J Biol Chem*. 281:6038-47.

Dulubova, I., X. Lou, J. Lu, I. Huryeva, A. Alam, R. Schneggenburger, T.C. Sudhof, and J. Rizo. 2005. A Munc13/RIM/Rab3 tripartite complex: from priming to plasticity? *EMBO J*. 24:2839-50.

Dulubova, I., S. Sugita, S. Hill, M. Hosaka, I. Fernandez, T.C. Sudhof, and J. Rizo. 1999. A conformational switch in syntaxin during exocytosis: role of munc18. *EMBO J*. 18:4372-82.

Ewart, M.A., M. Clarke, S. Kane, L.H. Chamberlain, and G.W. Gould. 2005. Evidence for a role of the exocyst in insulin-stimulated Glut4 trafficking in 3T3-L1 adipocytes. *J Biol Chem*. 280:3812-6.

Fatt, P., and B. Katz. 1950. Some observations on biological noise. *Nature*. 166:597-8.

Fatt, P., and B. Katz. 1951. An analysis of the end-plate potential recorded with an intracellular electrode. *J Physiol*. 115:320-70.

Fatt, P., and B. Katz. 1952. Spontaneous subthreshold activity at motor nerve endings. *J Physiol*. 117:109-28.

Finger, F.P., T.E. Hughes, and P. Novick. 1998. Sec3p is a spatial landmark for polarized secretion in budding yeast. *Cell*. 92:559-71.

Ford, M.C., B. Grothe, and A. Klug. 2009. Fenestration of the calyx of Held occurs sequentially along the tonotopic axis, is influenced by afferent activity, and facilitates glutamate clearance. *J Comp Neurol*. 514:92-106.

Friedrich, G.A., J.D. Hildebrand, and P. Soriano. 1997. The secretory protein Sec8 is required for paraxial mesoderm formation in the mouse. *Dev Biol*. 192:364-74.

Futerman, A.H., and G.A. Banker. 1996. The economics of neurite outgrowth--the addition of new membrane to growing axons. *Trends Neurosci*. 19:144-9.

Geppert, M., Y. Goda, R.E. Hammer, C. Li, T.W. Rosahl, C.F. Stevens, and T.C. Sudhof. 1994. Synaptotagmin I: a major Ca2+ sensor for transmitter release at a central synapse. *Cell*. 79:717-27.

Gerges, N.Z., D.S. Backos, C.N. Rupasinghe, M.R. Spaller, and J.A. Esteban. 2006. Dual role of the exocyst in AMPA receptor targeting and insertion into the postsynaptic membrane. *Embo J*. 25:1623-34.

Grimm, D., M.A. Kay, and J.A. Kleinschmidt. 2003. Helper virus-free, optically controllable, and two-plasmid-based production of adeno-associated virus vectors of serotypes 1 to 6. *Mol Ther*. 7:839-50.

Grindstaff, K.K., C. Yeaman, N. Anandasabapathy, S.C. Hsu, E. Rodriguez-Boulan, R.H. Scheller, and W.J. Nelson. 1998. Sec6/8 complex is recruited to cell-cell contacts and specifies transport vesicle delivery to the basal-lateral membrane in epithelial cells. *Cell*. 93:731-40.

Groemer, T.W., and J. Klingauf. 2007. Synaptic vesicles recycling spontaneously and during activity belong to the same vesicle pool. *Nat Neurosci*. 10:145-7.

Gromley, A., C. Yeaman, J. Rosa, S. Redick, C.T. Chen, S. Mirabelle, M. Guha, J. Sillibourne, and S.J. Doxsey. 2005. Centriolin anchoring of exocyst and SNARE complexes at the midbody is required for secretory-vesicle-mediated abscission. *Cell*. 123:75-87.

Guan, R., H. Dai, and J. Rizo. 2008. Binding of the Munc13-1 MUN domain to membrane-anchored SNARE complexes. *Biochemistry*. 47:1474-81.

Guo, W., A. Grant, and P. Novick. 1999a. Exo84p is an exocyst protein essential for secretion. *J Biol Chem*. 274:23558-64.

Guo, W., D. Roth, C. Walch-Solimena, and P. Novick. 1999b. The exocyst is an effector for Sec4p, targeting secretory vesicles to sites of exocytosis. *Embo J*. 18:1071-80.

Guo, W., F. Tamanoi, and P. Novick. 2001. Spatial regulation of the exocyst complex by Rho1 GTPase. *Nat Cell Biol*. 3:353-60.

Harata, N.C., A.M. Aravanis, and R.W. Tsien. 2006. Kiss-and-run and full-collapse fusion as modes of exo-endocytosis in neurosecretion. *J Neurochem*. 97:1546-70.

Hata, Y., S. Butz, and T.C. Sudhof. 1996. CASK: a novel dlg/PSD95 homolog with an N-terminal calmodulin-dependent protein kinase domain identified by interaction with neurexins. *J Neurosci*. 16:2488-94.

Hazuka, C.D., D.L. Foletti, S.C. Hsu, Y. Kee, F.W. Hopf, and R.H. Scheller. 1999. The sec6/8 complex is located at neurite outgrowth and axonal synapse-assembly domains. *J Neurosci*. 19:1324-34.

Held, Hans (1893) Die zentrale Gehörleitung. Arch Anat Physiol Anat Abtheil 17:201–248)

Hilfiker, S., V.A. Pieribone, A.J. Czernik, H.T. Kao, G.J. Augustine, and P. Greengard. 1999. Synapsins as regulators of neurotransmitter release. *Philos Trans R Soc Lond B Biol Sci*. 354:269-79.

Hodgkin, A.L., and A.F. Huxley. 1952. A quantitative description of membrane current and its application to conduction and excitation in nerve. *J Physiol*. 117:500-44.

Hsu, S.C., C.D. Hazuka, R. Roth, D.L. Foletti, J. Heuser, and R.H. Scheller. 1998. Subunit composition, protein interactions, and structures of the mammalian brain sec6/8 complex and septin filaments. *Neuron*. 20:1111-22.

Hsu, S.C., A.E. Ting, C.D. Hazuka, S. Davanger, J.W. Kenny, Y. Kee, and R.H. Scheller. 1996. The mammalian brain rsec6/8 complex. *Neuron*. 17:1209-19.

Ichtchenko, K., Y. Hata, T. Nguyen, B. Ullrich, M. Missler, C. Moomaw, and T.C. Sudhof. 1995. Neuroligin 1: a splice site-specific ligand for beta-neurexins. *Cell*. 81:435-43.

Inoue, M., L. Chang, J. Hwang, S.H. Chiang, and A.R. Saltiel. 2003. The exocyst complex is required for targeting of Glut4 to the plasma membrane by insulin. *Nature*. 422:629-33.

Inoue, M., S.H. Chiang, L. Chang, X.W. Chen, and A.R. Saltiel. 2006. Compartmentalization of the exocyst complex in lipid rafts controls Glut4 vesicle tethering. *Mol Biol Cell*. 17:2303-11.

Isaacson, J.S., and B. Walmsley. 1995. Counting quanta: direct measurements of transmitter release at a central synapse. *Neuron*. 15:875-84.

Junge, H.J., J.S. Rhee, O. Jahn, F. Varoqueaux, J. Spiess, M.N. Waxham, C. Rosenmund, and N. Brose. 2004. Calmodulin and Munc13 form a Ca2+ sensor/effector complex that controls short-term synaptic plasticity. *Cell*. 118:389-401.

Kandel, E.R. 2001. The molecular biology of memory storage: a dialogue between genes and synapses. *Science*. 294:1030-8.

Kandler, K., and E. Friauf. 1993. Pre- and postnatal development of efferent connections of the cochlear nucleus in the rat. *J Comp Neurol*. 328:161-84.

Katz, B., and R. Miledi. 1968. The role of calcium in neuromuscular facilitation. *J Physiol*. 195:481-92.

Kee, Y., J.S. Yoo, C.D. Hazuka, K.E. Peterson, S.C. Hsu, and R.H. Scheller. 1997. Subunit structure of the mammalian exocyst complex. *Proc Natl Acad Sci U S A*. 94:14438-43.

Kidd, T., K.S. Bland, and C.S. Goodman. 1999. Slit is the midline repellent for the robo receptor in Drosophila. *Cell*. 96:785-94.

Kobielak, A., and E. Fuchs. 2004. Alpha-catenin: at the junction of intercellular adhesion and actin dynamics. *Nat Rev Mol Cell Biol*. 5:614-25.

Koushika, S.P., J.E. Richmond, G. Hadwiger, R.M. Weimer, E.M. Jorgensen, and M.L. Nonet. 2001. A post-docking role for active zone protein Rim. *Nat Neurosci*. 4:997-1005.

Lalli, G. 2009. RalA and the exocyst complex influence neuronal polarity through PAR-3 and aPKC. *J Cell Sci*. 122:1499-506.

Lalli, G., and A. Hall. 2005. Ral GTPases regulate neurite branching through GAP-43 and the exocyst complex. *J Cell Biol*. 171:857-69.

Landau, E.M., A. Smolinsky, and Y. Lass. 1973. Post-tetanic potentiation and facilitation do not share a common calcium-dependent mechanism. *Nat New Biol*. 244:155-7.

Levinson, J.N., N. Chery, K. Huang, T.P. Wong, K. Gerrow, R. Kang, O. Prange, Y.T. Wang, and A. El-Husseini. 2005. Neuroligins mediate excitatory and inhibitory synapse formation: involvement of PSD-95 and neurexin-1beta in neuroligin-induced synaptic specificity. *J Biol Chem*. 280:17312-9.

Lim, K.H., A.T. Baines, J.J. Fiordalisi, M. Shipitsin, L.A. Feig, A.D. Cox, C.J. Der, and C.M. Counter. 2005. Activation of RalA is critical for Ras-induced tumorigenesis of human cells. *Cancer Cell*. 7:533-45.

Lipschutz, J.H., V.R. Lingappa, and K.E. Mostov. 2003. The exocyst affects protein synthesis by acting on the translocation machinery of the endoplasmic reticulum. *J Biol Chem*. 278:20954-60.

Lisman, J.E., S. Raghavachari, and R.W. Tsien. 2007. The sequence of events that underlie quantal transmission at central glutamatergic synapses. *Nat Rev Neurosci*. 8:597-609.

Liu, J., X. Zuo, P. Yue, and W. Guo. 2007. Phosphatidylinositol 4,5-bisphosphate mediates the targeting of the exocyst to the plasma membrane for exocytosis in mammalian cells. *Mol Biol Cell*. 18:4483-92.

Lizunov, V.A., I. Lisinski, K. Stenkula, J. Zimmerberg, and S.W. Cushman. 2009. Insulin Regulates Fusion of GLUT4 Vesicles Independent of Exo70-Mediated Tethering. *J Biol Chem*.

Llinas, R., I.Z. Steinberg, and K. Walton. 1981. Relationship between presynaptic calcium current and postsynaptic potential in squid giant synapse. *Biophys J*. 33:323-51.

Lois, C., E.J. Hong, S. Pease, E.J. Brown, and D. Baltimore. 2002. Germline transmission and tissue-specific expression of transgenes delivered by lentiviral vectors. *Science*. 295:868-72.

Lopez-Bendito, G., A. Cautinat, J.A. Sanchez, F. Bielle, N. Flames, A.N. Garratt, D.A. Talmage, L.W. Role, P. Charnay, O. Marin, and S. Garel. 2006. Tangential neuronal migration controls axon guidance: a role for neuregulin-1 in thalamocortical axon navigation. *Cell*. 125:127-42.

Lyons, P.D., G.R. Peck, A.N. Kettenbach, S.A. Gerber, L. Roudaia, and G.E. Lienhard. 2008. Insulin stimulates the phosphorylation of the exocyst protein Sec8 in adipocytes. *Biosci Rep*.

Magleby, K.L., and J.E. Zengel. 1982. A quantitative description of stimulation-induced changes in transmitter release at the frog neuromuscular junction. *J Gen Physiol*. 80:613-38.

Matern, H.T., C. Yeaman, W.J. Nelson, and R.H. Scheller. 2001. The Sec6/8 complex in mammalian cells: characterization of mammalian Sec3, subunit interactions, and expression of subunits in polarized cells. *Proc Natl Acad Sci U S A*. 98:9648-53.

McKinney, R.A., M. Capogna, R. Durr, B.H. Gahwiler, and S.M. Thompson. 1999. Miniature synaptic events maintain dendritic spines via AMPA receptor activation. *Nat Neurosci*. 2:44-9.

Mehta, S.Q., P.R. Hiesinger, S. Beronja, R.G. Zhai, K.L. Schulze, P. Verstreken, Y. Cao, Y. Zhou, U. Tepass, M.C. Crair, and H.J. Bellen. 2005. Mutations in Drosophila sec15 reveal a function in neuronal targeting for a subset of exocyst components. *Neuron*. 46:219-32.

Moskalenko, S., D.O. Henry, C. Rosse, G. Mirey, J.H. Camonis, and M.A. White. 2002. The exocyst is a Ral effector complex. *Nat Cell Biol*. 4:66-72.

Moskalenko, S., C. Tong, C. Rosse, G. Mirey, E. Formstecher, L. Daviet, J. Camonis, and M.A. White. 2003. Ral GTPases regulate exocyst assembly through dual subunit interactions. *J Biol Chem*. 278:51743-8.

Murthy, M., D. Garza, R.H. Scheller, and T.L. Schwarz. 2003. Mutations in the exocyst component Sec5 disrupt neuronal membrane traffic, but neurotransmitter release persists. *Neuron*. 37:433-47.

Murthy, M., R. Ranjan, N. Denef, M.E. Higashi, T. Schupbach, and T.L. Schwarz. 2005. Sec6 mutations and the Drosophila exocyst complex. *J Cell Sci*. 118:1139-50.

Murthy, V.N., T.J. Sejnowski, and C.F. Stevens. 1997. Heterogeneous release properties of visualized individual hippocampal synapses. *Neuron*. 18:599-612.

Naldini, L., U. Blomer, P. Gallay, D. Ory, R. Mulligan, F.H. Gage, I.M. Verma, and D. Trono. 1996. In vivo gene delivery and stable transduction of nondividing cells by a lentiviral vector. *Science*. 272:263-7.

Nishiki, T., and G.J. Augustine. 2004. Dual roles of the C2B domain of synaptotagmin I in synchronizing Ca2+-dependent neurotransmitter release. *J Neurosci*. 24:8542-50.

Novick, P., C. Field, and R. Schekman. 1980. Identification of 23 complementation groups required for post-translational events in the yeast secretory pathway. *Cell*. 21:205-15.

Ohtsuka, T., E. Takao-Rikitsu, E. Inoue, M. Inoue, M. Takeuchi, K. Matsubara, M. Deguchi-Tawarada, K. Satoh, K. Morimoto, H. Nakanishi, and Y. Takai. 2002. Cast: a novel protein of the cytomatrix at the active zone of synapses that forms a ternary complex with RIM1 and munc13-1. *J Cell Biol*. 158:577-90.

Okada, A., F. Charron, S. Morin, D.S. Shin, K. Wong, P.J. Fabre, M. Tessier-Lavigne, and S.K. McConnell. 2006. Boc is a receptor for sonic hedgehog in the guidance of commissural axons. *Nature*. 444:369-73.

Petrenko, A.G., M.S. Perin, B.A. Davletov, Y.A. Ushkaryov, M. Geppert, and T.C. Sudhof. 1991. Binding of synaptotagmin to the alpha-latrotoxin receptor implicates both in synaptic vesicle exocytosis. *Nature*. 353:65-8.

Pollard, T.D., and G.G. Borisy. 2003. Cellular motility driven by assembly and disassembly of actin filaments. *Cell*. 112:453-65.

Pommereit, D., and F.S. Wouters. 2007. An NGF-induced Exo70-TC10 complex locally antagonises Cdc42-mediated activation of N-WASP to modulate neurite outgrowth. *J Cell Sci*. 120:2694-705.

Prigent, M., T. Dubois, G. Raposo, V. Derrien, D. Tenza, C. Rosse, J. Camonis, and P. Chavrier. 2003. ARF6 controls post-endocytic recycling through its downstream exocyst complex effector. *J Cell Biol*. 163:1111-21.

Reim, K., M. Mansour, F. Varoqueaux, H.T. McMahon, T.C. Sudhof, N. Brose, and C. Rosenmund. 2001. Complexins regulate a late step in Ca2+-dependent neurotransmitter release. *Cell*. 104:71-81.

Richmond, J.E., R.M. Weimer, and E.M. Jorgensen. 2001. An open form of syntaxin bypasses the requirement for UNC-13 in vesicle priming. *Nature*. 412:338-41.

Riefler, G.M., G. Balasingam, K.G. Lucas, S. Wang, S.C. Hsu, and B.L. Firestein. 2003. Exocyst complex subunit sec8 binds to postsynaptic density protein-95 (PSD-95): a novel interaction regulated by cypin (cytosolic PSD-95 interactor). *Biochem J.* 373:49-55.

Rizo, J., and C. Rosenmund. 2008. Synaptic vesicle fusion. *Nat Struct Mol Biol*. 15:665-74.

Rizzoli, S.O., and W.J. Betz. 2005. Synaptic vesicle pools. *Nat Rev Neurosci*. 6:57-69.

Rosse, C., A. Hatzoglou, M.C. Parrini, M.A. White, P. Chavrier, and J. Camonis. 2006. RalB mobilizes the exocyst to drive cell migration. *Mol Cell Biol*. 26:727-34.

Sakaba, T., and E. Neher. 2001. Calmodulin mediates rapid recruitment of fast-releasing synaptic vesicles at a calyx-type synapse. *Neuron*. 32:1119-31.

Salinas, P.C., and S.R. Price. 2005. Cadherins and catenins in synapse development. *Curr Opin Neurobiol*. 15:73-80.

Sankaranarayanan, S., P.P. Atluri, and T.A. Ryan. 2003. Actin has a molecular scaffolding, not propulsive, role in presynaptic function. *Nat Neurosci*. 6:127-35.

Sans, N., K. Prybylowski, R.S. Petralia, K. Chang, Y.X. Wang, C. Racca, S. Vicini, and R.J. Wenthold. 2003. NMDA receptor trafficking through an interaction between PDZ proteins and the exocyst complex. *Nat Cell Biol*. 5:520-30.

Santos, M.S., H. Li, and S.M. Voglmaier. 2009. Synaptic vesicle protein trafficking at the glutamate synapse. *Neuroscience*. 158:189-203.

Sara, Y., T. Virmani, F. Deak, X. Liu, and E.T. Kavalali. 2005. An isolated pool of vesicles recycles at rest and drives spontaneous neurotransmission. *Neuron*. 45:563-73.

Scheiffele, P., J. Fan, J. Choih, R. Fetter, and T. Serafini. 2000. Neuroligin expressed in nonneuronal cells triggers presynaptic development in contacting axons. *Cell*. 101:657-69.

Schluter, O.M., F. Schmitz, R. Jahn, C. Rosenmund, and T.C. Sudhof. 2004. A complete genetic analysis of neuronal Rab3 function. *J Neurosci*. 24:6629-37.

Schneggenburger, R., and I.D. Forsythe. 2006. The calyx of Held. *Cell Tissue Res*. 326:311-37.

Schneggenburger, R., A.C. Meyer, and E. Neher. 1999. Released fraction and total size of a pool of immediately available transmitter quanta at a calyx synapse. *Neuron*. 23:399-409.

Schneggenburger, R., and E. Neher. 2000. Intracellular calcium dependence of transmitter release rates at a fast central synapse. *Nature*. 406:889-93.

Schoch, S., P.E. Castillo, T. Jo, K. Mukherjee, M. Geppert, Y. Wang, F. Schmitz, R.C. Malenka, and T.C. Sudhof. 2002. RIM1alpha forms a protein scaffold for regulating neurotransmitter release at the active zone. *Nature*. 415:321-6.

Schoch, S., F. Deak, A. Konigstorfer, M. Mozhayeva, Y. Sara, T.C. Sudhof, and E.T. Kavalali. 2001. SNARE function analyzed in synaptobrevin/VAMP knockout mice. *Science*. 294:1117-22.

Schoch, S., and E.D. Gundelfinger. 2006. Molecular organization of the presynaptic active zone. *Cell Tissue Res*. 326:379-91.

Serafini, T., S.A. Colamarino, E.D. Leonardo, H. Wang, R. Beddington, W.C. Skarnes, and M. Tessier-Lavigne. 1996. Netrin-1 is required for commissural axon guidance in the developing vertebrate nervous system. *Cell*. 87:1001-14.

Shapira, M., R.G. Zhai, T. Dresbach, T. Bresler, V.I. Torres, E.D. Gundelfinger, N.E. Ziv, and C.C. Garner. 2003. Unitary assembly of presynaptic active zones from Piccolo-Bassoon transport vesicles. *Neuron*. 38:237-52.

Shen, J., D.C. Tareste, F. Paumet, J.E. Rothman, and T.J. Melia. 2007. Selective activation of cognate SNAREpins by Sec1/Munc18 proteins. *Cell*. 128:183-95.

Shin, D.M., X.S. Zhao, W. Zeng, M. Mozhayeva, and S. Muallem. 2000. The mammalian Sec6/8 complex interacts with Ca(2+) signaling complexes and regulates their activity. *J Cell Biol*. 150:1101-12.

Stein, E., and M. Tessier-Lavigne. 2001. Hierarchical organization of guidance receptors: silencing of netrin attraction by slit through a Robo/DCC receptor complex. *Science*. 291:1928-38.

Sugihara, K., S. Asano, K. Tanaka, A. Iwamatsu, K. Okawa, and Y. Ohta. 2002. The exocyst complex binds the small GTPase RalA to mediate filopodia formation. *Nat Cell Biol*. 4:73-8.

Takamori, S., M. Holt, K. Stenius, E.A. Lemke, M. Gronborg, D. Riedel, H. Urlaub, S. Schenck, B. Brugger, P. Ringler, S.A. Muller, B. Rammner, F. Grater, J.S. Hub, B.L. De Groot, G. Mieskes, Y. Moriyama, J. Klingauf, H. Grubmuller, J. Heuser, F. Wieland, and R. Jahn. 2006. Molecular anatomy of a trafficking organelle. *Cell*. 127:831-46.

Takao-Rikitsu, E., S. Mochida, E. Inoue, M. Deguchi-Tawarada, M. Inoue, T. Ohtsuka, and Y. Takai. 2004. Physical and functional interaction of the active zone proteins, CAST, RIM1, and Bassoon, in neurotransmitter release. *J Cell Biol*. 164:301-11.

Tang, J., A. Maximov, O.H. Shin, H. Dai, J. Rizo, and T.C. Sudhof. 2006. A complexin/synaptotagmin 1 switch controls fast synaptic vesicle exocytosis. *Cell*. 126:1175-87.

Taschenberger, H., R.M. Leao, K.C. Rowland, G.A. Spirou, and H. von Gersdorff. 2002. Optimizing synaptic architecture and efficiency for high-frequency transmission. *Neuron*. 36:1127-43.

Taschenberger, H., and H. von Gersdorff. 2000. Fine-tuning an auditory synapse for speed and fidelity: developmental changes in presynaptic waveform, EPSC kinetics, and synaptic plasticity. *J Neurosci*. 20:9162-73.

TerBush, D.R., T. Maurice, D. Roth, and P. Novick. 1996. The Exocyst is a multiprotein complex required for exocytosis in Saccharomyces cerevisiae. *Embo J*. 15:6483-94.

TerBush, D.R., and P. Novick. 1995. Sec6, Sec8, and Sec15 are components of a multisubunit complex which localizes to small bud tips in Saccharomyces cerevisiae. *J Cell Biol*. 130:299-312.

Ting, A.E., C.D. Hazuka, S.C. Hsu, M.D. Kirk, A.J. Bean, and R.H. Scheller. 1995. rSec6 and rSec8, mammalian homologs of yeast proteins essential for secretion. *Proc Natl Acad Sci U S A*. 92:9613-7.

tom Dieck, S., L. Sanmarti-Vila, K. Langnaese, K. Richter, S. Kindler, A. Soyke, H. Wex, K.H. Smalla, U. Kampf, J.T. Franzer, M. Stumm, C.C. Garner, and E.D. Gundelfinger. 1998. Bassoon, a novel zinc-finger CAG/glutamine-repeat protein selectively localized at the active zone of presynaptic nerve terminals. *J Cell Biol*. 142:499-509.

Tsuboi, T., M.A. Ravier, H. Xie, M.A. Ewart, G.W. Gould, S.A. Baldwin, and G.A. Rutter. 2005. Mammalian exocyst complex is required for the docking step of insulin vesicle exocytosis. *J Biol Chem*. 280:25565-70.

Ushkaryov, Y.A., Y. Hata, K. Ichtchenko, C. Moomaw, S. Afendis, C.A. Slaughter, and T.C. Sudhof. 1994. Conserved domain structure of beta-neurexins. Unusual cleaved signal sequences in receptor-like neuronal cell-surface proteins. *J Biol Chem*. 269:11987-92.

Ushkaryov, Y.A., A.G. Petrenko, M. Geppert, and T.C. Sudhof. 1992. Neurexins: synaptic cell surface proteins related to the alpha-latrotoxin receptor and laminin. *Science*. 257:50-6.

Varoqueaux, F., A. Sigler, J.S. Rhee, N. Brose, C. Enk, K. Reim, and C. Rosenmund. 2002. Total arrest of spontaneous and evoked synaptic transmission but normal synaptogenesis in the absence of Munc13-mediated vesicle priming. *Proc Natl Acad Sci U S A*. 99:9037-42.

Vega, I.E., and S.C. Hsu. 2001. The exocyst complex associates with microtubules to mediate vesicle targeting and neurite outgrowth. *J Neurosci*. 21:3839-48.

Vega, I.E., and S.C. Hsu. 2003. The septin protein Nedd5 associates with both the exocyst complex and microtubules and disruption of its GTPase activity promotes aberrant neurite sprouting in PC12 cells. *Neuroreport*. 14:31-7.

Verhage, M., A.S. Maia, J.J. Plomp, A.B. Brussaard, J.H. Heeroma, H. Vermeer, R.F. Toonen, R.E. Hammer, T.K. van den Berg, M. Missler, H.J. Geuze, and T.C. Sudhof. 2000. Synaptic assembly of the brain in the absence of neurotransmitter secretion. *Science*. 287:864-9.

Vik-Mo, E.O., L. Oltedal, E.A. Hoivik, H. Kleivdal, J. Eidet, and S. Davanger. 2003. Sec6 is localized to the plasma membrane of mature synaptic terminals and is transported with secretogranin II-containing vesicles. *Neuroscience*. 119:73-85.

von Gersdorff, H., R. Schneggenburger, S. Weis, and E. Neher. 1997. Presynaptic depression at a calyx synapse: the small contribution of metabotropic glutamate receptors. *J Neurosci*. 17:8137-46.

Wang, L., G. Li, and S. Sugita. 2004a. RalA-exocyst interaction mediates GTP-dependent exocytosis. *J Biol Chem*. 279:19875-81.

Wang, S., and S.C. Hsu. 2003. Immunological characterization of exocyst complex subunits in cell differentiation. *Hybrid Hybridomics*. 22:159-64.

Wang, S., and S.C. Hsu. 2006. The molecular mechanisms of the mammalian exocyst complex in exocytosis. *Biochem Soc Trans*. 34:687-90.

Wang, S., Y. Liu, C.L. Adamson, G. Valdez, W. Guo, and S.C. Hsu. 2004b. The mammalian exocyst, a complex required for exocytosis, inhibits tubulin polymerization. *J Biol Chem*. 279:35958-66.

Wang, Y., M. Okamoto, F. Schmitz, K. Hofmann, and T.C. Sudhof. 1997. Rim is a putative Rab3 effector in regulating synaptic-vesicle fusion. *Nature*. 388:593-8.

Wasser, C.R., and E.T. Kavalali. 2009. Leaky synapses: regulation of spontaneous neurotransmission in central synapses. *Neuroscience*. 158:177-88.

Williams, S.E., F. Mann, L. Erskine, T. Sakurai, S. Wei, D.J. Rossi, N.W. Gale, C.E. Holt, C.A. Mason, and M. Henkemeyer. 2003. Ephrin-B2 and EphB1 mediate retinal axon divergence at the optic chiasm. *Neuron*. 39:919-35.

Wimmer, V.C., T. Nevian, and T. Kuner. 2004. Targeted in vivo expression of proteins in the calyx of Held. *Pflugers Arch*. 449:319-33.

Wojcik, S.M., and N. Brose. 2007. Regulation of membrane fusion in synaptic excitation-secretion coupling: speed and accuracy matter. *Neuron*. 55:11-24.

Wu, L.G., and J.G. Borst. 1999. The reduced release probability of releasable vesicles during recovery from short-term synaptic depression. *Neuron*. 23:821-32.

Wu, S., S.Q. Mehta, F. Pichaud, H.J. Bellen, and F.A. Quiocho. 2005. Sec15 interacts with Rab11 via a novel domain and affects Rab11 localization in vivo. *Nat Struct Mol Biol*. 12:879-85.

Xu, K.F., X. Shen, H. Li, G. Pacheco-Rodriguez, J. Moss, and M. Vaughan. 2005. Interaction of BIG2, a brefeldin A-inhibited guanine nucleotide-exchange protein, with exocyst protein Exo70. *Proc Natl Acad Sci U S A*. 102:2784-9.

Yeaman, C., K.K. Grindstaff, and W.J. Nelson. 2004. Mechanism of recruiting Sec6/8 (exocyst) complex to the apical junctional complex during polarization of epithelial cells. *J Cell Sci*. 117:559-70.

Yeaman, C., K.K. Grindstaff, J.R. Wright, and W.J. Nelson. 2001. Sec6/8 complexes on trans-Golgi network and plasma membrane regulate late stages of exocytosis in mammalian cells. *J Cell Biol*. 155:593-604.

Zhai, R.G., H. Vardinon-Friedman, C. Cases-Langhoff, B. Becker, E.D. Gundelfinger, N.E. Ziv, and C.C. Garner. 2001. Assembling the presynaptic active zone: a characterization of an active one precursor vesicle. *Neuron*. 29:131-43.

Zhang, X.M., S. Ellis, A. Sriratana, C.A. Mitchell, and T. Rowe. 2004. Sec15 is an effector for the Rab11 GTPase in mammalian cells. *J Biol Chem*. 279:43027-34.

Ziv, N.E., and C.C. Garner. 2004. Cellular and molecular mechanisms of presynaptic assembly. *Nat Rev Neurosci*. 5:385-99.

Zucker, R.S., and W.G. Regehr. 2002. Short-term synaptic plasticity. *Annu Rev Physiol*. 64:355-405.

Zuo, X., J. Zhang, Y. Zhang, S.C. Hsu, D. Zhou, and W. Guo. 2006. Exo70 interacts with the Arp2/3 complex and regulates cell migration. *Nat Cell Biol*. 8:1383-8.